Impact of basalt application on soil chemical properties and plant response, and enhanced rock weathering by plant

（玄武岩の施与が土壌の化学性と植物の生育に与える影響および植物による岩石風化促進の可能性）

北海道大学大学院農学院
作物生産生物学ユニット　博士後期課程

内林 大志

Contents page

Chapter 1 - General introduction

1.1. Necessity of carbon dioxide removal

Climate change is an urgent issue to be addressed, and anthropogenic carbon dioxide (CO_2) emission is considered its main cause (IPCC, 2023). Paris agreement established the goal aiming to hold global temperature changes well below 2 ℃ or 1.5 ℃ above the pre-industrial levels in order to avoid increasing risks due to the warming temperature. To achieve this goal, not only limitation of CO_2 emissions but also CO_2 removal (CDR) is necessary. The representative concentration pathway (RCP) that results in a likely temperature rise by 2100 below 2 ℃ is RCP2.6 (Van Vuuren et al., 2011) (Figure 1-1), which suggests a cumulative emission of 880 Gt C and includes 40-220 Gt C of CDR (Edenhofer, 2015). Wide range of approaches have been proposed as CDR strategies such as afforestation/reforestation (AF/RF), soil carbon sequestration (SCS), biochar, enhanced rock weathering (ERW), bioenergy with carbon capture and storage (BECCS), direct air carbon capture and storage (DACCS) as land-based CDR strategy (Minx et al., 2018). Among these approaches, ERW is a relatively new CDR strategy, which takes advantage of natural geochemical carbon cycle, and has attracted attention in recent years (Hartmann et al., 2013, Beerling et al., 2020, Renforth and Henderson, 2017).

1.2. Theory of carbon dioxide removal via Enhanced Rock Weathering (ERW)

The principle behind ERW is similar to that of natural chemical weathering of silicate minerals. In general, CO_2 in the atmosphere dissolves in rainwater to produce H^+ and HCO_3^-:

$$CO_2 + H_2O \rightarrow H^+ + HCO_3^- \quad \text{(eq. 1-1)}$$

Silicate minerals such as pyroxene (represented here as $CaMgSiO_2$) consume H^+ in the water to release base cations (e.g., Ca^{2+} and Mg^{2+}) and silicic acid (e.g., H_4SiO_4):

$$CaMgSi_2O_6 + 4H^+ + 2H_2O \rightarrow Ca^{2+} + Mg^{2+} + 2H_4SiO_4 \quad \text{(eq. 1-2)}$$

In summary, 1 mol of a silicate mineral such as pyroxene in soil reacts with 4 mol of CO_2.

$$CaMgSi_2O_6 + 4CO_2 + 6H_2O \rightarrow Ca^{2+} + Mg^{2+} + 2H_4SiO_4 + 4HCO_3^- \quad \text{(eq. 1-3)}$$

The products of the reaction are transported to the ocean by rivers and are stored as carbonate minerals on geological timescales:

$Ca^{2+} + 2HCO_3^- \rightarrow CaCO_3 + CO_2 + H_2O$ (eq. 1-4)

$Mg^{2+} + 2HCO_3^- \rightarrow MgCO_3 + CO_2 + H_2O$ (eq. 1-5)

A series of these reactions has locked up atmospheric CO_2 in ocean sediments (Kasting, 2019). Natural rock weathering sequestrates approximately 0.25 Pg C $year^{-1}$, or ~3% of fossil fuel emissions (Taylor et al., 2016). ERW strategy aims to artificially accelerate this weathering process by crushing the silicate rocks to particle sizes to make the rocks easy to be dissolved and applying the crushed rocks to land surface, coastal area, and the open ocean to facilitate dissolution of the rocks (Renforth and Henderson, 2017).

The CDR potential induced by ERW conceptually depends on realistic rates of mineral dissolution and carbon sequestration efficiency of cations released from mineral, i.e., how much HCO_3^- and CO_3^{2-} can bind with cations derived from silicate mineral weathering (Hartmann et al., 2013).

In respect of dissolution rate, one of the most important controlling factors is silicate mineral species (Figure 1-3). Dissolution rate per surface area varies among silicate mineral species, and olivine, pyroxene, Ca-plagioclase are highly reactive minerals compared with other silicate minerals (Goldich, 1938). Therefore, mafic and ultramafic rocks, predominantly containing these minerals, are considered appropriate materials for ERW strategy (Figure 1-4). Another important factor is surface area available for reaction; higher surface area per unit mass means higher dissolution rates and greater alkalinity flux for a given mass of mineral. The dissolution rates of silicate minerals is also highly affected by pH; at low pH, the dissolution of silicate minerals can generally proceed more rapid than at high pH (Hermanská et al., 2023). Moreover, high temperature, high pressure, and low saturation state of solution accelerate dissolution of minerals (Brantley et al., 2008).

On the other hand, carbon sequestration efficiency of cations from silicate mineral weathering depends on the behavior of inorganic carbon and cations in the ecosystem. The ERW strategy primarily aims to accelerate the dissolution of CO_2 in water and its precipitation as carbonate. However, CO_2 dissolution cannot proceed under highly acidic conditions, as CO_2

hardly dissolve in solutions with a pH below 6.36. Therefore, when the weathering of silicate minerals is driven by strong acids such as HNO_3 or H_2SO_4, common anthropogenic pollutants, it may not immediately sequester carbon because generation of bicarbonate ions doesn't occur (Hartmann et al., 2013). Moreover, if the released cations are bound with negative charge other than HCO_3^- or CO_3^{2-}, such as cation exchange site in soil or other anions derived from chemical fertilizer, carbon sequestration doesn't occur at that time, either (Hasemer et al., 2024). From a larger perspective, provision of basic cations to the ecosystem by dissolution of silicate minerals can directly or indirectly contribute to the absorption of carbonic acid, a weak acid, but how long it takes to absorb carbon will become the next question in that case.

1.3. ERW on agricultural land

1.3.1. ERW deployment on agricultural land

Silicate mineral dissolution rate is a fundamental key to the feasibility of ERW, and spreading finely ground easily weatherable silicate minerals on soils can proceed silicate weathering more rapidly than just leaving them on massive rock deposits. Particularly in hot and humid regions, there are acidic soils with enough precipitation, where silicate mineral dissolution is easy to occur. Moreover, considering the logistical infrastructure to apply rock powder including roads, rail, and spreading technology for mineral addition to the land, agricultural land is the most feasible site (Hartmann et al., 2013, Kantola et al., 2017). There have been increasing studies about ERW in agricultural land (Table 1-1). As mentioned above, mafic and ultramafic rocks including olivine, wollastonite, and basalt are used because of their high dissolution rate compared with other silicate minerals.

1.3.2. Advantages of agricultural land on rock weathering enhancement

There have been piecemeal reports of findings supporting rock weathering enhancement in agricultural lands so far. Swoboda et al. (2022) reported controlling factors of silicate mineral weathering in agricultural land. In summary, environmental factors controlling mineral dissolution in agricultural land are (i) climate, (ii) soil, (iv) cultivation management, and (iv) plant.

(i) Climate: Temperature and precipitation are two major climatic factors influencing rock

weathering rates. Warm temperatures tend to accelerate weathering rates of minerals due to increases in activation energy (Kump et al., 2000). Precipitation is crucial since water is central to all forms of chemical weathering in the soil. Additionally, high water flux enhances weathering by leaching elements and maintaining a soil solution in ionic disequilibrium with the mineral surface (Cipolla et al., 2021b). In these senses, humid areas are suitable for weathering enhancement (Guo et al., 2023a).

(ii) Soil: soil is a medium for weathering of silicate minerals, and soil pH and mineralogy are important factors controlling silicate mineral dissolution. As mentioned above, pH is a strong factor controlling mineral dissolution and low soil pH enhances weathering of silicate minerals. In this sense, pH buffering capacity of the soil is also important. van der Bauwhede et al. (2024) reported that the initial pH and cation exchange capacity affects dissolution rate of silicate rock powder as well as its reactive surface area and mineral species. In addition, soil mineralogy can be important, considering dissolution occurs when there is ionic disequilibrium between the mineral surface and the soil solution (White and Brantley, 2003). Soil mineralogy is also related with pH buffering capacity, i.e., the more soil contain clay minerals, the higher the pH buffering capacity is in general.

(iii) Cultivation management: Application of nitrogen-rich fertilizer can facilitate mineral dissolution by providing H^+ in the process of nitrification. In this case, silicate mineral dissolution does not always lead to carbon sequestration because the supplier of H^+ is not carbonic acid (Hasemer et al., 2024). However, when nitrate is removed from the soil solution through plant uptake, HCO_3^- may alternatively replace it to maintain charge balance, thereby contributing to carbon sequestration. In addition, agricultural tillage incorporates rock powder into the soil, where organic acids, metabolic activity of soil organisms, and higher CO_2 partial pressure promote mineral dissolution, although these effects are poorly quantified for lager areas (Hartmann et al., 2013). Furthermore, whether an agricultural land is managed as paddy field or upland field is crucial in Asia, because paddy field and upland field has quite different geochemical environment including redox conditions and water flux. Particularly in Japan, crop rotation between paddy fields and upland fields has been recommended as a governmental policy. This practice may also influence the weathering rate of silicate minerals, although its effects have not yet been investigated.

(iv) Plant : This factor will be described in the next section in detail.

1.3.3. Enhanced rock weathering by plant

Plants influence mineral dissolution in various biogeochemical ways, particularly in the rhizosphere, where conditions can differ greatly from those in the bulk soil. Moisture levels, pH, elemental and gas concentrations fluctuate in these spheres and thereby alter the rate and quasi-equilibrium of reactions between the solid mineral phase and the soil solution (Hinsinger et al., 2005). Its importance for ERW was also pointed out in a model simulation (Cipolla et al., 2021a).

(i) Respiration: Plant roots consume O_2 and release CO_2 into the soil through respiration. The released CO_2 can dissolve in soil water, and lowers its pH, thereby promoting silicate mineral dissolution. Moreover, O_2 consumption affects redox conditions. By reducing redox potential, Fe^{3+} and Mn^{4+}, which located in the structure of minerals, can be reduced and dissolved into soil water, and mineral weathering can be promoted (Colombo et al., 2014).

(ii) Release of organic substances: Plants release organic substances, some of which can chelate metal elements within mineral structures, thereby enhancing mineral dissolution. Phytosiderophores, a representative group of Fe chelators secreted by gramineous plants, play a key role in facilitating Fe uptake. Their contribution to mineral dissolution has been suggested by (Akter and Akagi, 2010, Hinsinger et al., 2001).

(iii) Absorption: plants take up elements for their growth, resulting in disturbance of equilibrium between soil solution and mineral surface. Moriizumi et al. (2021) suggested rice cultivars with different ability of Si uptake affected mineral dissolution rate. In addition, legumes release H^+ following excess uptake of cations over anions during N_2 fixation, leading to dissolution of minerals by acidification in the rhizosphere (HAYNES, 1983).

(iv) Symbiosis with microorganisms: Plants have symbiotic microbes in the rhizosphere. Mycorrhizal fungi is a representative symbiotic microbes and reported to enhance weathering of minerals (Burghelea et al., 2015). Some symbiotic bacteria also can dissolve minerals through their metabolisms (Ribeiro et al., 2020). Moreover, microbes in the rhizosphere metabolites root exudates and release CO_2, resulting in the increase of CO_2 partial pressure and dissolution of minerals (Hartmann et al., 2009).

1.3.4. Co-benefits of ERW on agricultural land

ERW on agricultural land also has a co-benefit on soil fertility and crop production (Swoboda et al. 2022). For example, Ca and Mg, essential elements for plant growth, are released from silicate minerals and supplied to crops as nutrients in the process of weathering (Kantola et al. 2017; Andrews and Taylor 2019). Silicon (Si) is provided as well and work as beneficial element for plant growth (Kelland et al. 2020). Further, the increase of Ca and Mg concentrations leads to the increase in soil pH, which is beneficial in acidic soil (Gillman et al. 2001). Also, Anda et al. (2015) reported the increase of cation exchange capacity (CEC) by applying basalt powder in Oxisols, which is highly weathered soil. Moreover, if the improvement of soil fertility enhances plant growth, that also leads to organic carbon sequestration by promoting carbon fixation by photosynthesis.

1.3.5. Possible adverse effects of ERW on agricultural land

On the other hand, it is also necessary to assess the potential of adverse effect of ERW on agricultural land. For example, olivine contains relatively high Ni and Cr and its application on agricultural land can cause the heavy metal pollution (Beerling et al., 2018). Therefore, wollastonite and basalt have been more appropriate candidates for ERW on agricultural land than olivine. Moreover, soil chemical and physical properties are also affected by rock powder application. In general, the particle size of rock powder is desirable to be small in terms of fast mineral dissolution, but some small particles of rock powder enter the pore space of soil, which can seal the route of air and water in soil and possibly degrade soil fertility. In addition, high pH of mafic and ultramafic rock powders increase soil pH and excessive pH increase can do harm on the crop growth by causing some nutrient deficiency including Fe and Mn (Haque et al., 2020).

1.4. Objectives of this study

Within a single agricultural field, the potential effectiveness of ERW can vary depending on crop species and cultivation practices. Different crops interact biogeochemically with soil in unique ways due to variations in root system size, nutrient requirements, and root secretions. Cultivation practices also differ, including the amounts of chemical fertilizers and irrigation applied, which are tailored to specific crops. Notably, paddy fields and upland fields exhibit distinct soil conditions, as previously mentioned, making it essential to investigate the potential of ERW under these varying conditions. Additionally, we used basalt as the silicate mineral, which is abundant and readily accessible in Japan. Basalt contains several elements, including Ca, Mg, Na, and Si, among others, and its effects on crop growth can differ depending on the crop species. Although several studies have reported the beneficial effects of basalt application on crop production (Kelland et al., 2020, Kantola et al., 2023, Skov et al., 2024, Luchese et al., 2023), only a limited number have analyzed the specific factors of basalt application that influence crop growth (Beerling et al., 2024).

In this study, we examined the differential impacts of basalt application on rice and soybean growth from the perspective of plant nutrition. In Chapter 2, we analyzed the effects of basalt application on paddy rice growth and the reciprocal impact of rice growth on basalt weathering. Chapter 3 focuses on the effects of basalt application on soybean growth and the reciprocal impact of soybean growth on basalt weathering. In Chapter 4, we expanded this investigation to a field scale, examining the effects of basalt application on soybean growth and its reciprocal influence on basalt weathering.

Chapter 2 – Rice cultivation in a pot experiment

2.1. Summary

Paddy rice was cultivated for 99 days in a pot experiment with Gray Lowland soil with six application rates of basalt equivalent to 0, 5, 10, 20, 50, 100 t ha^{-1}. Soil chemical properties, growth response of rice, and element concentration in rice were investigated. In addition, the release amount of Si from the basalt was estimated by calculating (i) changes in soil available Si pool and Si uptake by rice during cultivation, and (ii) its differences among the treatments. The release amounts of Ca, Mg, Na, and K were similarly calculated based on the soil exchangeable pool and the elemental uptake by rice. Moreover, carbon balance between before planting and after harvest in the whole system including soil and plant was calculated. The application of the basalt increased total amount of soil available Si and exchangeable Mg and Na in pot as well as the uptake of Si and Na in rice ($p < 0.05$). There was no significant increase in arsenic (As), cadmium (Cd), copper (Cu), Cr, and Ni concentrations in soil solution nor rice grain in the basalt applied treatments compared with Control treatment. The release of Si, Mg, and Na from the basalt increased corresponding to the application rate of the basalt, suggesting that the applied basalt was weathered during cultivation, though increased carbon sequestration by the basalt weathering was not detected in 99 days of this experiment. We clearly demonstrated that basalt powder got weathered and released Si, Mg and Na in paddy field condition and additional Si enhanced paddy rice growth.

2.2. Introduction

There have been several studies to investigate the effect of silicate mineral powder on the crops under upland field conditions (Table 1-1). However, as far as I know, there is only one study to report the effect of a silicate mineral under paddy field, where wollastonite powder, mainly composed of $CaSiO_3$, influenced positively the yield of paddy rice and soil inorganic carbon (Wang et al., 2024). On the other hand, basalt contains not only Si and Ca but also Mg and Na, and the release of these elements in weathering process and their effects on paddy rice growth have not yet been studied. In this study, I investigated (i) the impact of basalt application on soil chemical properties and paddy rice growth and (ii) release of cations from basalt under paddy

field conditions.

2.3. Materials and Methods

2.2.1. Basalt characteristics

Basalt rock was obtained from Kamigassanshita area, Odate city, Akita prefecture, Japan (Horie Kenzai. Ltd., Japan), and crushed in Aichi prefecture (Sobueclay Corporatio, Japan). The basalt characteristics are given in Table 2-1. The basalt pH(H_2O) was 9.68 and total carbon content was 0.333 g kg^{-1} basalt, measured by the protocols below. The particle size distribution was determined using a laser diffraction particle size distribution analyzer (SALD2100, Shimadzu, Kyoto, Japan), and 10 %, 50 % and 90 % of particles was smaller than 21.6, 120 and 370 μm, respectively. The mineral content of the basalt used in this study was determined using X-ray powder diffraction (XRPD) analysis using full-pattern summation method (Butler BM and Hillier 2021) following the procedure of Kurokawa et al. (2024). Samples were spiked by 20% with corundum (Al_2O_3) to aid quantitative analysis and ground with ethanol by using XRD-mill (McCrone, Retsch, Germany). The ethanol suspension samples were dried at room temperature and reground by using agate pestle and mortar. The XRPD patterns of the powdered samples were obtained by X-ray diffraction (XRD) instrument (MiniFlex600, Rigaku, Tokyo, Japan) using Cu-Kα radiation from 5-65° 2θ, with a step of 0.01° and a scan speed of 10° min^{-1} at 40 kV and 15 mA conditions. The mineral content was calculated from the XRPD patterns using the powdR package (Butler B and Hillier 2020) version 1.3.0 for R language (R Core Team, 2023). The most abundant mineral was bytownite (36.6 wt.%), followed by labradorite (25.7 wt.%) and pyroxene (10.2 wt.%). Bytownite and labradorite are subgroups of plagioclase feldspar, which is a solid solution with a predominance of albite ($NaAlSi_3O_8$) and anorthite ($CaAl_2Si_2O_8$). Bytownite contains 70-90 % anorthite, while labradorite contains 50-70 %. These major minerals in the basalt are easily weathered (Hermanská et al. 2023). The element content of the basalt was determined by energy-dispersive X-ray fluorescence spectroscopy (EDXRF: XEPOSC, SPECTRO Analytical Instruments, Germany) using pressed powder pellet sampling (Table 2-2). The major elements were SiO_2 (58 wt.%), Al_2O_3 (13 wt.%), Fe_2O_3 (9.9 wt.%), CaO (7.8 wt.%), MgO (4.7 wt.%) and Na_2O (3.8 wt.%). The element contents were considered within the general range when compared to basalts used in a previous study (Lewis et al. 2021).

2.2.2. Potential of element supply from basalt

To evaluate the potential of elemental supply from the basalt used in this study, Si, Ca, Mg, K, and Na were investigated by two extraction methods: (1) shaking for 1 h with 1.0 *M* ammonium acetate solution (pH = 7.0) at a soil solution ratio of 1:20 at room temperature followed by filtered with a filter paper (Advantec No. 6) to evaluate elements in exchangeable fraction (Kamewada 1997a), (2) shaking for 30 minutes with 2% citric acid solution at a soil solution ratio of 1:100 at room temperature followed by filtered with a filter paper (Advantec No. 6) to evaluate elements potentially dissolved from minerals in rhizosphere (De Medeiros et al. 2021). The elements in the extractions were analyzed by Inductively Coupled Plasma Mass Spectrometry (ICP-MS: ELAN DRC-e, PerkinElmer, Waltham, MA, USA).

2.2.3. Experimental setup

Experiments were conducted with 1/2000a Wagner pots (30 cm height, 25.2 cm diameter) in a greenhouse at Hokkaido University in Japan (43°04'18.2" N, 141°20'26.5" E). Soil was collected from a depth of 0-15 cm in an upland agricultural field in Field Science Center for Northern Biosphere (43°04'16.6" N, 141°20'24.8" E). The soil type was classified as a Gray Lowland soil (Nakamura et al. 2024) in Comprehensive Soil Classification System of Japan First Approximation (Obara et al. 2011) (Haplic Fluvisol in World reference base for soil resources (IUSS Working Group WRB 2022)). Soil texture was sandy clay loam. pH(H_2O) was 6.19 and soil total carbon content was 27.4 g kg^{-1} soil, measured by the protocols below. Soil was air-dried and passed through a 5 mm sieve, and thoroughly mixed. An 8 kg portion of air-dried soil was then mixed with 4.0 g of ammonium sulfate, 1.5 g of potassium dihydrogen phosphate, and 0.42 g of potassium chloride, which equals to 850 mg N pot^{-1}, 349 mg P pot^{-1}, and 664 mg K pot^{-1}, respectively. Crushed basalt, as described below, was mixed thoroughly with soil at six different application rates: which were 0, 25, 50, 100, 250, and 500 g per pot (equivalent to 0, 0.31, 0.63, 1.25, 3.13, 6.25 wt.% or 0, 5, 10, 20, 50, 100 t ha^{-1}, hereafter referred to as B0, B5, B10, B20, B50, B100), respectively. Each treatment was replicated four times. A small portion of soil was collected at this stage before planting for chemical analysis from each pot and composited in each basalt application rate treatment. The pot was filled with soil and flooded with tap water on June

13, 2022. Rice seed was sown in plastic trays on April 22 and grown in a greenhouse. Three individuals of 54-days-old seedlings of paddy rice (*Oryza sativa* L. cv. Nanatsuboshi) were transplanted in the flooded pot on June 15. The pots were flooded until ripening stage (August 26), with water leaching prevented using silicon plugs (Supplemental figure 2-1(a)). From August 26 onward, flooding conditions were discontinued, and the soil was watered as needed to prevent complete drying until harvest. Air temperature started to be hourly measured from June 17 (Ondotori TR-52i, T&D Corporation, Nagano, Japan). The mean daily air temperature during this experiment was between 15.0 ℃ and 27.4 ℃. Rice was harvested at physiological maturity (September 22). The aboveground parts of rice plants were harvested using scissors, and yield-related indices (i.e. panicle number, grain number, 1000-grain weight and setting rate) were investigated. The soil-root complex was removed from the pot and air-dried for several days. Once the soil was sufficiently dry, it was broken apart using a wood hammer to collect root samples, which were then washed with tap water. The remaining soil was thoroughly mixed and collected as a soil sample after harvest. The plant samples were separated into roots, stems, leaves, husks, and grains, then dried in a forced-air oven at 80 ℃ for at least 72 h. Soil samples were air-dried and sieved through a 2 mm mesh.

2.2.4. Soil chemical analysis

Soils before planting and after harvest were analyzed for pH, soil total carbon, available Si, and exchangeable cations. For soil pH measurements, 3.0 g of soil was weighed into a 50 mL of plastic bottle with 15 mL of Milli-Q water (1:5 mass ratio of soil:water) and shaken for 1 h at room temperature (150 rpm; TS-10N, Taitec Co., Ltd, Aichi, Japan). The solution was stood still for 1 h before pH measurement to 0.01 pH units (Kamewada 1997b). Soil total carbon was measured using an elemental analyzer (vario EL cube, Elementar Analysensysteme GmbH, Langenselbold, Germany) following powdered less than 250 μm with pestle and mortar. For available Si measurement, 1.0 g of soil was mixed with 10 mL of 0.02 *M* phosphate buffer solution (sodium dihydrogenphosphate (NaH_2PO_4) : disodium hydrogenphosphate (Na_2HPO_4) = 50:50, pH 6.9) in a 15-mL centrifugation tube and kept in a water bath at 40°C for 5 h. The centrifugation tube was reciprocally shaken 10 times at 40–50 cm width at the beginning of the water bath and again at 0.5, 1, 2, 3, 4 and 5 h after the start of the bath. The solution was then filtered with a filter paper (Advantec No. 6), and the Si concentration of the solution was determined by Inductively Coupled

Plasma Atomic Emissions Spectroscopy (ICP-AES: Avio 220 Max, PerkinElmer, Waltham, MA, USA) (Yanai et al. 2016). For soil exchangeable cations, Ca, Mg, K, and Na were extracted following the protocols of 2.2.2. and analyzed using ICP-MS. Total amount of elements in a pot was calculated by multiplying elemental concentration in soil by mass of soil in a pot.

2.2.5. Rice growth and elemental uptake

Dry weight of each sample was recorded, and samples were analyzed for element concentration according to the method as follows (Ishikawa et al. 2016). Dried samples were powdered using griding mill (Wonder Blender WB-1, Osaka Chemical Co., Ltd., Osaka, Japan). A 70 mg powdered sample was taken to a 65-mL polypropylene tube (DigiTUBE, SCP Sciences, Tokyo, Japan) with 2 mL of a 13 *M* HNO_3 solution (EL grade, Kanto Chemical Inc.) and left for 2 days at room temperature, then heated at 105°C for 1.5 h using a heating block system (Digi-PREP, SCP Science, Baie d'Urfé, Quebec, Canada) and cooled to room temperature. Then, a 70 mg of the same powdered sample was additionally taken to the same tube, and heated under the same condition and cooled to room temperature in order to increase concentration of Si in sample solution to be detected. After that, 0.4 mL of hydrogen peroxide (H_2O_2; atomic-absorption grade, Kanto Chemical Inc.) was added to the solution, which was then heated at 105°C for 0.5 h. The digested solution was adjusted to 10 mL by 2% HNO_3 solution and filtered through a filter paper (Advantec No. 5C). One mL of extracts was diluted to 10 mL by 2% HNO_3 and analyzed for 16 elements (Ca, Mg, K, Na, phosphorous (P), sulfate (S), manganese (Mn), iron (Fe), zinc (Zn), molybdenum (Mo), strontium (Sr), Cu, Cd, Cr, Ni, As) by ICP-MS. To determine Si concentration, the filter papers were washed with hot deionized water, compacted in small melting pots and dried at 80ºC for 2 h. Then, they were burned at 550ºC in a maffle for 5 h, and the weight of dry ash was measured for Si concentration (Kusa et al. 2021). Three empty tubes without sample were prepared as blank and subjected to the same procedure. The data were obtained after subtracting the blank values. To determine the N concentration, each 20 mg sample was digested with 1.25 mL of concentrated H_2SO_4 in a test tube at 200°C. At 15 min intervals, 0.5 mL of H_2O_2 was added to each tube for a total of six times, following which the N concentration in the digests was determined using the micro-Kjeldahl method (Obama et al., 2024). The data of micro-Kjeldahl method were obtained after subtracting blank values as well, which were prepared under the same procedure but without samples. Shoot element concentrations were calculated by multiplying the

dry weight and concentration of each part except for root, summing them up, and dividing by total dry weight of all parts except for root. In addition, the total uptake of Si, Ca, Mg, K, and Na by rice was calculated by multiplying the dry weight and concentration of each part for the calculation of elemental release from the basalt.

2.2.6. Soil solution analysis

Soil solution was sampled every two weeks during the pots were flooded. Three porous cups (5 cm length, 2 mm pore size) were inserted at 5 - 10 cm depth vertically per pot and connected with 25 cm length plastic tube each. 20 mL of soil solution was collected in total by using 10 mL syringes connected to the other end of plastic tube, filtered with a filter paper (Advantec No. 5C), and stored at 4 ^{o}C in a refrigerator until analysis. The concentrations of Si, Ca, Mg, K, Na, S, Fe, Mn, Sr, Zn, Mo, As, Cu, Ni, Cd, and Cr were analyzed by ICP-MS (Supplement table 2-4). Cd and Cr was under detection in some sampling points.

2.2.7. Calculation of release of Si and cations from the basalt during cultivation

Firstly, change in total amount of elements (Si, Ca, Mg, K, and Na) during cultivation contained by soil and plant in each treatment was calculated. The change in total amount of Si was calculated as follows:

Change in total amount of Si during cultivation (ΔSi) = (AvailableSi_{AH} + Uptake$_{plant}$ of Si) – AvailableSi_{BP} (eq. 2-1),

where AvailableSi_{AH} is total amount of soil available Si after harvest, Uptake$_{plant}$ of Si is Si uptake in rice, and AvailableSi_{BP} is total amount of soil available Si before planting. Units of change in total amount of Si during cultivation (ΔSi) is represented in g pot^{-1}.

The change in total amount of cations were similarly calculated as follows:

Change in total amount of M during cultivation (ΔM) = (Ex_{AH} of M + Uptake$_{plant}$ of M) – Ex_{BP} of M (eq. 2-2)

where Ex_{AH} of M is total amount of exchangeable cation in soil after harvest, Uptake$_{plant}$ of M is cation uptake in rice, and Ex_{BP} of M is total amount of exchangeable cation in soil before planting. Units of change in total amount of M during cultivation (ΔM) is represented in g pot^{-1}.

Then, Si and cation release from the basalt in each treatment was calculated by subtracting the

change in total amount of each element during cultivation in B0 from that in each treatment to eliminate the input from tap water and natural weathering of the mineral originally existed in the soil (Ten Berge et al. 2012). As an example of Si release from the basalt in B100, the calculation was as follows:

Calculated release of Si from the basalt = ($\Delta Si_{100} - \Delta Si_0$) / (M.W. of Si × 1000), (eq. 2-3)

where ΔSi_{100} is the change in total amount of Si during cultivation in B100 (g pot^{-1}), ΔSi_0 is the change in total amount of Si during cultivation in B0 (g pot^{-1}), and M.W. of Si is molar weight of Si (28.1 g mol^{-1}). Units of release of Si is represented in mmol pot^{-1}. As for ΔSi_0, the mean value was used in the calculation. Release of cations from the basalt was also calculated based on (eq.5).

2.2.8. Calculation of change in carbon content in the soil and in the whole system

Change in carbon content in the soil and in the whole system was calculated as follows:

Change in carbon content in the soil (ΔC_{soil}) = TC_{AH} - TC_{BP} (eq. 2-4)

Change in carbon content in the whole system (ΔC_{system})= (TC_{AH} - TC_{BP}) + [TC_{plant}] × DW_{plant} (eq. 2-5)

where TC_{AH} is total amount of total carbon in the soil after harvest (gC pot^{-1}), TC_{BP} is total amount of total carbon in the soil before planting (gC pot^{-1}), [TC_{plant}] is total carbon concentration in plant (0.413 g g^{-1} plant, Naser et al. 2020), and DW_{plant} is total dry weight of rice including shoot and root (g $plant^{-1}$). Units of change in carbon content in the soil (ΔC_{soil}) and in the whole system (ΔC_{system}) is represented in gC pot^{-1}.

2.2.9. Statistical analysis

Statistical differences between the element concentration of extracts from the basalt and soil were examined by Welch's t-test. Significant differences in soil pH, total amount of elements in soil, dry weight of plant, elemental uptake in plant, element concentration in grain, calculated release of Si and cations from the basalt, ΔC_{soil}, and ΔC_{system} were determined and compared among application rates of the basalt using one-way ANOVA and Tukey post hoc tests. The Pearson product moment correlation coefficient (*R*) was used to examine the correlation between soil chemical properties and element concentration in rice shoot and root, the total amount of available

Si in the soil and total Si uptake and dry weight of rice, as well as the total amount of exchangeable Na in the soil and total Na uptake and dry weight of rice. Outliers were statistically determined by the Smirnov–Grubbs test and excluded from the experimental analysis. All statistical analysis were performed using the computing environment R (R Core Team, 2023).

2.4. Results

2.3.1. Potential of elemental supply from basalt

Element concentrations of the basalt by two extraction methods are shown in Table 2-3, as well as the soil of B0 before planting. Si and Na were higher in the basalt than in the soil in both extraction methods, whereas K was lower in the basalt than in the soil. Ca was higher in the basalt in 1.0 *M* ammonium acetate extraction than in the soil, but showed no difference in 2 % citric acid extraction. Mg was lower in the basalt in 1.0 *M* ammonium acetate extraction, but higher in 2 % citric acid extraction than in the soil.

2.3.2. Soil chemical properties with different application rates of basalt

The soil chemical properties before planting and after harvest are shown in Table 2-4 and Supplemental table 1. Soil pH before planting increased with the higher basalt application rate and was significantly higher in B50 and B100 than other treatments. Total amount of soil total carbon, exchangeable Mg and K before planting showed no difference among the treatments. Total amount of soil available Si and exchangeable Ca in pot before planting showed significant difference by one-way ANOVA, and lowest in B5 and highest in B100. Total amount of soil exchangeable Na in pot before planting significantly increased with the higher basalt application rate. On the other hand, soil pH and total amount of soil total carbon after harvest didn't differ among the treatment. Total amount of soil available Si, exchangeable Mg and Na in pot after harvest significantly increased with the higher basalt application rate. Total amount of soil exchangeable Ca and K in pot after harvest showed no significant difference among the treatments. Basically, the exchangeable K and Mg concentration and Mg:K ratio in soil before planting and after harvest were higher than the diagnostic standard for paddy field fertilization in Hokkaido prefecture, i.e. 124 mg kg^{-1} soil for exchangeable K, 151 mg kg^{-1} soil for exchangeable Mg, and 2 in equivalent ratio for Mg:K ratio (Hokkaido Research Organization 2020) (Supplemental table 2-1). The available Si concentration extracted by phosphate buffer solution was higher than 34.4 mg kg^{-1} soil, which is the average in Gray Lowland soil in Japan (Yanai et al. 2016).

2.3.3. Rice growth and element uptake responding to basalt application

The dry weight of each part of rice is shown in Table 2-5. No significant difference was observed in dry weight of each part nor total of them among the treatments. There were no significant differences in yield-related indexes among the treatments either (Supplemental table 2-2). Table 2-6 shows the element concentration in shoot. The Na concentration increased with the higher basalt application rate ($p < 0.01$), but there was no significant differences among the treatments in other elements. Table 2-7 shows the element concentration in root. The Fe concentration was significantly different among the treatments ($p < 0.05$), but there was no significant difference in other elements. N concentration in shoot was not measured. Table 2-8 shows the total uptake of Si, Ca, Mg, K and Na in rice. The uptake of Si showed significant difference among the treatments by one-way ANOVA ($p < 0.05$), and Si uptake increased with the higher basalt application rate. The uptake of Ca, Mg, and K didn't show significant difference among the treatments, but the uptake of Na significantly increased with the higher basalt application rate ($p < 0.01$). Table 2-9 shows the concentration of As, Cd, Cu, Cu, and Ni in grain, and no significant difference was detected among the application rates of the basalt.

2.3.4. Relationships between Si and Na in the soil and paddy rice growth response

The relationships between soil available Si and paddy rice growth responses are shown in Figure 2-1. Total amount of soil available Si after harvest had positively significant correlation with total Si uptake of rice ($p < 0.001$) and total dry weight ($p < 0.01$). In addition, relationship between soil exchangeable Na and rice growth responses are shown in Figure 2-2. Total amount of soil exchangeable Na after harvest showed significantly positive correlation with Na concentration in paddy rice shoot ($p < 0.001$), whereas it had no significant correlation with shoot dry weight ($p > 0.05$).

2.3.5. Si and cation release from basalt during cultivation

Release of Si, Ca, Mg, K, and Na from the basalt are shown in Figure 2-3. Si release differed among the application rates and significantly increased with the higher application rates of the basalt. Ca release from the basalt didn't differ among the application rate of basalts. Mg release

significantly increased with the higher application rates of the basalt. K release showed significant difference among the application rates by one-way ANOVA and was lower in B20. Na release showed significant difference among the application rates by one-way ANOVA and increased with the higher application rates of basalt.

2.3.6. Change in carbon content in the soil and in the whole system

ΔC_{soil}, total amount of carbon in plant, and ΔC_{system} are shown in Table 2-10. ΔC_{soil} showed significant difference among the treatments by one-way ANOVA. Total amount of carbon in plant nor ΔC_{system} didn't differ among the treatments.

2.5. Discussion

2.4.1. Impact of basalt application on soil chemical properties and elemental uptake in rice

The application of the basalt increased total amount of soil available Si both before planting and after harvest (Table 2-4). Although the concentration of Si in shoot or root did not increase by the basalt application, the total Si uptake of rice was significantly increased with the higher basalt application (Tables 2-6, 2-7, and 2-8). In addition, a positive correlation was detected between soil available Si after harvest and total Si uptake of rice (Figure 2-1(a)). The available Si in this study was extracted by the phosphate buffer solution, and is considered monosilicate adsorbed on the surface of soil particles and easily desorbed and supplied to plants (Shigezumi et al., 2002). Therefore, the results in this experiment suggested that silicate minerals in the basalt got weathered during cultivation and released monosilicate to the soil particles and soil solutions as available Si, which was partly absorbed by rice plant. Wang et al. (2024) also reported the increase of available Si concentration in soil and Si concentration in paddy rice straw by application of wollastonite as well as this study, which confirms easily weatherable silicate mineral application is effective to supply Si to soil and plant in paddy rice field. Moreover, total amount of soil available Si after harvest was also positively correlated with total dry weight of rice, even though dry weight itself didn't significantly differ among the treatments (Table 2-5 and Figure 2-1(b)). Since Si has physical and chemical stress-relieving effects in rice, such as reducing salt and heat stress, improving physical strength and light-receiving attitude (Ma 2004; Ma and Yamaji 2008), the increase of available Si in soil and its uptake by rice could have contributed to rice growth in this study. Further, as the beneficial effects of Si have been observed not only in rice but also other crops regardless of monocotyledonous or dicotyledonous plants (Fawe et al., 1998, Tripathi et al., 2021), Si supply can be one of the important co-benefits in ERW strategy.

In addition, the application of basalt increased total amount of soil exchangeable Mg after harvest (Table 2-4). Since total amount of soil exchangeable Mg didn't differ among the basalt application rate before planting, the increase of Mg probably derived from the weathering of the basalt during cultivation. The soil exchangeable Mg concentration didn't increase by wollastonite application in paddy field (Wang et al., 2024), Mg supply was revealed to be a beneficial effect of basalt application compared to wollastonite application. However, the increase of soil

exchangeable Mg didn't affect the Mg concentration in rice (Tables 2-6, 2-7, and Supplemental figure 2-2), probably because the soil used in this study contained higher exchangeable Mg than the diagnostic standard for fertilization (Hokkaido Research Organization 2020) and was fertile enough to meet Mg demand by rice even without the basalt application. However, when basalt is applied to a Mg-deficient field or a field with an imbalance in soil base cation content, it can enhance Mg uptake by plants, potentially promoting growth.

Moreover, the application of the basalt increased the total amount of soil exchangeable Na before planting, after harvest, and the Na concentration in rice shoot (Tables 2-4 and 2-6). There was a positive correlation between the total amount of soil exchangeable Na after harvest and the Na concentration in rice shoot (Figure 2-2(a), and Supplemental figure 2-2), suggesting the increase of the total amount of soil exchangeable Na caused the increase of Na concentration in rice shoot. Rice is susceptible to Na salinity, and high Na concentration in soil antagonistically inhibits K uptake by rice and interferes metabolism because of ion imbalance in a cell (Coca et al. 2023). The threshold of EC of soil water is 3 dS/m (≈ 30 m*M* of NaCl) for rice (Chinnusamy et al., 2005), and salt stress reduces yield mainly due to the reduction in the number of tillers and spikelets per panicle (Zeng and Shannon, 2000). Fortunately, however, there was no significant correlation between the total amount of soil exchangeable Na and shoot dry weight of rice (Figure 2-2(b)). Moreover, no significant decrease by basalt application was observed in yield-related indices, suggesting Na concentration in soil was not high enough to inhibit rice growth in this study (Supplemental table 2-2). Also, Na is a monovalent cation and relatively easy to be leached (Gillman et al. 2001). Considering that this experiment was conducted under non-leaching conditions, it is less possible that Na supply from the basalt negatively affects rice growth in paddy field, where water derived from river leaches downward during most of the cultivation season. However, as basalt generally contains Na in easily weatherable plagioclase minerals, the effect of basalt application in paddy field should be carefully monitored particularly in the case of continuous application, with high application rate, or application to the area where soil Na salinity is originally high.

The increase of concentrations of As, Cd, Cu, Cr, and Ni in soil solution was not observed (Supplemental table 2-4), which reflected that the basalt contained low amount of heavy metals (Beerling et al. 2018). On the other hand, Vienne et al. (2022) reported the increase of Ni concentration in soil solution by basalt application in potato cultivation. Since the mobility of

these elements are affected by soil pH, redox conditions, and organic matter contents (El-Naggar et al., 2021, Kumar et al., 2021, Zulfiqar et al., 2023), it is necessary to consider the difference of soil properties, management practice, and the basalt characteristics to be applied, and to be careful in assessing the risk of pollution by As and heavy metal elements in ERW strategy. Furthermore, the concentrations of these elements in rice grain did not significantly differ among the treatments (Table 2-9). Kelland et al. (2020) also reported no significant increase in As and heavy metal elements concentration in sorghum grain by application of the basalt in upland condition and the consistent result was obtained even under submerged paddy condition.

As for soil pH, the basalt application increased soil pH before planting, but didn't affect soil pH after harvest (Table 2-4). In paddy field, it is known that soil solution pH converges to around 7.0 because production of protons by the dissolution of CO_2 comes to be balanced with consumption of protons by the reduction of ferric (Fe^{3+}) ions to ferrous (Fe^{2+}) ions in soil over time (Sahrawat, 2005). The soil pH after harvest were probably affected by the soil solution pH convergence, suggesting that basalt application will not influence soil pH or associated nutrient availability in paddy field.

2.4.2. Basalt weathering and release of Si and cations during cultivation

The increase of the release of Si, Mg and Na from the basalt during cultivation corresponded to the increase of the basalt application rate, which indicated the weathering of the basalt occurred during cultivation (Figure 2-3(a),(c), and (e)). These results were consistent with the mineralogical characteristic of the basalt, containing 10.2 wt.% of pyroxene and 62.3 wt.% of plagioclase (bytownite and labradorite) (Table 2-1). Pyroxene contains Si and Mg while plagioclase contains Si and Na, and both are easy to be weathered especially in the presence of plant (Moulton et al., 2000). The result of 2 % citric acid extraction also showed higher Si, Mg and Na concentration in the basalt than the soil, supporting the result of the release of these elements from the basalt by weathering (Table 2-3). On the other hand, the release of Ca didn't show the significant difference among the application rates (Figure 2-3(a)) though Ca-containing silicate minerals like plagioclase and pyroxene were presumed to be weathered. Considering the high exchangeable Ca content in the soil used in this study (Table 2-3), it might be possible that Ca in soil water reached saturation during cultivation and precipitated as secondary mineral and calcium salt which was insoluble in 1.0 *M* ammonium acetate. The release of K showed significant

differences among the treatments by one-way ANOVA but the reason for the negative value of K release in B20 treatment was unclear (Figure 2-3(c)). In any case, since the basalt used in this study contained little K (Table 2-2), K was probably hardly supplied from the basalt.

When we compared the rate for Mg and Na release with the previous study by Kelland et al. (2020), in which sorghum was cultivated in a pot under upland condition, the rate for Mg release in B100 (6.5 mmol m^{-2} day^{-1}) was similar order of magnitude to that observed in Kelland et al. (2020) (4.2 mmol m^{-2} day^{-1} in 100 t ha^{-1} application of basalt) (Supplemental table 2-3). This result suggests that paddy rice cultivation with basalt powder has comparable ERW potential with their study. Moreover, the potential in a real paddy field can be higher than the present results, considering that this experiment was conducted under non-leaching conditions (Cipolla et al., 2021b). Based on eq. 1 and 2, gross C sequestration by the basalt weathering amounts to 0.012 g C per mmol of Mg in the form of carbonate precipitation, and if 100 t ha^{-1} of the basalt powder is applied to all of paddy field in Japan (2,319,000 ha) (Ministry of Agriculture, Forestry and Fisheries. 2024) and weathered in a rate of 6.5 mmol m^{-2} day^{-1}, the sequestrated carbon by the basalt weathering will be 663,234 t CO_2 in one cultivation cycle (99 days) in Japan. Moreover, rate for Na release in B100 (4.6 mmol m^{-2} day^{-1}) was one order of magnitude higher than that observed in Kelland et al. (2020) (0.33 mmol m^{-2} day^{-1}) (Supplemental table 2-3), indicating the weathering of the basalt used in this study can release considerable amount of Na, not only Mg. Since Na cannot precipitate as carbonate in water because of its high solubility, it cannot sequestrate carbon directly. However, Na electrically binds to nitric and sulfuric acid which derive from fertilizer and may help increase the alkalinity of leachate from agricultural land and maintain the alkalinity of rivers and oceans (Renforth and Henderson 2017; Kelland et al. 2020).

2.4.3. Change in carbon content in the soil and in the whole system

ΔC_{soil} significantly differed among the treatments by one-way ANOVA (Table 2-10). However, the difference of ΔC_{soil} didn't correspond to the application rate of the basalt. This result suggests that the basalt weathering didn't affect ΔC_{soil}, though we observed the release of Mg and Na from the basalt. Based on (eq. 1-5), 32 mmol of Mg release from the basalt in B100 treatment only equaled to 0.77 g C pot^{-1} even if all of Mg released from the basalt contributed to carbon sequestration. Therefore, the potential of additional inorganic carbon storage was less than 0.5 % of total amount of soil total carbon in pot at most, which was little to detect its impact on carbon

balance. Moreover, the mean value of total amount of carbon in plant increased by the basalt application, but didn't significantly differ among the treatments, neither did ΔC_{soil}, which was calculated as the sum of the ΔC_{soil} and total amount of carbon in plant (Table 2-10).

In this study, carbon sequestration by the basalt application was not detected probably because of the insufficient amount of weathering of the basalt in 99 days of cultivation as mentioned above. However, rock weathering continues to occur over time and its impact should be evaluated in longer-term. In addition, most of previous studies of ERW have been conducted assuming aerobic field condition. However, quite different biogeochemical reactions happen in a paddy field under an anaerobic environment. For example, Fe^{3+} in mineral structure can be reduced to Fe^{2+} due to anaerobic condition, which can result in enhancement of weathering as ferrous ion is much more soluble than ferric ion. On the other hand, an increase in HCO_3^- in the soil solution due to mineral weathering can lead to the release of methane (CH_4) by increasing the reaction substrate for methanogenic bacteria (Conrad, 2007). As a future perspective, it is necessary to evaluate the potential of basalt application on carbon sequestration considering the unique carbon dynamics to paddy field condition in long term.

Chapter 3 – Soybean cultivation in a pot experiment

3.1. Summary

The effects of basalt and lime application were investigated in a pot experiment. Seven treatments were established: a conventional treatment (Control), treatments with 5, 10, and 20 wt% basalt application (BA5, BA10, and BA20, corresponding to 75, 150, and 300 t ha^{-1}, respectively), and treatments with 0.005, 0.01, and 0.02 wt% lime application (Lime5, Lime10, and Lime20, respectively). Planted treatments and unplanted treatments were established only in Control, BA5, BA10, and BA20 treatments. Soil chemical properties, growth response of soybean, and elemental concentration in soybean were investigated. In addition, the release of Ca, Mg, Na, and K was estimated by calculating (i) changes in soil exchangeable pools and element uptake by soybean during cultivation, and (ii) their differences among the treatments. Both basalt and lime applications increased soil pH and the total amount of exchangeable Ca in the soil. Additionally, the basalt application increased the total amount of exchangeable Mg and Na in the soil, whereas lime application did not influence them. The application of the basalt and the lime commonly increased the concentrations of N and Mo and decreased the concentrations of Mn and Ni in shoot by increasing the soil pH. On the other hand, the shoot dry weight of soybeans was significantly higher only in BA10 and BA20 compared to Control. Since there was a significant positive correlation between the total amount of soil exchangeable Mg and shoot dry weight, the increase of soil exchangeable Mg could have contributed to the increase of the shoot dry weight. Furthermore, the release of Mg from basalt was clearly observed in both planted and unplanted treatments, with higher Mg release in planted treatments, which suggested that the basalt was weathered during cultivation and soybean growth accelerated the basalt weathering.

3.2. Introduction

The effect of silicate minerals on soybean growth has been investigated recently (Beerling et al., 2024, Luchese et al., 2023, Haque et al., 2020, Guo et al., 2023b). These studies reported the increase of soybean growth by the application of silicate minerals. Luchese et al. (2023)

evaluated the effect of basalt and lime on soybean growth until flowering stage, and suggested the additional effect of basalt apart from the increase of soil pH. However, the effect of basalt application on soybean growth until full maturity has not been investigated yet. In addition, while the weathering of wollastonite was shown to be enhanced by soybean cultivation, whether soybean cultivation also enhances the weathering of basalt has not yet been investigated (Haque et al., 2020). In this study, I investigated (i) the differences in the effects of basalt and lime on soybean growth up to the harvest stage and (ii) the potential enhancement of basalt weathering by soybean cultivation.

3.3. Materials and methods

3.2.1. Basalt characteristics

Basalt rock was obtained from Kamigassanshita area, Odate city, Akita prefecture, Japan (Horie Kenzai. Ltd., Japan), and crushed in Aichi prefecture (Sobueclay Corporatio, Japan), the same as the basalt used in Chapter 2. As to the particle size distribution used in this study, 10 %, 50 % and 90 % of particles was smaller than 5.26, 30.7 and 75.6 μm, respectively. The other characteristics of the basalt were the same as Tables 2-1 and 2-2.

3.2.2. Experimental setup

Experiments were conducted with replicated mesocosms in a greenhouse at Hokkaido University in Japan (43°07’15.5” N, 141°34’02.9” E). 1/5000a Wagner pots (19.75 cm height, 7.98 cm diameter) were used and water leaching was prevented with silicon plugs during cultivation. Soil was collected from a depth of 0-15 cm in an upland agricultural field in Field Science Center for Northern Biosphere (43°04’16.6” N, 141°20’24.8” E). The soil type was classified as a Gray Lowland soil (Nakamura et al., 2024) in Comprehensive Soil Classification System of Japan First Approximation (Obara et al. 2011) (Haplic Fluvisol in World reference base for soil resources (IUSS Working Group WRB 2022)). Soil texture was sandy clay loam. pH(H_2O) was 5.55 and soil total carbon content was 27.4 g kg^{-1} soil. Soil was air-dried and passed through a 5 mm sieve, and thoroughly mixed. A 3 kg portion of soil was then mixed with 0.838 g of ammonium sulfate, 1.13 g of monoammonium phosphate, and 1.45 g of potassium sulfate (300 mg N pot^{-1}, 300 mg P

pot^{-1}, and 300 mg K pot^{-1}, respectively). Chemical fertilizers were applied more than the local fertilizer recommendation for soybean field in order to avoid depletion of nutrients in a pot (Hokkaido Research Organization 2020). Crushed basalt, described above, was mixed thoroughly with soil in four different application rates, which were 0, 150, 300, 600 g per pot (equivalent to 0, 5, 10, 20 wt.% or 0, 75, 150, 300 t ha^{-1}, hereafter Control, BA5, BA10, BA20, respectively) with seven replicates per treatment. Soybeans were planted in four of the seven replicates, and nothing was planted in other three replicates. Moreover, lime was mixed thoroughly with soil in 3 different application rates, which were 1.5, 3 and 6 g per pot (hereafter Lime5, Lime10 and Lime20, respectively) with three replicates per treatment and soybean was planted. The application rates of lime were determined to make soil pH of Lime5, Lime10 and Lime20 corresponding to the soil pH of BA5, BA10 and BA20 based on the neutralization curve by lime and the basalt, measured by following the protocols below.

The pots were filled with soil on June 25, 2023 and placed on a tray filled with deionized water, allowed to absorb water overnight through the drainage holes. After the water was confirmed to reach the soil surface, three soybean seeds (*Glycine max* L. cv. Yukihomare) per pot were sown on June 26, 2023. The pot was watered with deionized water when the surface of the soil was dry. Roughly, about 300 ml of deionized water was added to a pot once in a few days during vegetative stage, once in a day from R1 to R3, twice in a day from R4 to R6, and once in a few days until harvest (October 18). Soil temperature at 5-cm soil depth was started to be measured from June 30 and hourly recorded (Ondotori Jr.TR-42, T&D Corporation, Nagano, Japan). The mean daily soil temperature during this experiment was between 32.5 ℃ and 11.1 ℃ (Supplemental figure 3-2). Soybeans were harvested at physiological maturity. Although soybeans grew well, the grain yield was low, possibly due to the high temperature during seed development stage in August (Supplemental figures 3-1 and 3-2). Plant samples were separated into root, shoot, and seed, then dried in a forced-air oven at 80 ºC for at least 72 h. Soils were collected after harvest. In the planted treatments, soil in a pot was mixed thoroughly and collected for about 100 g of portion after soybean plant was removed. In the unplanted treatments, 3 cm of surface layer was removed in order to avoid local accumulation salt and soil in a pot was mixed and collected. Soils before planting and after harvest were air-dried and sieved with 2 mm mesh before analysis for pH and exchangeable cations.

3.2.3. Lime neutralization curve for determination of lime application rate

For lime neutralization curve determination, 4 g of air-dried soil with < 2 mm particle was weighed into a 50 mL of plastic tube. The basalt or the lime used in this study was added to the soil at seven application rates: 0, 80, 200, 400, 600, 800, and 1200 mg of the basalt or 0, 4, 10, 20, 30, 40, and 60 mg of the lime. Afterward, 20 mL of deionized water was added to each sample. The tubes were thoroughly shaken by hand and then left to stand for 24 hours at room temperature. They were subsequently shaken again for 5 hours at 150 rpm using a shaker (TS-10N, Taitec Co., Ltd, Aichi, Japan) to allow sufficient reaction between the soil and the basalt or the lime. After standing for an additional hour, pH of the suspension was measured. The results of the neutralization curves by the basalt and the lime are shown in Supplemental figure 3-3.

3.2.4. Soil chemical analysis

For soil pH measurements, 0.8 g of soil was weighed into a 5 mL of plastic tube with 4 mL of deionized water (1:5 mass ratio of soil:water) and shaken for 1 h at room temperature (150 rpm; TS-10N, Taitec Co., Ltd, Aichi, Japan). The solution was stood still for 1 h before pH measurement to 0.01 pH units (Kamewada, 1997b). For soil exchangeable cations, 2.0 g of soil was mixed with 40 mL of 1.0 *M* of ammonium acetate (pH=7.0; 1:20 mass ratio of soil:solution), shaken for 1 h at room temperature, filtered with a filter paper (Advantec No. 6) (Kamewada, 1997a). The concentrations of Ca, Mg, K, and Na in the extracts were analyzed using Inductively Coupled Plasma Atomic Emissions Spectroscopy (ICP-AES: Avio 220 Max, PerkinElmer, Waltham, MA, USA). Total amount of elements in a pot was calculated by multiplying elemental concentration in soil by mass of soil in a pot.

3.2.5. Soybean growth and elemental uptake

Dry weight of each sample was recorded and samples were analyzed for element concentration according to the method as follows (Ishikawa et al., 2016). Dried samples were powdered using griding mill (Wonder Blender WB-1, Osaka Chemical Co., Ltd., Osaka, Japan). A 40 mg powdered sample was taken to a 65-mL polypropylene tube (DigiTUBE, SCP Sciences, Tokyo, Japan) with 2 mL of a 13 *M* HNO_3 solution (EL grade, Kanto Chemical Inc.) and cooled to room temperature. Then, 0.4 mL of hydrogen peroxide (H_2O_2; atomic-absorption grade, Kanto

Chemical Inc.) was added to the solution, which was then heated at 105°C for 0.5 h. The digested solution was adjusted to 20 mL by 2% HNO_3 solution and filtered through a filter paper (Advantec No. 5C). Solution samples were analyzed for 15 elements (Ca, Mg, K, Na, P, S, Mn, Fe, Zn, Cu, Mo, Sr, Cd, Cr, Ni) using ICP-AES. To determine the N concentration, each 20 mg sample was digested with 1.25 mL of concentrated H_2SO_4 in a test tube at 200°C. At 15 min intervals, 0.5 mL of H_2O_2 was added to each tube for a total of six times, following which the N concentration in the digests was determined using the micro- Kjeldahl method (Obama et al., 2024). Shoot element concentrations were calculated by multiplying the dry weight and concentration of each part except for root, summing them up, and dividing by total dry weight of all parts except for root. In addition, total uptake of Ca, Mg, K, and Na in soybean was calculated by multiplying elemental concentration in soybean by dry weight for the calculation of elemental release from the basalt.

3.2.6. Calculation of release cations from the basalt during cultivation

Firstly, change in total amount of elements (Ca, Mg, K and Na) during cultivation contained by soil and plant in each treatment was calculated as follows:

Change in total amount of M during cultivation (ΔM) = (Ex_{AH} of M + $Uptake_{plant}$ of M) – Ex_{BP} of M (eq. 3-1)

where Ex_{AH} of M is total amount of exchangeable cation in soil after harvest, $Uptake_{plant}$ of M is cation uptake in rice, and Ex_{BP} of M is total amount of exchangeable cation in soil before planting. Units of change in total amount of M during cultivation (ΔM) is represented in g pot^{-1}.

Then, cation release from the basalt in each treatment was calculated by subtracting ΔM in Control from ΔM in each basalt applied treatment to eliminate the input from natural weathering of the mineral originally existed in the soil (Ten Berge et al. 2012). As an example of Mg release from the basalt in BA5, the calculation was as follows:

Calculated release of Mg from the basalt = ($\Delta Mg_{BA5} - \Delta Mg_{control}$) × (charge amount of Mg) / (M.W. of Mg × 100), (eq. 3-2)

where ΔMg_{BA5} is the change in total amount of Mg during cultivation in BA5 (g pot^{-1}), $\Delta Mg_{control}$ is the change in total amount of Mg during cultivation in Control (g pot^{-1}), charge amount of Mg is 2, and M.W. of Mg is molar weight of Mg (24.31 g mol^{-1}). Units of calculated Mg release is represented in $cmol_c$ pot^{-1}. Release of other cations from the basalt was also calculated based on (eq. 3-2).

3.2.7. Statistical analysis

Significant differences in soil pH, total amount of elements in soil, dry weight of plant, elemental uptake in plant, cation release from the basalt were determined and compared among application rates of the basalt and lime using one-way ANOVA and Tukey post hoc tests. The Pearson's correlation coefficient (R) was used to examine the correlation of the pH and total amount of each exchangeable cation in the soil with the dry weight and uptake of elements in soybean. All statistical analysis were performed using the computing environment R (R Core Team, 2023).

3.4. Results

3.3.1. Soil chemical property

Soil pH and total amount of exchangeable cations in pot are shown in Figure3-1. Soil pH and total amount of exchangeable Ca were significantly increased by basalt and lime application ($p < 0.001$) (Figure 3-1(a) and (b)). The increase of pH and exchangeable Ca in BA5, BA10 and BA20 corresponded to Lime5, Lime10 and Lime20, respectively, both before planting and after harvest in planted treatments. On the other hand, total amount of exchangeable Mg and Na were significantly increased by basalt application, but not increased by lime application ($p < 0.001$) (Figure 3-1(c) and (d)). The increase of exchangeable Mg and Na by basalt application were observed before planting, after harvest in planted treatments, and after harvest in unplanted treatment, but the amount of exchangeable Na after harvest in unplanted treatment was lower than before planting. Total amount of exchangeable K didn't differ among application treatments except for after harvest in unplanted treatment, where exchangeable K was higher in BA20 than other application treatments ($p < 0.01$) (Figure 3-1(e)). Moreover, the amount of exchangeable K after harvest in planted and unplanted treatments were lower than before planting.

3.3.2. Plant growth response

The stem length and dry weight in each part of soybean are shown in Table 3-1. The dry weight of leaf, pod, and root was significantly different among the treatments by one-way ANOVA, while stem length, dry weight of stem and grain was not significantly different. Shoot and total dry weight of soybean was higher in BA10 and BA20 than Control by Tukey post-hoc analysis. The element concentration in soybean shoot is shown in Table 3-2. The concentrations of N, K, Mg, S, Fe, Na, Cu, Sr, and Cr in shoot showed no significant differences among the treatments. The concentrations of P, Zn, and Cd in shoot were significantly lower with higher basalt application rates. The concentration of Ca in shoot was higher in lime application treatments. The concentration of Mo in shoot significantly increased with higher application rates of both basalt and lime whereas the concentrations of Mn and Ni in shoot significantly decreased under these conditions. The element concentration in soybean root is shown in Table 3-3. The concentrations of N, Mg, Ni, Sr, Cd, and Cr in root showed no significant differences among the

treatments. The concentrations of P, K, and Mn in root significantly decreased with higher application rate of basalt whereas the concentration of Na in root increased. The concentration of Ca in root was higher with higher lime application rate. The concentrations of Zn and Cu in root were significantly lower with higher application rate of both basalt and lime. Mo in root was not detected. The total uptakes of Ca, Mg, Na, and K are shown in Table 3-4. The total uptake of C and Na significantly increased with higher application rate of basalt. The total uptake of Mg was significantly higher in all basalt application treatments. The total uptake of K didn't differ significantly among the treatments.

3.3.3. Relationship of soil chemical properties with soybean growth responses

The relationships between soil pH at R8 and the concentrations of N, Mo, Mn, and Ni in shoot are shown in Figure 3-2. Soil pH had significantly positive correlations with the N and Mo concentration in shoot, while it had significantly negative correlations with the Mn and Ni concentration in shoot. In addition, the relationships of soil exchangeable Mg and soil pH with shoot dry weight are shown in Figure 3-3. The total amount of exchangeable Mg at R8 was significantly positively correlated with shoot dry weight, whereas soil pH at R8 showed no significant correlation with shoot dry weight.

3.3.4. Elemental release from basalt

Calculated cation releases from basalt are shown in Figure 3-4. Calculated Ca release didn't differ among application rates either in planted or unplanted treatments (Figure 3-4(a)). Calculated Mg release increased significantly with higher application rate of basalt both in planted and unplanted treatments (Figure 3-4(b)). Calculated Na release didn't differ among application rate in planted treatment but significantly decreased in unplanted treatment with higher application rate of basalt (Figure 3-4(c)). Calculation K release differed among the application rate of basalt in both planted and unplanted treatment by one-way ANOVA, and tend to increase with higher application rate of basalt (Figure 3-4(d)).

3.5. Discussion

3.4.1. Common effect of basalt and lime application on soybean element concentrations

The application of the basalt and the lime commonly increased soil pH and the total amount of soil exchangeable Ca both before planting and at R8 (Figure 3-1 (a) and (b)). Particularly, the increase of soil pH influenced the concentration of specific elements in shoot at R8. The concentrations of N and Mo in shoot showed significant positive correlations with soil pH (Figures 3-2 (a), (b), and Supplemental figure 3-4). The availability of Mo highly depends on soil pH and its availability increases with higher soil pH (Ahmed et al., 2020). Since Mo is involved with nitrogen assimilation and biological nitrogen fixation by legumes, the increase of Mo concentrations may have led to the increase of the concentration of N (Banerjee and Nath, 2022, Kaiser et al., 2005).

On the other hand, soil pH had significant negative correlations with the concentrations of Mn and Ni in shoot (Figure 3-2 (c) and (d)) probably because the availability of these elements decreased with the increase of soil pH (Kumar et al., 2019; He et al., 2005). Although Mn is one of the essential elements for plants, soybean in this study did not show the symptom of Mn deficiency, which implied this decrease of Mn concentration had no significant negative effect on the growth. Moreover, the decrease of Ni concentration in shoot was observed not only in the lime applied treatments but also in the basalt applied treatments. The Ni concentration in the basalt was 8.3 mg kg^{-1} (Table 2-2), which is lower than the standard for any fertilizer material specified in the *Act on the Quality Control of Fertilizers* (MAFF, 2024). Therefore, these results suggest the application of the basalt is unlikely to lead to excessive accumulation of Ni in plants.

The increase of Mo concentration or the decrease of Mn concentration by basalt application was observed in soybean, wheat, and spring oats, so far (Skov et al., 2024, Buss et al., 2024, Beerling et al., 2024). Therefore, the findings in this study were consistent with those of previous studies. However, when it comes to accumulation of heavy metals in soil, Vienne et al. (2022) reported the increase of Ni concentrations in soil solution and soil exchangeable Ni concentration by basalt application. Although another study observed no increase of heavy

metals in soil (Beerling et al., 2024), it is necessary to pay attention to not only accumulation in plants but also in soil (Dupla et al., 2023b). It is also possible that the mobility of heavy metals derived from rock powder can be influenced by various factors such as a change of soil pH, cultivation management, and organic matter content, and the variability of the risks depending on these factors should be assessed in the long run.

3.4.2. Different effects of basalt and lime application on soybean growth

The application of the basalt increased the total amount of soil exchangeable Mg and Na both before planting and at R8, but the application of the lime did not increase them (Figure 3-1 (c),(d), and Supplemental table 3-1). In addition, the basalt application significantly increased the shoot dry weight of soybean, but lime application did not significantly increase it (Table 3-1). A significant positive correlation was observed between the total amount of soil exchangeable Mg at R8 and shoot dry weight, but no correlation was observed between soil pH at R8 and total dry weight of soybean (Figure 3-3 (a) and (b), Supplemental figure 3-4). Furthermore, Mg promotes soybean growth by stimulating nitrate transporter gene expression and nodulation in root through facilitation of carbohydrate allocation in soybean (Peng et al., 2018, Peng et al., 2020). Therefore, although the concentration of Mg in shoot and root didn't differ significantly among the treatments at R8, Mg may have enhanced N metabolism and promoted growth subsequently (Table 3-2 and 3-3). The correlation analysis among shoot dry weight and element concentrations in shoot showed significant negative correlations between shoot dry weight and many macro and micronutrients, but the concentration of N and Mo showed slight positive correlations (Supplemental figure 3-5 (a)). These results may have implied that N concentration was a main driving force for the increase of soybean growth, resulting in the dilution of other elements. Although the total amount of exchangeable Na showed positive correlation with the dry weight, that was considered pseudo-correlations because Na is neither an essential element or beneficial element for soybean (Supplemental figure 3-4).

Beerling et al. (2024) reported basalt application increased soybean yield, and our result supported the positive effect of the basalt application on soybean growth. They also suggested the additional positive effect of basalt application other than the increase of soil pH on maize by

comparing basalt with lime. Moreover, Luchese et al. (2023) compared the effects of basalt and lime on soybean growth in a pot experiment, and observed better growth of soybean at R2 stage with basalt application than lime. Our study confirmed the additional effect of basalt on soybean other than pH increase even at the later growth stage and suggested the involvement of the increase of soil exchangeable Mg.

3.4.3. Basalt weathering and cation release

In planted treatment, the calculated release of Mg from the basalt significantly increased with higher application rates of the basalt, while no significant increase of the calculated release of Ca, Na, and K was observed in the basalt application treatments compared with Control by Tukey post-hoc test (Figure 3-4). The increase of the calculated Mg release was probably due to the weathering of the basalt because it contained easily weatherable Mg-rich minerals such as pyroxene (Figure 3-4 (b) and Table 2-1). Mg release from basalt is also observed in previous studies, which indicates that basalt commonly releases Mg in the process of the weathering reaction (Kelland et al., 2020, Vienne et al., 2022, Luchese et al., 2023). On the other hand, the significant increase of the calculated release of Ca or Na was not observed, though the basalt contained bytownite and labradorite, which are easily weatherable and abundant with Ca and Na (Hermanská et al., 2023) (Figure 3-4 (a) and (c)). This result implied that these plagioclase minerals were harder to be weathered than pyroxene under the conditions of this study. In contrast, the release of Na was observed under the paddy field condition with almost the same soil and basalt, which may have proposed the importance of cultivation condition in the weathering of plagioclase minerals (Figures 2-1 (e) and 3-4 (c)). No significant higher K release was observed compared with Control possibly because the basalt used in this study contained little K (Figure 3-4 (d)).

In unplanted treatment, similar trend to planted treatment was observed in each element except for the calculated Na release (Figure 3-4 (c)). The decrease of calculated Na release with higher basalt application rate was likely to be attributed to the salt accumulation on the surface layer of the pot. When a silicate mineral in the basalt is weathered and releases divalent cations like Mg, Na adsorbing to cation exchange site gets easy to be compelled to liquid phase because of its relatively weak electrically binding (Gillman et al., 2001). This effect could have

transported Na to the surface layer by evaporation in this study. As we sampled soil excluding the 3 cm surface layer to avoid localized ion accumulation layer, this possibly resulted in the decrease of Na release with higher application rates of the basalt. On the other hand, this result was not observed in the planted treatment probably because enough cation exchange sites were available for released cations from the basalt as soybeans absorbed cations for their growth. Another possible reason for the absence of surface salt accumulation in planted treatment was that water may have moved toward the soybean roots rather than to the surface layer as the roots absorbed water.

When comparing the calculated release of Mg, the planted treatment showed the higher calculated release than the unplanted treatment by 3.3 times in BA5, 1.9 times in BA10, and 1.3 times in BA20 (Figure 3-4 (b)). These results indicated soybean enhanced the weathering of the basalt. Akter and Akagi (2005) also reported significant increase of element release from the basalt in hydroponic cultivation of soybean with the roots in contact with basalt. As soybean absorbs considerable amounts of cations including Ca and Mg, the removal of these cations from the soil solution may have promoted the dissolution of minerals in the basalt because of disturbance of equilibrium between soil solution and minerals in the basalt. In addition, leguminous plants acidify the rhizosphere in the process of nutrient absorption and nitrogen fixation, which also could lead to the dissolution of minerals (Epihov et al., 2021, Epihov et al., 2017, Haque et al., 2019). Moreover, there are several studies reporting the influence of symbiosis microbes including mycorrhizae on enhanced weathering of minerals (Burghelea et al., 2015, Verbruggen et al., 2021). However, we couldn't identify the main driving force of the weathering of the basalt in the planted treatment, and further research is required to determine the biogeochemical mechanisms of enhanced weathering by plants.

Chapter 4 – soybean cultivation in a field experiment

4.1. Summary

The impact of the basalt application on soybean was investigated at the field scale in Hokkaido University campus, which is located in a subarctic area. Five treatments were established: a conventional plot (Control), plots with 5, 10, and 20 wt% basalt application (BA5, BA10, and BA20, corresponding to 75, 150, and 300 t ha^{-1}, respectively), and a plot with 0.01 wt% lime application (Lime). The basalt was applied on May 19, and soybean was grown from June 1 to September 23 in 2023. The basalt application significantly increased soil pH and exchangeable Mg and Na concentration in the soil. Although there was no significant difference in the soybean yield among the treatments, the number of pods showed slight difference among the treatments ($p < 0.1$), and its average tended to increase by basalt application. There was a significant positive correlation between soil pH and the number of pods ($r = 0.52$, $p < 0.05$). In addition, shoot N concentration in soybean at flowering stage showed significant difference among Control, BA10, and Lime ($p < 0.05$), and it was higher in BA10. There was a significant positive correlation between shoot N concentration at R2 and both soil pH at R2 ($r = 0.69$, $p < 0.05$) and the number of pods at R8 ($r = 0.79$, $p < 0.05$), which indicated the increase of soil pH by the basalt application enhanced the N acquisition by soybean, resulting in the increase of the number of pods at harvest. XRPD analysis showed the higher Ca-plagioclase and pyroxene content in BA10 and BA20 than Control at R8 ($p < 0.001$). Moreover, the pyroxene content was lower in planted plot than unplanted plot at R8 ($p < 0.05$). These results suggested soybean growth enhanced the weathering of pyroxene in the basalt at the field scale.

4.2. Introduction

The effect of basalt application on crops at the field scale has been investigated in tropical area and temperate area (Beerling et al., 2024, Skov et al., 2024, Kantola et al., 2023, Larkin et al., 2022, Guo et al., 2023b). However, the effect of basalt application at the field scale has not yet been studied in subarctic areas. In general, climatic conditions such as temperature and precipitation influence the reactivity and weathering rate of silicate minerals, as well as the

effect of silicate mineral application on crop growth (Guo et al., 2023b, Guo et al., 2023a). In this study, I evaluated (i) the effects of basalt application on soybean growth and yield and (ii) the weathering of basalt and its potential enhancement by soybean cultivation in a subarctic field setting.

4.3. Materials and Methods

4.2.1. Basalt characteristics

The basalt used in this study was completely the same as the basalt used in Chapter 3. The detailed information is described in Chapter 2 and 3.

4.2.2. Experimental setup

A field experiment was conducted from May 19 to September 21, 2023 at the Experimental Farm of Field Science Center for Northern Biosphere, Hokkaido University, in Sapporo, Hokkaido, Japan (43°04′17.4″ N 141°20′24.6″ E). The soil type was classified as a Gray Lowland soil (Nakamura et al. 2024) in Comprehensive Soil Classification System of Japan First Approximation (Obara et al. 2011) (Haplic Fluvisol in World reference base for soil resources (IUSS Working Group WRB 2022)). The soil texture was sandy clay loam, with an initial pH(H_2O) of 5.55 and soil total carbon content of 27.4 g kg^{-1} soil. Experimental design in the field was a split-plot with three replicates. The main plots included five treatments, which were a conventional plot (Control), plots with 75, 150, 300 t ha^{-1} of basalt application (about 5, 10, 20 wt.% of the soil weight based on the bulk density of the 0–20 cm soil layer, hereafter BA5, BA10, BA20, respectively), and a plot with 1.5 t ha^{-1} of lime application (Lime). The application rate of lime was determined to make soil pH of Lime plot corresponding to the soil pH of BA10 based on the lime neutralization curve, measured in Chapter 3. The size of each plot had an area of 14.7 m2 (4.2 m × 3.5 m) with a 0.4 m of buffer zone between plots (Supplemental figure 4-1).

On May 19, the basalt powder and lime were evenly applied to BA5, BA10, BA20, and Lime plots and then thoroughly mixed with the 0–15 cm soil layer through tillage. On May 24, 17.8 g m^{-2} of monoammonium phosphate and 14.8 g m^{-2} of potassium sulfate (equivalent to 22 kg N ha^{-1}, 48 kg P ha^{-1}, 66 kg K ha^{-1}, based on the local fertilizer recommendations for soybean field

(Hokkaido Research Organization 2020)) were evenly applied to all plots and mixed through tillage again. On June 1, soybean seeds (*Glycine max* L. cv. Yukihomare) were sown in 7 rows with a row spacing of 0.60 m and an interhill spacing of 0.15 m by hand. The sowing rate per plant was four (44.4 seeds m^{-2}). An unplanted area of 4.2 m × 1.0 m was established in the southern part of each plot. Then, non-woven fabric was covered on the ground to prevent bird damage for the first two weeks. On June 22, soybean plants were thinned out to retain two plants; thus, plant density during the growing seasons was 22.2 plants m^{-2}. Weeds were removed by hand and pesticide was applied appropriately during cultivation. After harvesting grains, the aboveground residues were removed from the field.

4.2.3. Soil and plant sampling

Soybean sampling was conducted at three stages of development: R2, flowering stage (July 20); R6, seed development stage (August 14); and R8, full maturity stage (September 21). Samplings at R2 and R6 were conducted only in Control, BA10, and Lime treatments, while sampling at R8 was conducted in all treatments. Soybean plants were randomly sampled in one row at R2 and R6, and in two different rows at R8 per plot. The sampling area in each plot was 0.18 m^2 (0.60 m × 0.30 m; 4 plants) at R2, 0.27 m^2 (0.6 m× 0.45 m; 6 plants) at R6, and 0.90 m^2 (0.60 m × 0.75 m × 2; 20 plants) at R8. The soybean plants sampled at each stage were divided as follows: at R2 into leaves, stems, and roots; at R6 into leaves, stems, roots, pods, and grains; and at R8 into stems, roots, pods, and grains. The yield-related indices (i.e., yield, the number of pods per plant, 100-grain weight) were investigated at R8 before separation. Then, samples were dried in a forced-air oven at 80°C at least 72 h.

Soil sampling was conducted before planting (BP) (May 19) and at R2, R6, R8. Samplings at R2 and R6 were conducted only in Control, BA10, and Lime treatments as well as plant sampling, while sampling at BP and R8 was conducted in all treatments. Soil samples were collected from the surface layer (0–15 cm). At R2 and R6, soil samples in the planted plot were collected by shaking the roots in the air to separate the attached soil. At R8, soil was excavated with a shovel, focusing on the soybeans, to create a block measuring 25 cm in width, 15 cm in length, and 15 cm in depth. The soil was then mixed uniformly, and a portion was collected for sampling. For soil samples in unplanted plots, soil was collected with a soil probe. Soil samples were air-dried and sieved to < 2 mm before analysis.

4.2.4. Soil chemical analysis

For soil pH measurements, 0.8 g of soil was weighed into a 5 mL of plastic tube with 4 mL of deionized water (1:5 mass ratio of soil:water) and shaken for 1 h at room temperature (150 rpm; TS-10N, Taitec Co., Ltd, Aichi, Japan). The solution was stood still for 1 h before pH measurement to 0.01 pH units (Kamewada, 1997b). For soil exchangeable cations, 2.0 g of soil was mixed with 40 mL of 1.0 *M* of ammonium acetate (pH=7.0; 1:20 mass ratio of soil:solution), shaken for 1 h at room temperature, filtered with a filter paper (Advantec No. 6) (Kamewada, 1997a). The concentrations of Ca, Mg, K, and Na in the extracts were analyzed using Inductively Coupled Plasma Atomic Emissions Spectroscopy (ICP-AES: Avio 220 Max, PerkinElmer, Waltham, MA, USA).

4.2.5. Soybean growth and element concentration

Dry weight of each sample was recorded and samples were analyzed for element concentration according to the method as follows (Ishikawa et al., 2016). Dried samples were powdered using griding mill (Wonder Blender WB-1, Osaka Chemical Co., Ltd., Osaka, Japan). A 40 mg powdered sample was taken to a 65-mL polypropylene tube (DigiTUBE, SCP Sciences, Tokyo, Japan) with 2 mL of a 13 *M* HNO_3 solution (EL grade, Kanto Chemical Inc.) and cooled to room temperature. Then, 0.4 mL of hydrogen peroxide (H_2O_2; atomic-absorption grade, Kanto Chemical Inc.) was added to the solution, which was then heated at 105°C for 0.5 h. The digested solution was adjusted to 20 mL by 2% HNO_3 solution and filtered through a filter paper (Advantec No. 5C). Solution samples were analyzed for 15 elements (Ca, Mg, K, Na, P, S, Mn, Fe, Zn, Cu, Mo, Sr, Cd, Cr, Ni) for samples at R2 and R6 using ICP-AES, and for grain at R8 using Inductively Coupled Plasma Mass Spectrometry (ICP-MS: ELAN DRC-e, PerkinElmer, Waltham, MA, USA). To determine the N concentration, each 20 mg sample was digested with 1.25 mL of concentrated H_2SO_4 in a test tube at 200°C. At 15 min intervals, 0.5 mL of H_2O_2 was added to each tube for a total of six times, following which the N concentration in the digests was determined using the micro- Kjeldahl method (Obama et al., 2024). Shoot element concentrations were calculated by multiplying the dry weight and concentration of each part except for root, summing them up, and dividing by total dry weight of all parts except for root.

4.2.6. X-ray Powder Diffraction Analysis

The mineral content of the soil samples at BP and R8 was determined by following the procedure of Kurokawa et al. (2024). Briefly, 1.00 g of a soil sample was mixed with 0.25 g of corundum (α-Al2O3; Baikalox 3.0CR, Baikowski, France) in 7 mL of ethanol, which was then ground with an XRD-Mill (McCrone, Retsch, Germany) for 10 min. The mixture was dried at room temperature, ground into a homogeneous powder, and loaded onto the sample plate of an X-ray diffraction (XRD) instrument (MiniFlex600, Rigaku, Tokyo, Japan). The XRPD diffractogram was obtained at a scan range of 5°–65° (2θ) using Cu K-alpha radiation with a Ni filter and one-dimensional silicon strip detector (Rigaku D/teX Ultra 2) at a scan speed of 60 s/10° with a step of 0.01°. The diffractogram was modeled as the sum of scaled pure patterns including crystalline, paracrystalline, and amorphous phases (Kurokawa et al., 2024) using an automated full-pattern summation function in the powdR package (Butler & Hillier, 2020, 2021) version 1.3.0 for R (R Core Team, 2023). Then, a change in mineral (Δmineral) in the soil during cultivation was calculated by subtracting the mineral content at BP from the mineral content at R8. In addition, based on the change in pyroxene, one of easily weatherable minerals contained in the basalt, the ERW-induced CDR was estimated by assuming that the consumption of 1 mol of pyroxene ($CaMgSi_2O_6$) potentially sequesters 4 mol of CO_2 from the atmosphere as per Eq. 1-3.

4.2.7. Statistical analysis

Significant differences in soil pH, exchangeable cation concentration in soil, dry weight of plant, element concentration in plant and grain, and easily weatherable minerals were determined and compared among the treatments using split-plot ANOVA and Tukey post hoc tests. The Pearson's correlation coefficient (R) was used to examine the correlation among the yield-related indices, and between soil chemical properties and growth parameters of soybean. All statistical analysis were performed using the computing environment R (R Core Team, 2024).

4.4. Results

4.3.1. Soil chemical property

Soil chemical properties are shown in Table 4-1. Soil pH significantly differed among the treatments through cultivation period and was higher with basalt and lime application than Control. In addition, soil pH was lower in planted treatments than unplanted treatments at R6. Soil exchangeable Ca concentration significantly differed among the treatments at R2 and R6 and was higher with lime application. Soil exchangeable Mg concentration significantly differed among the treatments at R2, R6, and R8 and was higher with basalt application than Control and Lime. Soil exchangeable Na concentration was significantly higher with higher application rates of basalt through cultivation periods. Soil exchangeable K concentration significantly differed among the treatments at BP and was lower with higher application rates of basalt. At R6 and R8, soil exchangeable K concentration was lower in planted plots than unplanted plots.

4.3.2. Soybean growth response and yield-related indices

Stem length, shoot dry weight, and root dry weight at different growth stages are shown in Table 4-2. No significant differences were observed except for stem length at R8, which was significantly lower with higher application rates of basalt. Yield-related indices are shown in Table 4-3. The number of pods per plant showed slight difference among the treatments by split-plot ANOVA ($p < 0.1$), and tended to be higher with basalt application. No significant difference was observed in yield, 100-grain weight, or the number of grains per pod. The correlation matrix among the yield-related indices is shown in Figure 4-1. The yield had significant positive correlation with the number of pods per plant and the number of grains per pod. The 100-grain weight had a significant positive correlation with the number of grains and a significant negative correlation with the number of pods.

4.3.3. Element concentration in soybean

The concentration in soybean shoot and root at R2 are shown in Table 4-4 and

Supplemental table 4-2. The N, Mn, and Zn concentration in shoot significantly differed among the treatments by split-plot ANOVA. The N concentration tended to be higher in BA10, while the Mn and Zn concentration were lower in BA10 and Lime. In addition, the concentration of Zn, Mo, Sr, and Na in root were significantly different among the treatments, and the Mo, Sr, and Na concentration was higher in BA10 while the Zn concentration was lower in BA10. The other elements showed no significant differences among the treatments. The element concentrations in soybean shoot and root at R6 are shown in Table 4-5 and Supplemental table 4-3. The Mn and Ni concentration in shoot were significantly different among the treatments by split-plot ANOVA and lower in BA10 and Lime. Additionally, the Ca concentration in root significantly differed among the treatments by split-plot ANOVA and Na concentration in root was higher in BA10 by Tukey post-hoc analysis. No significant difference was observed in other elements. The element concentrations in grain at R8 are shown in Table 4-6. The concentration of Mn slightly differed among the treatments by split-plot ANOVA and tended to be lower with the application of the basalt and the lime. The concentration of Mo was significantly higher in BA20 than Control. The concentration of Ni was significantly lower with the application of the basalt and the lime. No significant difference was observed in the other elements.

4.3.4. Relationship of soil chemical properties with soybean growth and element concentration in grain

Relationships between soil pH and soybean growth responses are shown in Figure 4-2. Soil pH at R2 had significant positive correlation with the N concentration in shoot at R2. In addition, soil pH at R8 was positively correlated with the number of the pod at R8. Furthermore, the N concentration at R2 was positively correlated with the number of pods at R8. Relationships between soil pH and element concentration in grain at R8 are shown in Figure 4-3. Soil pH at R8 had significantly negative correlation with the Ni and Mn concentration in grain while it had significantly positive correlation with the Mn concentration.

4.3.5. Changes in easily weatherable mineral contents during cultivation

The changes in contents of Ca-plagioclase and pyroxene during cultivation period are shown in Table 4-7. Ca-plagioclase was higher with higher application rates of the basalt at BP and R8. No significant difference was observed in ΔCa-plagioclase. Significant difference among the treatments was not observed in pyroxene BP. However, pyroxene content at R8 significantly differed among the treatments by split-plot ANOVA and was higher with higher application rates of the basalt. In addition, it was significantly lower in planted plots than unplanted plots at R8. No significant difference was observed in ΔPyroxene.

4.5. Discussion

4.4.1. Positive effects of basalt application on soybean growth on field scale

The application of basalt influenced the soil chemical properties at the field scale. Soil pH and exchangeable Na concentration were higher with basalt application throughout the cultivation period (Table 4-1). Furthermore, exchangeable Mg concentration in the soil was higher with basalt application from the R2 to R8 growth stage. In contrast, lime application increased soil pH and soil exchangeable Ca concentration but had no significant effect on exchangeable Mg or Na concentrations. These results were generally consistent with those of the pot experiment, which demonstrated that basalt application not only raised soil pH but also supplied elements such as Mg and Na, distinguishing its effects from those of lime application.

The application of the basalt also had a positive impact on soybean N acquisition at R2 and pod formation. The shoot N concentration at R2 was significantly different among the treatments by split-plot ANOVA and was the highest in BA10 (Table 4-4). In addition, the number of pods per plant at R8 was slightly higher with the basalt application (Table 4-3). As soil pH at R2 and R8 had a significant positive correlation with shoot N concentration at R2 and pod number at R8, respectively, the basalt application could influence N acquisition and pod formation by increasing soil pH (Figure 4-2 (a), (b), and Supplemental figure 4-3). Moreover, shoot N concentration at R2 was significantly correlated with the number of pods at R8 in Control, BA10, and Lime treatment (Figure 4-2 (c)). These results suggest that the increase of pod number at R8 could derive from the enhanced N acquisition at R2 due to the soil pH increase. The optimal soil pH for nodulation is above 5.5 and an increase in soil pH increases the number of nodules (Thilakarathna and Raizada, 2017, Lin et al., 2012). Moreover, Tsubouchi and Saito (2010) observed the increase of acetylene reduction activity in soybean with higher soil pH. Therefore, the increase of soil pH by the basalt application may have promoted the nodulation of soybean and N acquisition at R2. In addition, Beerling et al. (2024) observed the increased N uptake and biological N_2 fixation of soybean by basalt application. They suggested the increase of soil pH enhanced Mo uptake, which in turn prompted nitrogen metabolism including nitrogen assimilation and transport of soybean. There was a possibility that the soybean in this study responded to the application of the basalt similarly, as the concentration of Mo in root at R2 and grain at R8 were significantly higher in the basalt applied

plots (Supplemental table 4-2 and Table 4-6). Regarding the number of pods, it is closely related to the yield and influenced by the net assimilation rate (NAR) around the flowering stage (Kohri et al., 1998, Saitoh et al., 1998). Thus, the increase of N concentration may have contributed to NAR, thereby increasing pod numbers in this study, as indicated by the positive correlation between shoot N concentration at R2 and pod number at R8. Although the yield itself did not significantly differ among the treatments, the basalt application could contribute to soybean yield indirectly since the number of pods was significantly correlated with the yield (Table 4-3 and Figure 4-1).

Compared with the results of the pot experiment, the increased N concentration due to the increase of soil pH was consistent both in the pot and the field experiment (Figure 3-2 (a) and 4-2 (a)). However, there was not a significant correlation between soil exchangeable Mg and shoot N concentration at R2 (Supplemental figure 4-4). Although the soil exchangeable Mg was considered to be the potential factor of enhanced N acquisition and the increased dry weight of soybean in the pot experiment (Figure 3-3 (a)), soybean in the field experiment did not respond to the increase of the soil exchangeable Mg by the basalt application. Since the volume of soil and amount of the nutrient in the soil are limited in the pot experiment, Mg supply from the basalt may have effectively promoted soybean growth.

Beerling et al. (2024) reported the soybean yield significantly increased by 16 % after 3 years of 50 t ha^{-1} of annual basalt application (cumulatively 150 t ha^{-1} of basalt application), while we observed 7.2 % increase in BA10 (150 t ha^{-1} of the basalt application) and 4.7 % increase in BA20 (300 t ha^{-1} of the basalt application). These results implied that relatively low positive impact of the basalt application was observed on soybean yield in this study. Although various factors must have been involved in this difference including basalt properties, climate condition, soil environment, etc., the duration of the experiment could be one of the reasons. In general, the longer the basalt is exposed to soil, the more it weathers and provides nutrients (Swoboda et al., 2022). Beerling et al. (2024) also reported the insignificant impact of basalt application on maize in the 1st and 2nd year but observed significant positive impact on maize in the 4th year. Therefore, the positive impact of the applied basalt can be strengthened over time and long-term monitoring for co-benefit is required.

4.4.2. Potentially adverse effects of basalt application

The application of the basalt negatively influenced the early growth of soybean. The dry weight at R2 tended to be lower in BA10 (Table 4-2, Supplemental figure 4-1). In addition, the stem length at R8 was significantly lower with higher basalt application rates (Table 4-2). The soybean cultivar used in this study has a determinate growth habit of stem growth, which usually terminates stem growth immediately after flowering (BERNARD, 1972). Therefore, these results indicated soybean growth at early stage was suppressed by the basalt application. As the particle size of the basalt powder used in this study was small (D90 < 75.6 μm), the hydraulic conductivity could be deteriorated, and wet stress could have occurred. Particularly, the precipitation which continued for 10 days after the seeding may have delayed the germination and seedling establishment of soybean in the basalt applied plots (Supplemental figure 4-2). The lower stem length in the basalt applied treatments was not observed in pot experiment, which could be because the pots were irrigated appropriately at early growth stage (Table 3-1). Although the yield in the basalt applied plots did not decrease in this study, it should be noted that the application of large amounts of fine rock powder can expose the crops to wet stress.

However, the application of the basalt did not increase heavy metal concentrations in soybean grain (Table 4-6). Rather, the Ni concentration in grain decreased by basalt application (Table 4-6). Since Ni concentration had a significant negative correlation with soil pH at R8, the increase of the soil pH by basalt application influenced Ni concentration in grain as well as the pot experiment (Figures 4-3 (a), 3-2 (d), and Supplemental figure 4-3). The decrease of Ni concentration in soybean grain was also observed in (Beerling et al., 2024). Although excessive accumulation of heavy metals in edible parts of crops is one of the concerns of ERW on agricultural land (Beerling et al., 2018), these results indicated the less possibility of elevated concentrations of heavy metals in crop and involvement of pH increase by the basalt application. However, the possibility of their accumulation in soil shouldn't be ignored (Dupla et al., 2023a) and their long-term behavior should be evaluated. In addition, the basalt application influenced the concentration of Mn and Mo in grain (Table 4-6). They were positively or negatively correlated with the soil pH, which were consistent with the results of the pot experiment (Figures 4-3 (b), (c) and 3-2 (b), (d)). Mn is an essential micronutrient, and its availability decrease with higher soil pH. Therefore, the reduction of availability of essential

micronutrients including Mn and Fe is a potential adverse effect in the field, in particular where soil pH is originally high.

4.4.3. Enhanced weathering and carbon accumulation in rhizosphere

Soybean growth enhanced the weathering of easily weatherable silicate mineral in the basalt. XRPD analysis showed that the pyroxene content in the soil significantly differed between planted and unplanted plots at R8 and was lower in planted plots than unplanted plots (Table 4-7). Although ΔPyroxene showed no significant differences by split-plot ANOVA, ΔPyroxene in planted plots decreased with higher application rates of the basalt, which suggested the weathering of pyroxene was enhanced in the rhizosphere of soybean. The enhancement of the basalt weathering in the rhizosphere of soybean was observed in hydroponic condition (Akter and Akagi, 2005, Akter and Akagi, 2010), and our results proved the weathering enhancement by soybean under soil condition as well as the results in Chapter 3 (Figure 3-4). The enhanced weathering of pyroxene in planted plot may have attributed to acidification in the rhizosphere as leguminous plants release H^+ following excess uptake of cations over anions during N_2 fixation (HAYNES, 1983). On the other hand, the Ca-plagioclase content didn't differ significantly between planted and unplanted plots at R8, neither did ΔCa-plagioclase, which indicated Ca-plagioclase was not weathered during cultivation (Table 4-7). The dissolution rate of Ca-plagioclase (Bytownite: $\log k_H = -5.85$ to -9.82, Laboradorite: $\log k_H = -7.87$ to -10.91) is mostly overlapped with pyroxene (Augite: $\log k_H = -6.82$ to -11.97) (Palandri and Kharaka, 2004). However, since soil exchangeable Mg concentration was about 10 times lower than the exchangeable Ca concentration (Table 4-1), the saturation state of Mg was lower than that of Ca, and pyroxene, a Mg-rich mineral, may have dissolved faster than Ca-plagioclase, a Ca-rich mineral. Also, the dissolution of pyroxene may have been promoted by Fe chelator including siderophore produced by microbes and plants (Epihov et al., 2024).

The CDR potential in planted plot was estimated solely from the decrease in pyroxene, and the mean value and standard error were 52.8±66.2 gC m^{-2} (1.9±2.4 t CO_2 ha^{-1}) in BA10 and 139±152 gC m^{-2} (5.1±5.6 t CO_2 ha^{-1}) in BA20. On the other hand, Kantola et al. (2023) estimated the CDR potential by 50 t ha^{-1} of annual basalt application to be 102 gC m^{-2} $year^{-1}$ (3.7 t CO_2 ha^{-1} $year^{-1}$) in their 4-year maize-soybean rotation system. Although the methods of

estimation of CDR potential are different between Kantola et al. (2023) and this study, these results implied the lower CDR potential in our results. This may be attributed to many factors including the shorter duration of this study as mentioned above. Furthermore, considering the growth of soybean in their study was almost doubled of our study (Beerling et al., 2024), it can be possible that the weathering enhancement by soybean worked much more than this study.

Chapter 5 - General discussion

5.1. The different effects of the basalt application on rice and soybean growth

I cultivated paddy rice in a pot and soybean both in a pot and in field and evaluated their responses to the application of the basalt. Interestingly, the basalt positively affected both of them but in a different way (Figures 5-1 and 5-2).

In a pot experiment for paddy rice cultivation, we observed the significant increase of soil available Si at harvest by the basalt application (Table 2-1). Moreover, it had a significantly positive correlation with total Si uptake and total dry weight of rice (Figure 2-1), indicating the basalt improved Si uptake by rice and growth by increasing soil available Si. Si plays an important role in reducing biotic and abiotic stresses (Ma, 2004). In particular, rice is a Si accumulator and there has been many studies reporting the beneficial effect of Si in rice production including improvement of the light-receiving attitude, and reducing salt stress and heat stress (Ma and Yamaji, 2008). The application of the basalt is considered to have a positive impact on paddy rice production by supplying Si. However, the uptake of Na was raised as a potential adverse effect. Although we didn't observe the decrease of rice dry weight or yield-related indices, the application of basalt significantly increased soil exchangeable Na as well as Na uptake by rice (Table 2-2). Since rice is susceptible to Na toxicity (Coca et al., 2023), high application rate of basalt could have a bad impact on rice production. However, it is likely that Na is leached out from a field immediately after the application of the basalt as Na is a monovalent cation and highly mobile in soil compared with other cations (Gillman et al., 2001). Therefore, it is needed to examine the positive or negative impact of the basalt application on paddy rice in field scale.

In a pot experiment of soybean cultivation, the basalt application significantly increased soil pH and soil exchangeable Ca, Mg, and Na as well as soybean dry weight (Figure3-1 and Table 3-1) . Correlation test across treatments including the basalt and the lime application showed a significant positive correlation between exchangeable Mg and dry weight, which indicated the basalt promoted soybean growth by increasing soil exchangeable Mg (Figure 3-5(a)). These results were reasonable as Mg enhances N acquisition of soybean by enhancing the nodulation and expression of nitrate transporter (Peng et al., 2018, Peng et al.,

2020). In a field experiment, the basalt application significantly increased soil pH and soil exchangeable Mg and Na concentration (Table 4-1). Among the yield-related indices, the number of pods tended to increase by the application of the basalt and it had a significantly positive correlation with soil pH (Table 4-3 and Figure 4-2(c)). Moreover, shoot N concentration at R2 was higher in the basalt applied plot and it had a significant positive correlation with soil pH at R2 and the number of pods at R8 (Figure 4-2(a) and 4-3). These result suggested the basalt application positively affected the shoot N concentration at R2 and pods number at R8 by increasing soil pH. Tsubouchi and Saito (2010) reported the increase of soil pH increased soybean yield by enhancing nitrogen fixation capacity. Therefore, these results showed a positive impact of the basalt application on N acquisition, soybean growth and yield by increasing soil pH and soil exchangeable Mg concentration. However, we observed the significant lower stem length in the basalt application treatments in the field experiment (Table 4-2). The high application rate of the fine basalt powder probably lowered hydraulic conductivity, possibly resulting in wet stress on soybean growth at early growth stage. Although the yield didn't significantly decrease by the application of the basalt, this potential adverse effect should be evaluated particularly in high precipitation areas.

5.2. The difference of the basalt weathering rate between paddy rice pot and soybean pot

The calculated release rate of cations in both rice and soybean experiments were compared based on the application rates of the basalt (t ha^{-1}) (Figure 5-3). The data of the previous study by (Kelland et al., 2020) was also shown as a reference.

The Ca release rate did not differ among the application rates in all studies (Figure 5-3(a)) because of large standard errors. Kelland et al. (2020) also reported a large standard error (3.6 ± 2.8 $cmol_c$ m^{-2} day^{-1}), which was removed from the figure. If pyroxene in the basalt was weathered as the result shown in the field experiment (Table 4-6), the release rate of Ca should have increased with higher application rates of basalt as well as Mg. However, the pattern of Ca release rate was not consistent with that of Mg release rate (Figure 5-3(b)). Since the soil used in this study contained high exchangeable Ca, released Ca may have reprecipitated as secondary mineral which cannot be extracted with 1.0 *M* ammonium acetate solution. It is necessary to

investigate Ca release rate using different soils in the future.

A clear difference was observed in Mg release rate (Figure 5-3(b)). The release rate of Mg increased with the higher application rates of basalt in all studies, and the highest release rate at 100 t ha^{-1} was observed in paddy rice followed by sorghum, soybean and unplanted treatment. These results proposed the high potential of mineral weathering in paddy rice cultivation system. In paddy field conditions, abundant water may have enhanced the weathering of silicate minerals because a high soil water content lowers ion saturation state in soil solution and leads to mineral dissolution (Cipolla et al., 2021b). Moreover, since rice absorbed considerable amount of Si, the equilibrium between minerals and soil solution can have been altered, resulting in dissolution of minerals (Kusa et al., 2021) (Table 2-8).

Interestingly, a clear increase of Na release rate was observed in paddy rice whereas almost no release was observed in sorghum and soybean (Figure 5-3(c)). The unplanted plot showed negative value possibly because of the salt accumulation at the surface layer, which was mentioned in Chapter 3. Na was probably derived from the weathering of plagioclase, and this result may have indicated that paddy field condition could be more advantageous than upland field in enhancing plagioclase weathering.

The release rate of K was quite low compared with other cation elements (Figure 5-3(d)). The low release rate possibly reflected the low K content of the basalt used in this study and indicated the low potential of K supply from the basalt (Table 2-1). The potential for K supply has been suggested to vary with the mineral composition of basalt, highlighting the need to consider mineralogical differences when aiming to utilize basalt as a K supplier (Lewis et al., 2021).

Overall, the results in these experiments suggested that paddy rice had a larger potential than upland field in the weathering of the basalt. However, it remains unclear if weathering enhancement in paddy field is attributed to the submerged condition of the soil or Si uptake by rice, and further research is required to evaluate the contributions of each factor in order to estimate the accurate prediction of the mineral weathering potential in paddy rice condition.

5.3. Conclusion

I cultivated paddy rice in a pot and soybean both in a pot and in field and evaluated their responses to the application of the basalt. In the paddy rice cropping system, the application of the basalt provided Si to the soil and the paddy rice, which enhanced paddy rice growth. the application of the basalt also increased exchangeable Na in the soil and Na concentration in the paddy rice, but there were no decrease in dry weight or yield-related indices of paddy rice, which indicated little possibility for the basalt to affect paddy rice growth negatively. In the soybean cropping system, the increase of soil pH enhanced soybean N acquisition. In addition, the increased exchangeable Mg concentration could have positively affected soybean growth. Moreover, the excessive accumulation of heavy metals was not observed either in paddy rice nor soybean, suggesting the risk of heavy metal pollution by the basalt application was low. Rather, the Ni concentration in soybean was lowered due to the increased soil pH by the basalt application. The results of the pot and field experiments showed that soybean enhanced the weathering of the basalt, particularly the pyroxene in it, which suggested the possibility of the enhanced carbon sequestration by plant root in ERW strategy on agricultural land.

Figures and Tables

List of Figures and Tables

Chapter 1

Chapter 2

Chapter 3

Chapter 4

Chapter 5

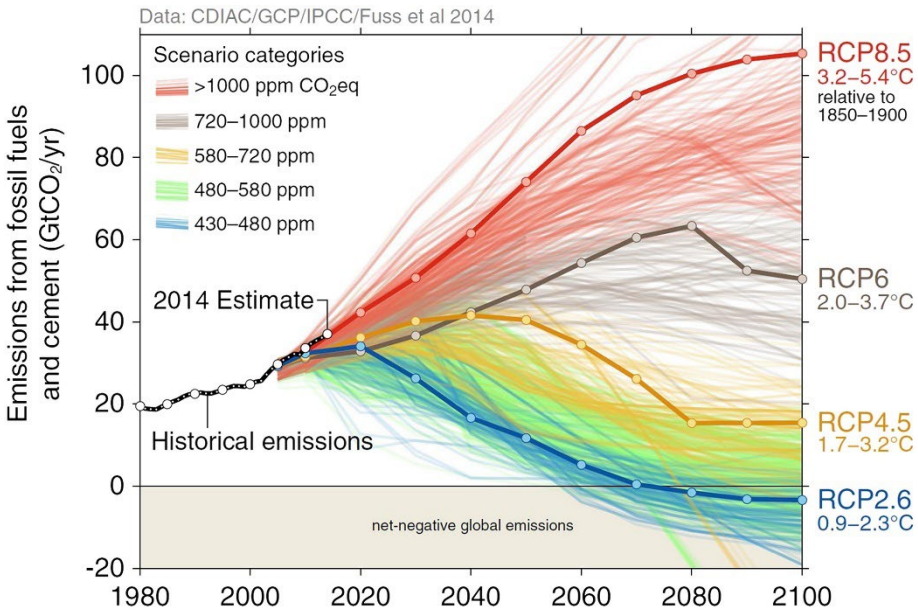

Figure 1-1. Different RCP scenarios and prediction of yearly carbon dioxide emissions. (Renforth and Henderson 2017)

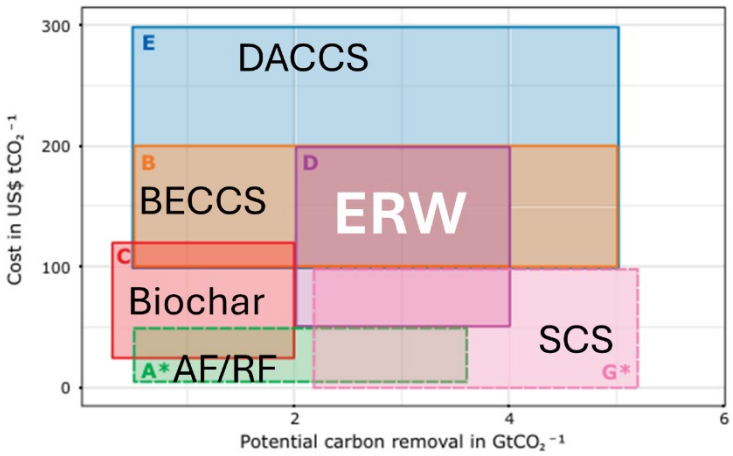

Figure 1-2. 2050 potentials and costs of various land-based CDR technologies. “AF/RF” indicates afforestation/reforestation, “SCS” indicates soil carbon sequestration, “ERW” indicates enhanced rock weathering, “BECCS” indicates bioenergy with carbon capture and storage, “DACCS” indicates direct air carbon capture and storage. (Minx et al. 2018 with modifications)

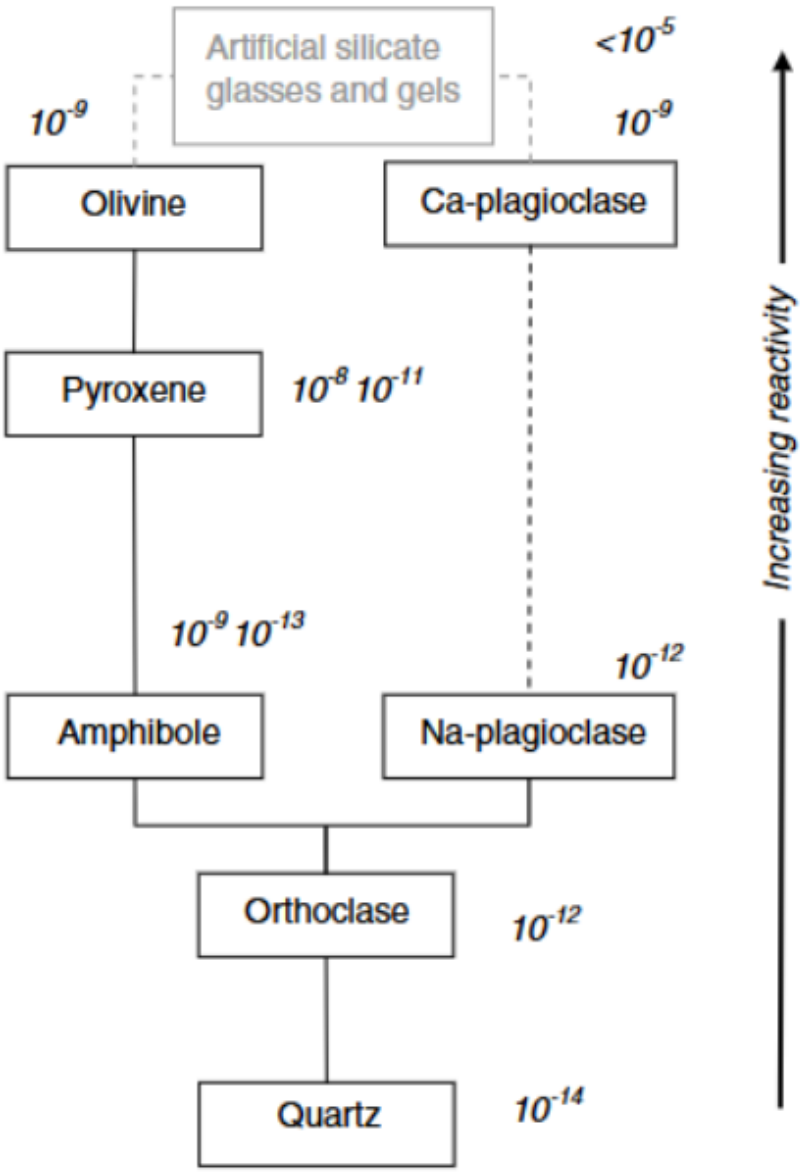

Figure 1-3. Representative dissolution rate of different silicate minerals. (Hartmann et al., 2013)

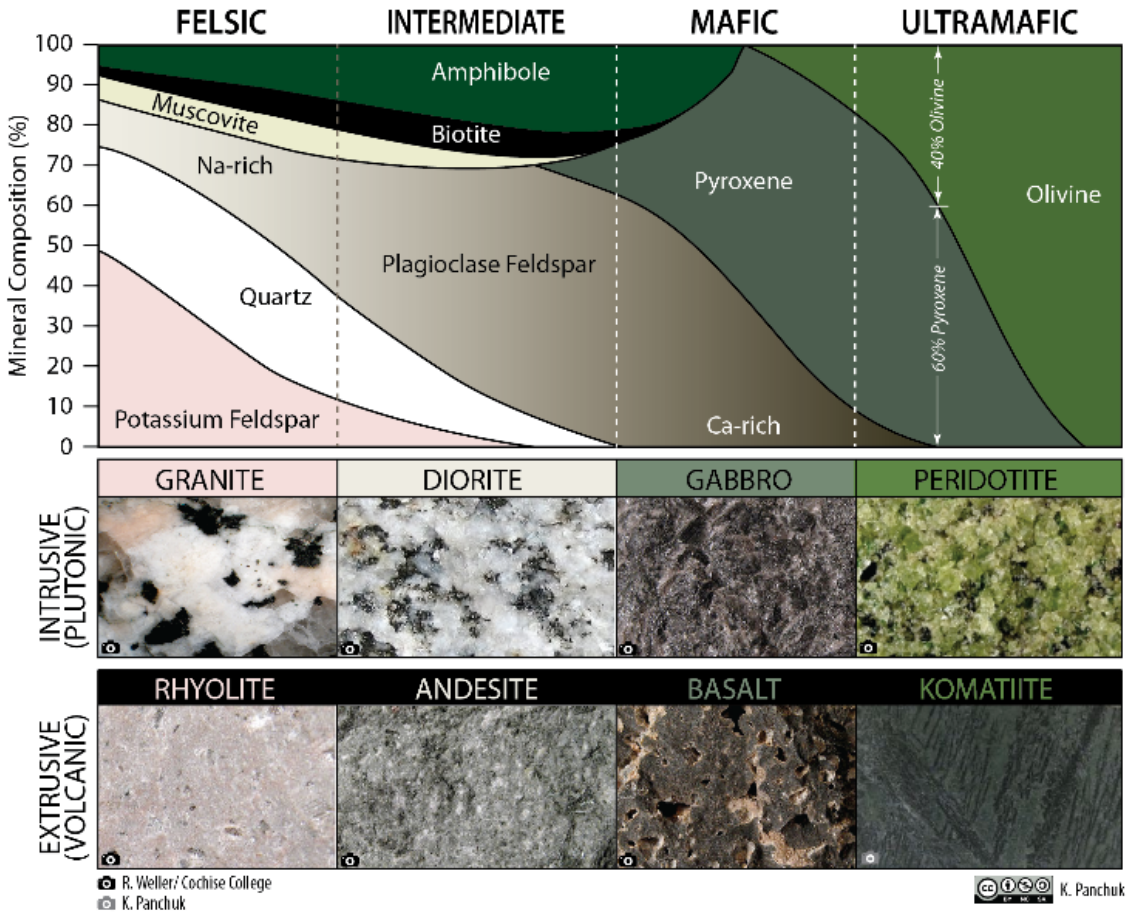

Figure 1-4. Igneous rock classification based on mineral composition. (Karla Panchuk (2018) CC BY-NC-SA 4.0, modified after Steven Earle (2015) CC BY 4.0 view source and others, with photos by R. Weller/Cochise College)

Table 1-1. Recent studies related to ERW on agricultural land.

Rock type	**Application rate (t/ha)**	**plant**	**Trial type**	**CDR (t CO_2/ha)**	**Crop growth promotion**	**Source**
Olivine	204	Ryegrass	Pot	2.7	Biomass increase	(Ten Berge et al. 2012)
Dunnite	220	Wheat and barley	Pot	0.049	-	(Amann et al. 2020)
Wollastonite	221	Maize and bean	Pot	39	Biomass increase	(Haque et al. 2019)
Wollastonite	300	Alfalfa and soybean	Rooftop field	9.6	Biomass increase	(Haque et al. 2020)
Wollastonite	5	Paddy rice	Field	1.2	Yield increase	(Wang et al. 2024)
Basalt	100	Sorghum	Pot	2.4-3.0	Yield increase	(Kelland et al. 2020)
Basalt	50	Potato	Pot	0.77	No difference	(Vienne et al. 2022)
Basalt	160	Maize and soybean	field	3.7	Biomass increase	(Kantola et al. 2023), (Beerling et al., 2024)
Basalt	18.9	Spring oat	field	-	Yield increase	(Skov et al. 2024)

Table 2-1. Characteristics of the basalt powder used in this study.

Chemical properties	
pH(H_2O)	9.68
TC (g kg^{-1} soil)	0.333
Particle size distribution (μm)	
D10	21.6
D50	120
D90	370
Mineralogical composition (wt.%)	
Bytownite	36.6
Labradorite	25.7
Pyroxene	10.2
Magnetite	6.77
Smectite	5.64
Cristobalite	4.45
Quartz	4.10
Olivine	4.27
Oligoclase	2.25

"TC" means total carbon. D10, 50, 90 means 10 %, 50 %, 90 % of particles was smaller than the given diameter, respectively.

Table 2-2. Total elemental composition of basalt used in experiment, derived from energy-dispersive X-ray fluorescence spectroscopy runs.

Oxide	Content (wt.%)	Element	Content (mg kg^{-1})
SiO_2	58 ± 0	As	0.21 ± 0.00
Al_2O_3	13 ± 0	Ba	166 ± 8
Fe_2O_3	9.9 ± 0.0	Cd	0.43 ± 0.40
CaO	7.8 ± 0.0	Cl	75 ± 3
MgO	4.7 ± 0.0	Co	1.0 ± 0.0
Na_2O	3.8 ± 0.1	Cr	29 ± 0
K_2O	0.34 ± 0.00	Cu	28 ± 1
P_2O_5	0.22 ± 0.00	Hg	0.94 ± 1.27
TiO_2	0.81 ± 0.00	Mo	0.21 ± 0.00
MnO	0.15 ± 0.00	Ni	8.3 ± 0.9
SO_3	0.00 ± 0.00	Pb	10 ± 0
		Rb	13 ± 0
		Sn	1.8 ± 0.3
		Sr	206 ± 2
		V	249 ± 2
		Zn	66 ± 1

Mean values ± one standard division are shown (n=3).

Table 2-3. Element concentrations of basalt and soil by two extraction methods.

Element	1.0 *M* ammonium acetate (mg kg^{-1})			2 % citric acid (mg kg^{-1})		
	basalt	soil		basalt	soil	
Si	82.3 ± 10.4	30.0 ± 5.2	*	565 ± 25	169 ± 11	**
Ca	5033 ± 26	4600 ± 44	**	4185 ± 50	4014 ± 264	
Mg	385 ± 2	512 ± 6	**	946 ± 16	545 ± 30	**
K	90.2 ± 1.6	592 ± 27	***	87.6 ± 0.7	506 ± 4	***
Na	1575 ± 13	45.5 ± 7.9	***	1611 ± 16	50.6 ± 5.7	***

Mean values ± one standard error are shown (n=3). Welch's t-test was performed to detect the significant differences of element concentrations in each extract between the basalt and the soil of B0 before planting. Asterisks (*, **, ***) denote $p < 0.05$, 0.01, 0.001, respectively.

Table 2-4. Soil chemical properties before planting and after harvest.

	Treatment	pH(H_2O)			Total amount of elements in soil (g pot^{-1})																			
					Total carbon				Available Si				Exchangeable Ca				Exchangeable Mg				Exchangeable K				Exchangeable Na			
before planting	B0	6.08	±	0.02	b	219	±	1	a	0.45	±	0.01	ab	36.80	±	0.35	ab	4.10	±	0.05	a	4.74	±	0.22	a	0.36	±	0.06	bc
	B5	6.11	±	0.03	b	225	±	2	a	0.43	±	0.01	b	36.28	±	0.63	b	4.19	±	0.05	a	4.56	±	0.20	a	0.33	±	0.02	c
	B10	6.12	±	0.03	b	223	±	3	a	0.43	±	0.01	b	37.11	±	0.38	ab	4.16	±	0.02	a	4.59	±	0.07	a	0.43	±	0.08	bc
	B20	6.11	±	0.00	b	223	±	3	a	0.44	±	0.01	b	36.71	±	0.77	b	4.15	±	0.07	a	5.31	±	0.64	a	0.45	±	0.05	bc
	B50	6.21	±	0.01	a	230	±	2	a	0.48	±	0.01	ab	37.06	±	0.38	ab	4.17	±	0.05	a	4.94	±	0.47	a	0.58	±	0.02	b
	B100	6.26	±	0.01	a	220	±	2	a	0.50	±	0.01	a	38.96	±	0.36	a	4.32	±	0.05	a	4.79	±	0.19	a	0.94	±	0.05	a
	ANOVA	***			**n.s.**				**				*				**n.s.**				**n.s.**				***			
after harvest	B0	6.52	±	0.11	a	226	±	1	a	0.39	±	0.01	c	43.59	±	0.40	a	6.30	±	0.05	c	2.02	±	0.11	a	1.71	±	0.11	b
	B5	6.54	±	0.11	a	225	±	6	a	0.37	±	0.01	c	43.81	±	1.22	a	6.60	±	0.23	bc	1.97	±	0.11	a	2.03	±	0.17	b
	B10	6.66	±	0.09	a	218	±	5	a	0.41	±	0.01	bc	44.31	±	0.90	a	6.76	±	0.12	abc	2.10	±	0.08	a	1.76	±	0.11	b
	B20	6.60	±	0.09	a	227	±	3	a	0.41	±	0.01	bc	43.93	±	0.32	a	6.58	±	0.08	bc	1.99	±	0.06	a	2.01	±	0.08	b
	B50	6.67	±	0.08	a	222	±	2	a	0.43	±	0.01	ab	44.40	±	0.38	a	6.94	±	0.11	ab	2.09	±	0.09	a	2.23	±	0.11	ab
	B100	6.64	±	0.20	a	230	±	3	a	0.47	±	0.01	a	46.06	±	1.18	a	7.30	±	0.13	a	1.94	±	0.14	a	2.74	±	0.12	a
	ANOVA	**n.s.**			**n.s.**				***				**n.s.**				**				**n.s.**				***			

Mean values ± one standard error are shown. Sample size before planting was three, while after harvest was four. “ANOVA” shows the results of one-way ANOVA, which was performed for detecting the significant differences among the treatments. Asterisks (*,**,***) denote $p < 0.05$, 0.01, 0.001, respectively. “n.s.” denotes not significant ($p > 0.05$). Different letters indicate significant differences among the treatments determined via

Tukey post hoc test. Each pot contained 8 kg of soil and basalt was additionally applied depending on the treatment of application rate.

Table 2-5. Dry weight of each part of rice at harvest.

Treatment	Dry weight (g plant^{-1})					
	root	stem	leaf	husk	grain	total
B0	4.43 ± 0.29 a	47.0 ± 1.8 a	15.0 ± 0.1 a	21.3 ± 0.3 a	80.5 ± 1.8 a	168 ± 3.6 a
B5	4.87 ± 0.77 a	48.0 ± 2.3 a	15.7 ± 1.1 a	20.0 ± 0.6 a	74.1 ± 2.7 a	163 ± 7.1 a
B10	4.94 ± 0.42 a	51.3 ± 0.9 a	15.8 ± 0.9 a	22.1 ± 0.9 a	81.3 ± 3.2 a	175 ± 4.4 a
B20	5.90 ± 0.82 a	52.0 ± 2.7 a	14.7 ± 0.4 a	21.1 ± 0.1 a	76.8 ± 2.6 a	170 ± 5.5 a
B50	6.23 ± 0.62 a	52.3 ± 1.1 a	16.2 ± 0.7 a	21.2 ± 0.4 a	77.6 ± 1.0 a	174 ± 1.8 a
B100	5.64 ± 0.31 a	51.5 ± 1.5 a	17.4 ± 0.8 a	22.2 ± 0.5 a	80.7 ± 1.8 a	177 ± 4.3 a
ANOVA	**n.s.**	**n.s.**	**n.s.**	**n.s.**	**n.s.**	**n.s.**

Mean values ± one standard error are shown (n=4). “ANOVA” shows the results of one-way ANOVA, which was performed for detecting the significant differences among the treatments. “n.s.” denotes not significant ($p > 0.05$). No significant difference among the treatments was determined via Tukey post hoc test.

Table 2-6. Element concentration in rice shoot.

Treatment	Element concentration in shoot (mg g^{-1} plant)																					
	N		P		K		Ca		Mg		S		Fe		Mn		Si		Na			
B0	5.38 ± 0.15	a	1.28 ± 0.02	a	14.6 ± 0.5	ab	1.50 ± 0.02	a	2.40 ± 0.03	a	0.746 ± 0.036	a	0.116 ± 0.005	a	0.573 ± 0.067	a	22.0 ± 0.6	a	0.725 ± 0.080	b
B5	5.07 ± 0.29	a	1.26 ± 0.02	a	15.3 ± 0.4	a	1.48 ± 0.04	a	2.32 ± 0.04	a	0.764 ± 0.054	a	0.138 ± 0.011	a	0.683 ± 0.115	a	22.4 ± 0.6	a	0.644 ± 0.031	b
B10	5.01 ± 0.18	a	1.24 ± 0.03	a	14.2 ± 0.1	ab	1.46 ± 0.12	a	2.35 ± 0.03	a	0.661 ± 0.059	a	0.136 ± 0.009	a	0.553 ± 0.042	a	21.9 ± 0.6	a	0.724 ± 0.037	b
B20	5.02 ± 0.18	a	1.27 ± 0.03	a	14.6 ± 0.3	ab	1.55 ± 0.09	a	2.26 ± 0.09	a	0.767 ± 0.062	a	0.138 ± 0.007	a	0.585 ± 0.034	a	21.9 ± 1.0	a	0.766 ± 0.018	b
B50	4.98 ± 0.20	a	1.28 ± 0.02	a	14.0 ± 0.2	b	1.37 ± 0.04	a	2.25 ± 0.06	a	0.757 ± 0.037	a	0.121 ± 0.003	a	0.546 ± 0.050	a	23.0 ± 0.4	a	0.851 ± 0.092	ab
B100	4.66 ± 0.19	a	1.29 ± 0.02	a	14.3 ± 0.1	ab	1.39 ± 0.05	a	2.28 ± 0.06	a	0.771 ± 0.019	a	0.122 ± 0.008	a	0.542 ± 0.069	a	23.0 ± 0.3	a	1.111 ± 0.074	a
ANOVA	**n.s.**		**n.s.**		**n.s.**		**n.s.**		**n.s.**		**n.s.**		**n.s.**		**n.s.**		**n.s.**		**	

Treatment	Element concentration in shoot (μg g^{-1} plant)															
	Zn		Cu		Mo		Ni		Sr		Cd		Cr		As	
B0	28.7 ± 0.2	a	3.81 ± 0.19	a	0.640 ± 0.027	a	1.54 ± 0.10	a	2.82 ± 0.04	a	0.0291 ± 0.0058	a	5.31 ± 0.39	a	6.35 ± 0.22	a
B5	29.5 ± 0.5	a	4.23 ± 0.45	a	0.623 ± 0.037	a	1.98 ± 0.32	a	2.76 ± 0.08	a	0.0419 ± 0.0132	a	8.79 ± 1.67	a	6.31 ± 1.00	a
B10	26.7 ± 0.8	a	3.81 ± 0.04	a	0.595 ± 0.025	a	1.97 ± 0.11	a	2.80 ± 0.18	a	0.0289 ± 0.0038	a	8.06 ± 0.78	a	7.37 ± 0.38	a
B20	30.0 ± 1.7	a	3.92 ± 0.19	a	0.587 ± 0.020	a	1.87 ± 0.11	a	3.07 ± 0.18	a	0.0340 ± 0.0049	a	7.94 ± 0.33	a	6.91 ± 0.10	a
B50	27.2 ± 0.8	a	3.46 ± 0.11	a	0.583 ± 0.021	a	1.65 ± 0.06	a	2.64 ± 0.05	a	0.0297 ± 0.0055	a	7.19 ± 0.38	a	6.95 ± 0.71	a
B100	29.4 ± 1.4	a	3.67 ± 0.32	a	0.567 ± 0.016	a	1.52 ± 0.07	a	2.77 ± 0.12	a	0.0351 ± 0.0110	a	6.63 ± 0.13	a	6.70 ± 0.56	a
ANOVA	**n.s.**		**n.s.**		**n.s.**		**n.s.**		**n.s.**		**n.s.**		**n.s.**		**n.s.**	

Mean values ± one standard error are shown (n=4). “ANOVA” shows the results of one-way ANOVA, which was performed for detecting the significant differences among the treatments. Asterisks (**) denote $p < 0.01$. “n.s.” denotes not significant ($p > 0.05$). Different letters indicate significant differences among the treatments determined via Tukey post hoc test.

Table 2-7. Element concentration in rice root.

Treatment	Element concentration in root (mg g^{-1} plant)									
	N	P	K	Ca	Mg	S	Fe	Mn	Si	Na
B0	not measured	3.87 ± 0.17 a	8.47 ± 0.41 a	2.62 ± 0.16 a	2.12 ± 0.13 a	2.91 ± 0.15 a	73.7 ± 3.0 a	1.49 ± 0.10 a	1.39 ± 0.11 a	1.47 ± 0.06 a
B5		3.62 ± 0.72 a	7.80 ± 0.53 a	3.09 ± 0.55 a	2.11 ± 0.07 a	3.01 ± 0.26 a	64.5 ± 11.1 a	1.34 ± 0.13 a	1.27 ± 0.11 a	1.63 ± 0.11 a
B10		2.52 ± 0.26 a	8.07 ± 0.44 a	2.95 ± 0.80 a	1.86 ± 0.06 a	2.96 ± 0.14 a	49.0 ± 4.9 a	1.20 ± 0.12 a	1.18 ± 0.11 a	1.71 ± 0.22 a
B20		3.01 ± 0.33 a	8.53 ± 1.04 a	3.65 ± 0.77 a	2.13 ± 0.12 a	3.09 ± 0.19 a	56.2 ± 5.5 a	1.41 ± 0.17 a	1.48 ± 0.16 a	1.87 ± 0.25 a
B50		2.87 ± 0.25 a	8.76 ± 0.73 a	2.68 ± 0.76 a	2.06 ± 0.10 a	2.58 ± 0.09 a	47.7 ± 4.9 a	1.16 ± 0.15 a	1.42 ± 0.17 a	1.81 ± 0.25 a
B100		3.34 ± 0.27 a	8.33 ± 0.27 a	2.32 ± 0.27 a	2.08 ± 0.09 a	2.76 ± 0.10 a	52.5 ± 2.8 a	1.35 ± 0.11 a	1.38 ± 0.08 a	1.69 ± 0.11 a
ANOVA		**n.s.**	**n.s.**	**n.s.**	**n.s.**	**n.s.**	*****	**n.s.**	**n.s.**	**n.s.**

Treatment	Element concentration in root (μg g^{-1} plant)							
	Zn	Cu	Mo	Ni	Sr	Cd	Cr	As
B0	93.4 ± 6.7 a	45.5 ± 7.4 a	4.99 ± 0.10 a	640 ± 17 a	45.8 ± 1.6 a	0.668 ± 0.194 a	84.5 ± 19.2 a	497 ± 27 a
B5	95.7 ± 8.1 a	40.1 ± 2.8 a	4.55 ± 0.62 a	564 ± 87 a	41.7 ± 3.1 a	0.634 ± 0.117 a	67.0 ± 1.7 a	448 ± 57 a
B10	79.6 ± 2.0 a	53.3 ± 12.3 a	3.77 ± 0.39 a	461 ± 36 a	42.5 ± 3.1 a	0.391 ± 0.021 a	120.3 ± 31.7 a	349 ± 37 a
B20	86.7 ± 2.6 a	48.2 ± 8.1 a	4.54 ± 0.52 a	529 ± 24 a	46.6 ± 6.1 a	0.706 ± 0.146 a	117.7 ± 56.8 a	403 ± 34 a
B50	88.6 ± 2.5 a	58.4 ± 10.5 a	4.23 ± 0.38 a	466 ± 48 a	45.5 ± 4.2 a	0.983 ± 0.468 a	105.5 ± 22.6 a	368 ± 34 a
B100	94.0 ± 5.1 a	66.5 ± 5.4 a	4.82 ± 0.32 a	548 ± 35 a	45.0 ± 1.3 a	0.551 ± 0.089 a	77.0 ± 13.7 a	444 ± 33 a
ANOVA	**n.s.**	**n.s.**	**n.s.**	**n.s.**	**n.s.**	**n.s.**	**n.s.**	**n.s.**

Mean values ± one standard error are shown (n=4). “ANOVA” shows the results of one-way ANOVA, which was performed for detecting the significant differences among the treatments. Asterisks (*) denote $p < 0.05$. “n.s.” denotes not significant ($p > 0.05$). Different letters indicate significant differences among the treatments determined via Tukey post hoc test.

Table 2-8. Total uptake of elements in rice.

Treatment	Total uptake of elements in rice (mg plant^{-1})											
	Si		Ca		Mg		K		Na			
B0	3603 ± 62	ab	284 ± 5	a	402 ± 7	a	2412 ± 106	a	126 ± 15	b		
B5	3539 ± 147	b	273 ± 18	a	376 ± 10	a	2430 ± 69	a	110 ± 10	b		
B10	3736 ± 50	ab	288 ± 16	a	410 ± 7	a	2437 ± 53	a	132 ± 7	b		
B20	3615 ± 163	ab	293 ± 20	a	390 ± 8	a	2447 ± 68	a	138 ± 4	b		
B50	3859 ± 45	ab	285 ± 17	a	388 ± 8	a	2349 ± 44	a	154 ± 17	ab		
B100	3959 ± 60	a	285 ± 9	a	402 ± 6	a	2468 ± 68	a	201 ± 17	a		
ANOVA	*****		**n.s.**		**n.s.**		**n.s.**		******			

Mean values ± one standard error are shown (n=4). “ANOVA” shows the results of one-way ANOVA, which was performed for detecting the significant differences among the treatments. Asterisks (*,**) denote $p < 0.05$, 0.01, respectively. “n.s.” denotes not significant ($p > 0.05$). Different letters indicate significant differences among the treatments determined via Tukey post hoc test.

Table 2-9. Concentrations of As and heavy metals in grain of rice.

Treatment	Element concentration in grain (μg g^{-1} grain)											
	As		Cd		Cu		Cr		Ni			
B0	0.646 ± 0.017	a	0.0066 ± 0.0005	a	4.75 ± 0.04	a	1.88 ± 0.14	a	0.159 ± 0.013	a		
B5	0.654 ± 0.071	a	0.0100 ± 0.0021	a	5.40 ± 0.32	a	2.19 ± 0.27	a	0.177 ± 0.018	a		
B10	0.723 ± 0.045	a	0.0075 ± 0.0008	a	4.93 ± 0.10	a	1.85 ± 0.10	a	0.224 ± 0.037	a		
B20	0.691 ± 0.035	a	0.0080 ± 0.0008	a	4.67 ± 0.09	a	1.84 ± 0.11	a	0.138 ± 0.012	a		
B50	0.743 ± 0.061	a	0.0078 ± 0.0008	a	4.75 ± 0.46	a	2.66 ± 0.10	a	0.200 ± 0.036	a		
B100	0.746 ± 0.033	a	0.0079 ± 0.0018	a	4.97 ± 0.24	a	2.08 ± 0.29	a	0.142 ± 0.014	a		
ANOVA	**n.s.**		**n.s.**		**n.s.**		**n.s.**		**n.s.**			

Mean values ± one standard error are shown (n=4). “ANOVA” shows the results of one-way ANOVA, which was performed for detecting the significant differences among the treatments. “n.s.” denotes not significant ($p > 0.05$). No significant difference among the treatments was determined via Tukey post hoc test.

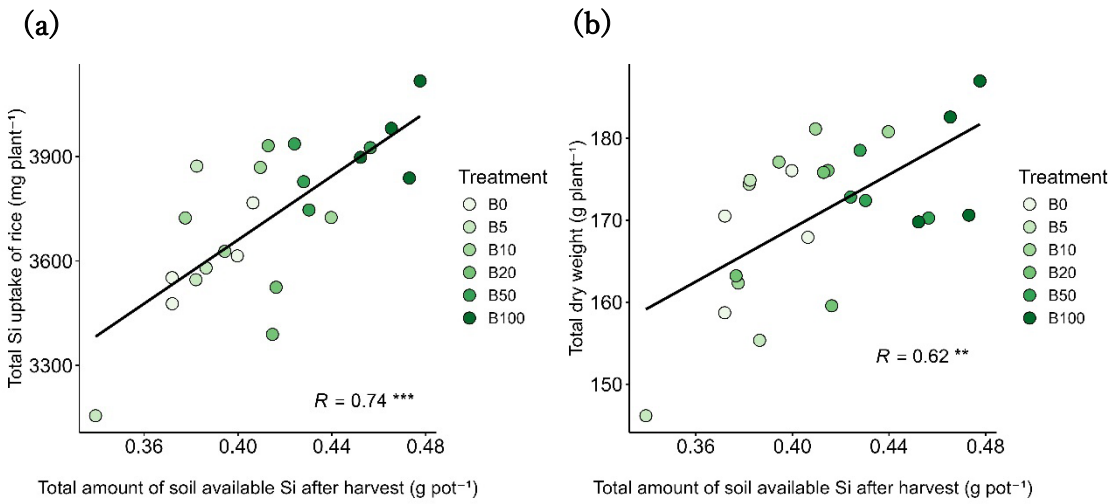

Figure 2-1. Relationship between total amount of soil available Si after harvest and total Si uptake of rice **(a)** and shoot dry weight **(b)**. **(a)** Points represents values of each sample. Linear regression analysis was performed. *R* denotes the Pearson product moment correlation coefficient. Asterisks (***) denotes $p < 0.001$. **(b)** Points represents values of each sample. Linear regression analysis was performed. *R* denotes the Pearson product moment correlation coefficient. Asterisks (**) denotes $p < 0.01$.

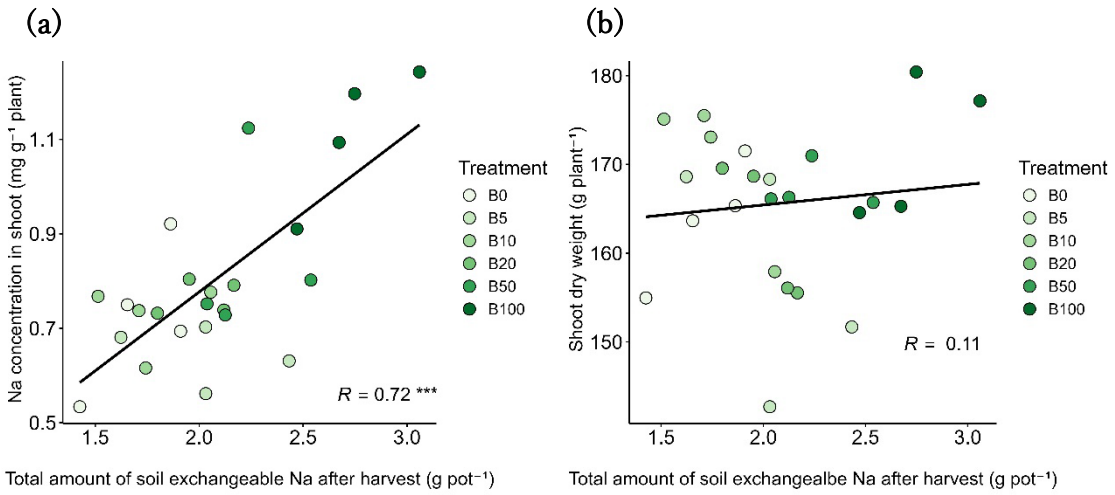

Figure 2-2. Relationship between total amount of soil exchangeable Na after harvest and Na concentration in shoot **(a)** and shoot dry weight **(b)**. **(a)**Points represent values of each sample. Linear regression analysis was performed. *R* denotes Pearson's correlation coefficient. Asterisks (***) denotes $p < 0.001$. **(b)**Points represent values of each sample. Linear regression analysis was performed. *R* denotes Pearson's correlation coefficient. No significance was observed ($p > 0.05$).

(a)

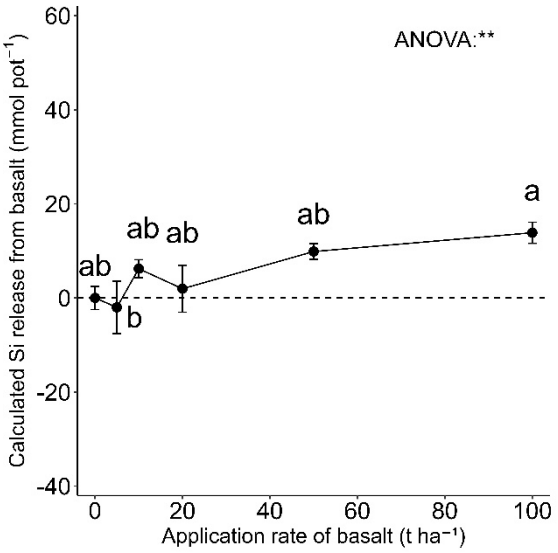
ANOVA:**
Calculated Si release from basalt (mmol pot^{-1})
Application rate of basalt (t ha^{-1})
ab
b
ab
ab
ab
a

(b)

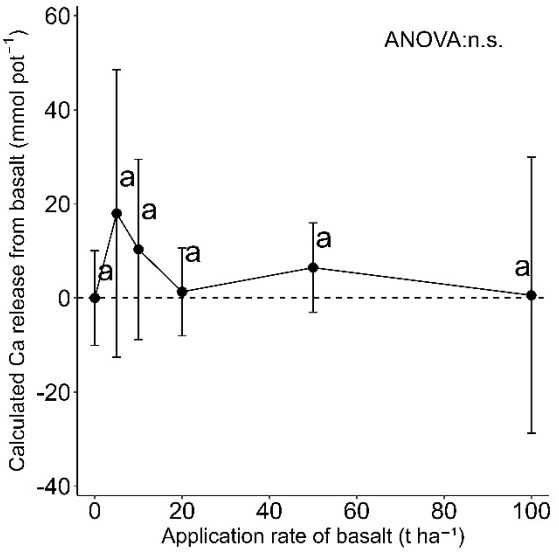
ANOVA:n.s.
Calculated Ca release from basalt (mmol pot^{-1})
Application rate of basalt (t ha^{-1})
a
a
a
a
a
a

(c)

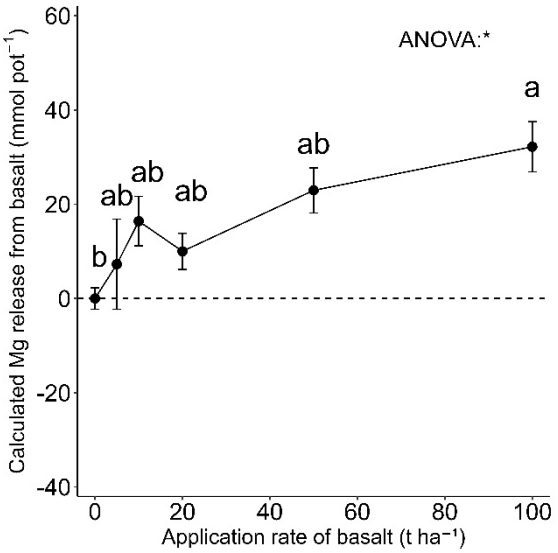
ANOVA:*
Calculated Mg release from basalt (mmol pot^{-1})
Application rate of basalt (t ha^{-1})
b
ab
ab
ab
ab
a

(d)

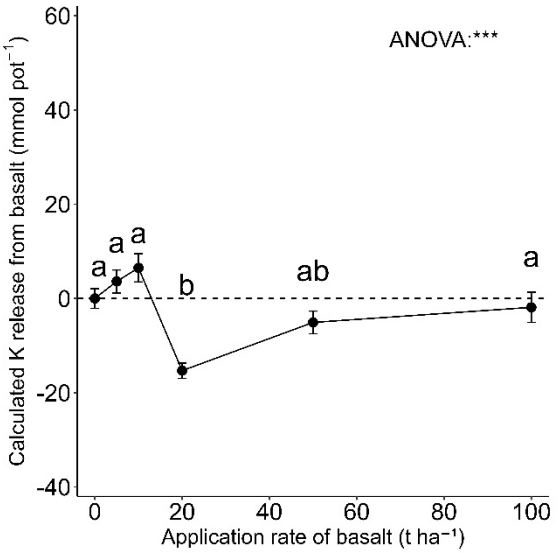
ANOVA:***
Calculated K release from basalt (mmol pot^{-1})
Application rate of basalt (t ha^{-1})
a
a
a
b
ab
a

(e)

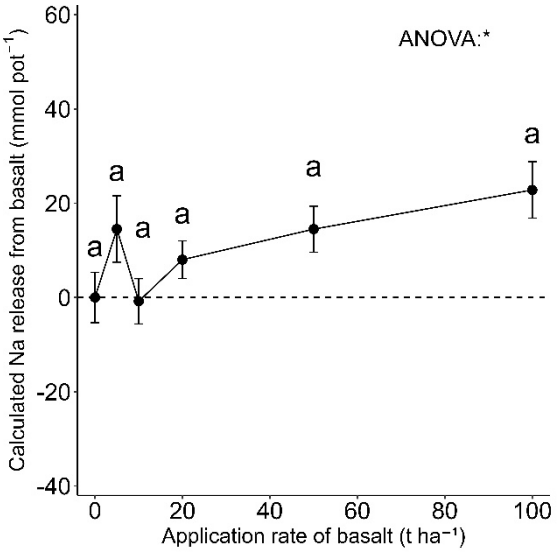

Figure 2-3. Release of Si **(a)**, Ca **(b)**, Mg **(c)**, K **(d)**, and Na **(e)** from basalt during cultivation. Points represent mean values ± one standard error (n=4). "ANOVA" shows the results of one-way ANOVA, which was performed to detect the significant differences among the application rates of basalt. Asterisks (*,**,***) denotes $p < 0.05$, 0.01, 0.001, respectively. "n.s." denotes not significant ($p > 0.05$). Different letters indicate significant differences among the application rates of basalt determined via Tukey post hoc test.

Table 2-10. Change in carbon content between before planting and after harvest in the soil (ΔC_{soil}) and in the whole system (ΔC_{system}).

Treatment	ΔC_{soil} (gC pot^{-1})	Total amount of carbon in plant (gC pot^{-1})	ΔC_{system} (gC pot^{-1})
B0	7.1 ± 1.4 a	69.6 ± 2.1 a	76.7 ± 3.2 a
B5	-0.1 ± 5.7 a	67.2 ± 3.0 a	67.1 ± 8.0 a
B10	-4.9 ± 5.4 a	72.4 ± 1.8 a	67.5 ± 6.9 a
B20	6.4 ± 2.0 a	70.4 ± 2.3 a	76.9 ± 4.3 a
B50	-7.3 ± 2.5 a	71.7 ± 0.7 a	64.4 ± 2.7 a
B100	10.1 ± 3.4 a	73.3 ± 1.8 a	83.4 ± 4.6 a
ANOVA	*	**n.s.**	**n.s.**

Mean values ± one standard error are shown (n=4). "ANOVA" shows the results of one-way ANOVA, which was performed for detecting the significant differences among the treatments. Asterisk (*) denotes $p < 0.05$. "n.s." denotes not significant ($p > 0.05$). No significant difference among the treatments was determined via Tukey post hoc test.

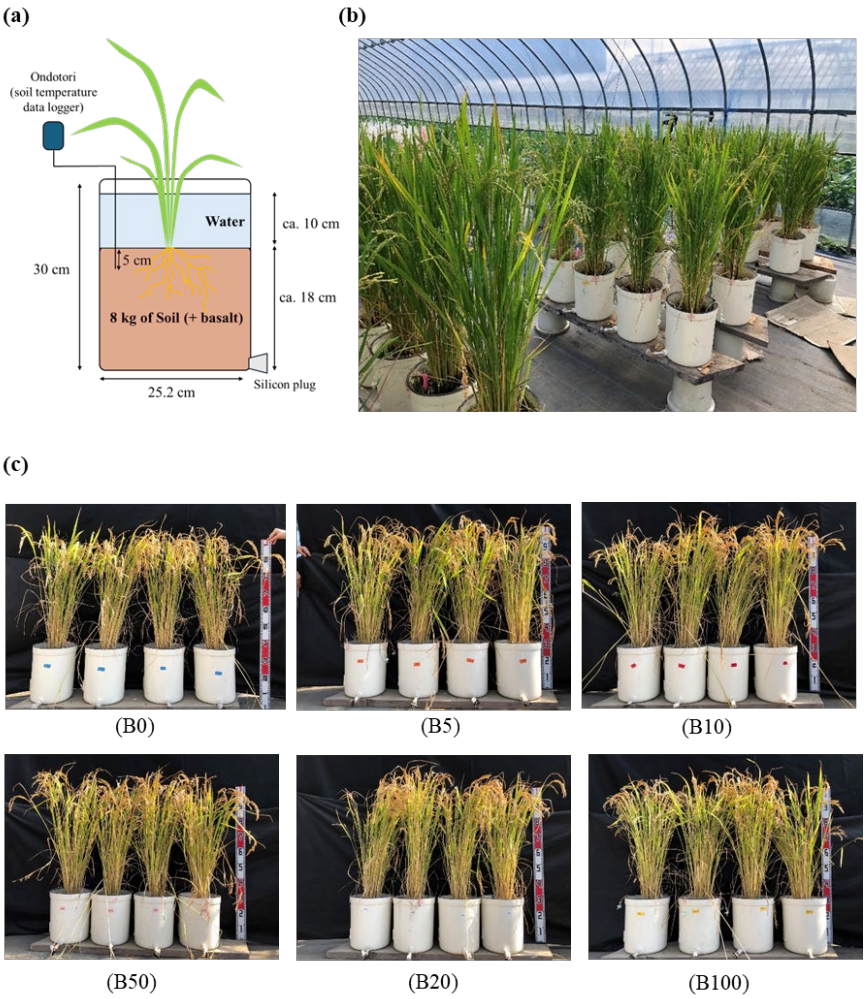

Supplemental figure 2-1. Schematic diagram of the pot **(a)** and photograph of status of the experiment on 20th August 2022 (2 months in) **(b)** and on 22nd September (at harvest) **(c)**.

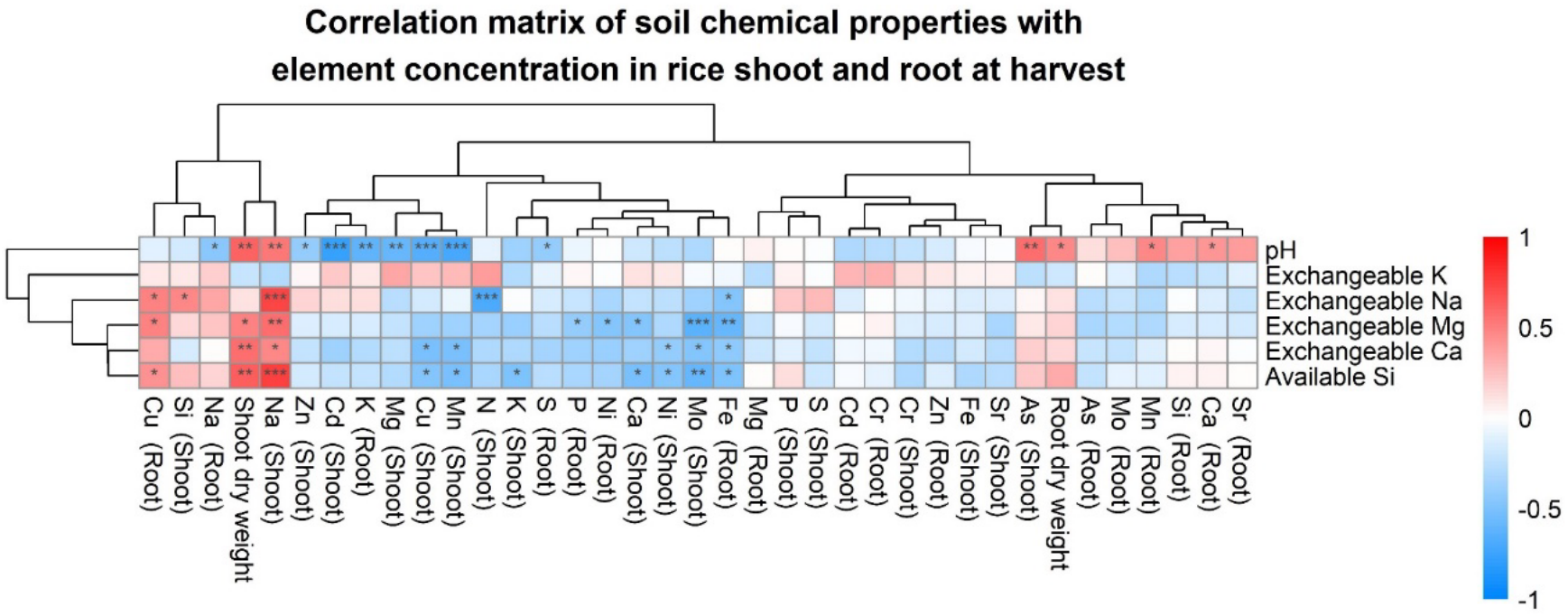

Supplemental figure 2-2. Correlation heatmap matrix of soil chemical properties with element concentration in rice shoot and root at harvest. The heatmap was constructed using R with complete clustering method. Color expresses Pearson correlation coefficient based on the color scale bar. Asterisk (*, **, ***) denotes *p*-value < 0.05, 0.01, 0.001, respectively.

Supplemental table 2-1. Element concentration in the soil.

	Basalt	Total carbon	Element concentration in soil (mg kg⁻¹ soil)				
	(t ha⁻¹)	(g kg^{-1} soil)	Available Si	Exchangeable Ca	Exchangeable Mg	Exchangeable K	Exchangeable Na
before planting	B0	27.4 ± 1.5 a	56.8 ± 1.0 a	4600 ± 44 a	512 ± 6 a	592 ± 27 a	45 ± 8 b
	B5	28.1 ± 2.2 a	53.8 ± 1.7 a	4521 ± 79 a	522 ± 7 a	569 ± 25 a	41 ± 2 b
	B10	27.7 ± 4.2 a	53.6 ± 1.6 a	4610 ± 47 a	517 ± 2 a	570 ± 8 a	54 ± 10 b
	B20	27.5 ± 3.2 a	54.2 ± 1.4 a	4532 ± 96 a	512 ± 8 a	655 ± 79 a	56 ± 6 b
	B50	27.8 ± 2.7 a	58.3 ± 1.7 a	4492 ± 47 a	505 ± 6 a	599 ± 57 a	70 ± 3 b
	B100	25.8 ± 2.0 b	58.9 ± 1.6 a	4584 ± 42 a	508 ± 6 a	563 ± 23 a	111 ± 6 a
	ANOVA	**	**n.s.**	**n.s.**	**n.s.**	**n.s.**	***
after harvest	B0	28.3 ± 1.7 a	48.4 ± 1.1 bc	5449 ± 50 a	788 ± 6 a	253 ± 14 a	214 ± 14 b
	B5	28.1 ± 7.1 a	46.4 ± 1.4 c	5459 ± 152 a	822 ± 29 a	246 ± 13 a	253 ± 21 b
	B10	27.1 ± 6.7 a	50.3 ± 1.6 abc	5504 ± 111 a	839 ± 15 a	261 ± 10 a	218 ± 14 b
	B20	28.0 ± 3.3 a	50.0 ± 1.2 abc	5423 ± 39 a	812 ± 10 a	246 ± 8 a	248 ± 10 b
	B50	27.0 ± 3.0 a	52.7 ± 0.9 ab	5381 ± 46 a	841 ± 13 a	253 ± 11 a	271 ± 13 ab
	B100	27.0 ± 3.9 a	54.9 ± 0.7 a	5419 ± 138 a	859 ± 15 a	228 ± 17 a	322 ± 14 a
	ANOVA	**n.s.**	**	**n.s.**	**n.s.**	**n.s.**	***

Mean values ± one standard error are shown. Sample size before planting was three, while after harvest was four. “ANOVA” shows the results of one-way ANOVA, which was performed for detecting the significant differences among the application rate of basalt. Asterisks (*,**,***) denote $p < 0.05$, 0.01, 0.001, respectively. “n.s.” denotes not significant ($p > 0.05$). Different letters indicate significant differences among the treatments

determined via Tukey post hoc test.

Supplemental table 2-2. Yield-related indices of rice.

Treatment	panicle number (plant^{-1})	grain number (panicle^{-1})	1000 grain weight (g)	setting rate (%)
B0	58.3 ± 1.0 a	65.4 ± 1.9 a	22.4 ± 0.1 a	0.889 ± 0.039 a
B5	55.8 ± 1.1 a	66.0 ± 2.7 a	22.7 ± 0.3 a	0.892 ± 0.041 a
B10	60.3 ± 2.1 a	65.3 ± 4.5 a	22.4 ± 0.2 a	0.927 ± 0.011 a
B20	55.0 ± 1.5 a	68.4 ± 1.9 a	22.4 ± 0.4 a	0.914 ± 0.009 a
B50	59.5 ± 2.1 a	64.9 ± 3.0 a	22.7 ± 0.1 a	0.891 ± 0.024 a
B100	61.0 ± 2.9 a	65.0 ± 1.9 a	22.3 ± 0.2 a	0.918 ± 0.011 a
ANOVA	**n.s.**	**n.s.**	**n.s.**	**n.s.**

Mean values ± one standard error are shown (n=4). “ANOVA” shows the results of one-way ANOVA, which was performed for detecting the significant differences among the application rate of basalt. “n.s.” denotes not significant ($p > 0.05$). No significant difference among the treatments was determined via Tukey post hoc test.

Supplemental table 2-3. Release rate of Si, Ca, Mg, K, and Na from the basalt.

Source	Basalt application rate		Release rate (mmol m^{-2} day^{-1})				
	(t ha^{-1})	(wt. %)	Si	Ca	Mg	K	Na
This study	0	0	0.0 ± 0.5	0.0 ± 2.0	0.0 ± 0.5	0.0 ± 0.4	0.0 ± 1.1
	5	0.31	-0.4 ± 1.1	3.6 ± 6.2	1.5 ± 1.9	0.7 ± 0.5	2.9 ± 1.4
	10	0.63	1.3 ± 0.4	2.1 ± 3.9	3.3 ± 1.1	1.3 ± 0.6	-0.2 ± 1.0
	20	1.25	0.4 ± 1.2	0.3 ± 2.2	2.0 ± 0.9	-3.1 ± 0.4	1.6 ± 0.9
	50	3.13	2.0 ± 0.3	1.3 ± 1.9	4.6 ± 1.0	-1.0 ± 0.6	2.9 ± 1.0
	100	6.25	2.8 ± 0.5	0.1 ± 5.9	6.5 ± 1.1	0.4 ± 0.6	4.6 ± 1.2
Kelland et al. (2020)	100	3.63	1.9 ± 0.4	18 ± 14	4.2 ± 0.9	1.1 ± 1.4	0.33 ± 0.53

Mean values ± one standard error are shown (n=4). “wt. %” means the proportion of applied basalt powder to soil mixed with by weight. The surface area of the pot was 0.05 m^{-2} and the cultivation duration was 99 days.

Supplemental table 2-4. Element concentration in soil solution.

Days after planting (DAP)	Treatment	Element concentration in soil solution (mg L^{-1})																							
		Si			Ca			Mg			K			Na			S			Fe			Mn		
16	B0	10.0 ±	0.7	a	152 ±	7	a	36.4 ±	1.7	a	42.5 ±	5.1	a	27.5 ±	0.5	**d**	125 ±	5	a	2.34 ±	0.72	a	7.58 ±	0.47	a
	B5	10.6 ±	0.4	a	133 ±	15	a	32.6 ±	3.3	a	37.1 ±	6.0	a	28.6 ±	2.1	**d**	114 ±	11	a	1.24 ±	0.24	a	5.59 ±	0.78	a
	B10	11.2 ±	0.1	a	149 ±	14	a	35.5 ±	2.6	a	41.4 ±	9.4	a	32.6 ±	2.4	**cd**	125 ±	9	a	3.32 ±	1.68	a	7.78 ±	1.41	a
	B20	10.2 ±	0.2	a	154 ±	6	a	35.6 ±	2.2	a	44.1 ±	3.7	a	41.3 ±	1.3	**bc**	136 ±	5	a	1.39 ±	0.27	a	6.57 ±	0.71	a
	B50	11.1 ±	0.8	a	150 ±	7	a	36.0 ±	0.5	a	33.4 ±	3.0	a	45.8 ±	2.1	**b**	139 ±	7	a	1.19 ±	0.28	a	6.60 ±	0.14	a
	B100	11.7 ±	0.9	a	149 ±	9	a	35.2 ±	2.6	a	35.2 ±	2.8	a	67.1 ±	4.5	**a**	141 ±	6	a	1.61 ±	0.31	a	7.24 ±	0.55	a
	ANOVA	**n.s.**			**n.s.**			**n.s.**			**n.s.**			***			**n.s.**			**n.s.**			**n.s.**		
30	B0	3.95 ±	1.08	a	137 ±	6	a	35.1 ±	1.7	a	7.43 ±	2.17	a	25 ±	1	**b**	110 ±	9	a	1.61 ±	1.09	a	10.4 ±	0.4	a
	B5	3.76 ±	0.53	a	73 ±	12	a	22.5 ±	1.6	a	6.64 ±	1.12	a	24 ±	1	**b**	60 ±	2	a	0.79 ±	0.29	a	5.4 ±	0.5	a
	B10	3.58 ±	0.54	a	114 ±	26	a	32.5 ±	5.6	a	6.25 ±	2.08	a	27 ±	2	**b**	103 ±	23	a	0.88 ±	0.60	a	9.0 ±	1.7	a
	B20	3.13 ±	0.45	a	125 ±	14	a	30.4 ±	5.3	a	7.42 ±	0.86	a	32 ±	2	**b**	104 ±	19	a	0.68 ±	0.05	a	8.5 ±	1.2	a
	B50	3.40 ±	0.82	a	86 ±	4	a	27.3 ±	4.4	a	4.22 ±	0.61	a	55 ±	9	**b**	88 ±	19	a	0.43 ±	0.09	a	6.1 ±	0.8	a
	B100	3.01 ±	0.35	a	118 ±	20	a	35.3 ±	8.3	a	4.44 ±	1.16	a	104 ±	21	**a**	128 ±	35	a	0.45 ±	0.21	a	8.7 ±	1.1	a
	ANOVA	**n.s.**			**n.s.**			**n.s.**			**n.s.**			***			**n.s.**			**n.s.**			*		
44	B0	1.54 ±	0.33	a	92.9 ±	2.3	a	22.6 ±	0.5	a	2.37 ±	0.73	a	32.4 ±	2.8	**b**	36.4 ±	5.8	a	0.421 ±	0.156	a	7.19 ±	0.15	a
	B5	1.90 ±	0.23	a	71.3 ±	6.3	a	17.7 ±	1.5	a	3.00 ±	0.51	a	28.7 ±	1.9	**b**	23.6 ±	3.6	a	0.324 ±	0.108	a	5.06 ±	0.47	a
	B10	2.18 ±	0.92	a	96.8 ±	24.2	a	23.8 ±	5.6	a	2.49 ±	0.60	a	34.1 ±	3.3	**ab**	43.0 ±	18.8	a	0.431 ±	0.121	a	7.16 ±	1.93	a
	B20	1.46 ±	0.26	a	81.3 ±	3.6	a	20.4 ±	1.6	a	2.09 ±	0.16	a	35.3 ±	1.8	**ab**	29.6 ±	3.4	a	0.483 ±	0.139	a	5.50 ±	0.12	a
	B50	1.30 ±	0.37	a	79.3 ±	7.2	a	19.6 ±	1.6	a	1.74 ±	0.06	a	39.1 ±	4.1	**ab**	26.7 ±	8.1	a	0.246 ±	0.007	a	5.27 ±	0.70	a
	B100	1.35 ±	0.22	a	89.5 ±	13.4	a	24.4 ±	4.6	a	1.70 ±	0.61	a	61.4 ±	12.8	**a**	36.8 ±	8.6	a	0.427 ±	0.094	a	4.81 ±	0.39	a
	ANOVA	**n.s.**			**n.s.**			**n.s.**			**n.s.**			*			**n.s.**			**n.s.**			**n.s.**		
59	B0	1.24 ±	0.25	a	110 ±	1	a	32.8 ±	0.9	a	2.34 ±	0.48	a	62.0 ±	3.6	a	9.0 ±	3.7	a	0.198 ±	0.006	a	6.66 ±	0.69	a
	B5	1.35 ±	0.08	a	98 ±	7	a	27.1 ±	2.7	a	3.03 ±	0.43	a	54.6 ±	1.7	a	11.9 ±	5.0	a	0.290 ±	0.079	a	7.08 ±	0.15	a
	B10	2.39 ±	1.31	a	114 ±	23	a	35.3 ±	9.1	a	2.52 ±	0.42	a	62.7 ±	13.6	a	15.3 ±	5.8	a	0.230 ±	0.036	a	5.69 ±	0.41	a
	B20	1.36 ±	0.24	a	113 ±	5	a	32.5 ±	1.4	a	2.41 ±	0.17	a	62.3 ±	1.3	a	8.3 ±	4.1	a	0.240 ±	0.005	a	8.02 ±	1.74	a
	B50	1.13 ±	0.17	a	114 ±	11	a	33.7 ±	2.4	a	2.14 ±	0.20	a	70.0 ±	6.1	a	8.2 ±	4.2	a	0.190 ±	0.016	a	6.31 ±	0.52	a
	B100	1.08 ±	0.10	a	113 ±	6	a	42.0 ±	7.6	a	2.05 ±	0.75	a	95.3 ±	21.6	a	10.3 ±	1.5	a	0.203 ±	0.023	a	4.33 ±	1.75	a
	ANOVA	**n.s.**			**n.s.**			**n.s.**			**n.s.**			**n.s.**			**n.s.**			**n.s.**			**n.s.**		
72	B0	0.795 ±	0.064	a	153 ±	8	a	49.9 ±	3.3	a	1.99 ±	0.31	a	117 ±	8	a	4.35 ±	0.30	a	0.221 ±	0.020	a	5.72 ±	0.10	a
	B5	0.776 ±	0.060	a	114 ±	14	a	34.4 ±	6.5	a	2.03 ±	0.15	a	90 ±	9	a	5.56 ±	2.22	a	0.157 ±	0.020	a	6.63 ±	1.07	a
	B10	0.973 ±	0.115	a	144 ±	6	a	50.7 ±	8.7	a	2.06 ±	0.21	a	112 ±	15	a	4.78 ±	0.64	a	0.207 ±	0.017	a	5.66 ±	0.80	a
	B20	0.809 ±	0.120	a	125 ±	2	a	40.5 ±	3.3	a	2.09 ±	0.13	a	104 ±	8	a	3.61 ±	1.30	a	0.189 ±	0.006	a	5.63 ±	1.30	a
	B50	0.884 ±	0.071	a	141 ±	12	a	49.3 ±	3.3	a	1.64 ±	0.11	a	115 ±	7	a	3.18 ±	1.23	a	0.271 ±	0.055	a	4.41 ±	0.66	a
	B100	0.862 ±	0.023	a	146 ±	10	a	61.1 ±	13.5	a	1.63 ±	0.45	a	160 ±	37	a	4.28 ±	0.45	a	0.227 ±	0.032	a	5.14 ±	1.86	a
	ANOVA	**n.s.**			**n.s.**			**n.s.**			**n.s.**			**n.s.**			**n.s.**			**n.s.**			**n.s.**		

Supplemental table 2-4. continued.

Days after planting (DAP)	Treatment	Element concentration in soil solution (μg L^{-1})																							
		Sr		Zn		Mo		As		Cu		Ni		Cd		Cr	
16	B0	607 ± 26	a	36.5 ± 2.4	a	2.47 ± 0.08	a	25.3 ± 2.8	a	2.79 ± 0.18	a	17.2 ± 4.9	a	0.0438 ± 0.0044	a	0.385 ± 0.105	a
	B5	544 ± 47	a	30.6 ± 1.1	a	2.34 ± 0.91	a	19.4 ± 1.8	a	3.67 ± 0.71	a	10.3 ± 0.6	a	0.0373 ± 0.0037	a	0.255 ± 0.046	a
	B10	593 ± 42	a	33.2 ± 2.2	a	2.19 ± 0.41	a	25.4 ± 3.9	a	3.87 ± 0.79	a	24.2 ± 12.1	a	0.0352 ± 0.0091	a	0.140 ± 0.073	a
	B20	606 ± 24	a	34.7 ± 1.2	a	1.65 ± 0.21	a	17.2 ± 1.2	a	3.57 ± 0.38	a	11.2 ± 2.4	a	0.0582 ± 0.0138	a	0.468 ± 0.125	a
	B50	606 ± 18	a	32.2 ± 3.5	a	1.59 ± 0.11	a	17.6 ± 1.8	a	3.09 ± 0.34	a	11.1 ± 2.0	a	0.0523 ± 0.0153	a	0.194 ± 0.031	a
	B100	598 ± 33	a	29.4 ± 2.4	a	1.84 ± 0.29	a	20.5 ± 2.9	a	3.23 ± 0.51	a	14.5 ± 1.7	a	0.0398 ± 0.0027	a	0.295 ± 0.044	a
		n.s.		**n.s.**		**n.s.**		**n.s.**		**n.s.**		**n.s.**		**n.s.**		**n.s.**	
30	B0	538 ± 2	a	18.3 ± 0.9	a	1.16 ± 0.12	a	7.56 ± 2.28	a	2.85 ± 0.39	a	19.5 ± 10.1	a	0.0180 ± 0.0029	a		
	B5	324 ± 11	a	13.4 ± 0.9	a	1.20 ± 0.29	a	8.46 ± 0.91	a	2.36 ± 0.28	a	11.3 ± 2.0	a	0.0215 ± 0.0052	a		
	B10	480 ± 80	a	19.0 ± 1.0	a	1.29 ± 0.45	a	7.43 ± 1.37	a	2.59 ± 0.13	a	11.6 ± 4.6	a	0.0311 ± 0.0083	a	**N.D.**	
	B20	488 ± 52	a	19.7 ± 3.5	a	0.97 ± 0.06	a	7.41 ± 0.77	a	2.57 ± 0.06	a	9.8 ± 0.8	a	0.0405 ± 0.0109	a		
	B50	394 ± 50	a	17.2 ± 3.4	a	1.58 ± 0.45	a	6.45 ± 1.04	a	3.06 ± 0.70	a	9.1 ± 1.3	a	0.0361 ± 0.0054	a		
	B100	506 ± 95	a	21.5 ± 5.1	a	1.86 ± 0.82	a	5.35 ± 0.89	a	3.17 ± 0.43	a	9.0 ± 2.6	a	0.0334 ± 0.0138	a		
		n.s.		**n.s.**		**n.s.**		**n.s.**		**n.s.**		**n.s.**		**n.s.**		**-**	
44	B0	358 ± 11	a	9.7 ± 2.3	a	0.49 ± 0.34	a	9.9 ± 1.7	a	5.73 ± 1.86	a	10.2 ± 4.1	a			3.21 ± 3.07	a
	B5	277 ± 20	a	8.9 ± 1.7	a	0.64 ± 0.70	a	9.0 ± 0.4	a	3.47 ± 0.26	a	6.4 ± 1.2	a			1.54 ± 1.33	a
	B10	364 ± 85	a	8.6 ± 2.1	a	0.35 ± 0.17	a	9.5 ± 1.9	a	3.18 ± 0.39	a	7.6 ± 1.1	a	**N.D.**		0.10 ± 0.04	a
	B20	323 ± 17	a	8.1 ± 0.8	a	0.57 ± 0.18	a	11.4 ± 1.5	a	4.09 ± 0.55	a	9.4 ± 1.8	a			1.43 ± 1.32	a
	B50	302 ± 26	a	13.1 ± 4.0	a	0.37 ± 0.19	a	9.5 ± 2.1	a	3.67 ± 0.31	a	8.9 ± 3.0	a			1.27 ± 0.22	a
	B100	362 ± 57	a	8.1 ± 1.9	a	1.51 ± 0.13	a	8.8 ± 0.9	a	4.27 ± 0.55	a	9.2 ± 0.7	a			2.99 ± 2.94	a
		n.s.		**n.s.**		**n.s.**		**n.s.**		**n.s.**		**n.s.**		**-**		**n.s.**	
59	B0	416 ± 2	a	7.8 ± 0.9	a	8.1 ± 0.5	a	12.3 ± 1.5	a	9.8 ± 0.4	a	2.45 ± 0.73	a	0.0221 ± 0.0015	a		
	B5	363 ± 25	a	10.7 ± 2.4	a	7.5 ± 2.1	a	11.9 ± 1.3	a	8.9 ± 2.6	a	2.59 ± 0.63	a	0.0258 ± 0.0051	a		
	B10	439 ± 97	a	9.6 ± 1.6	a	8.4 ± 1.4	a	11.3 ± 1.1	a	10.5 ± 1.6	a	2.06 ± 0.84	a	0.0254 ± 0.0021	a	**N.D.**	
	B20	421 ± 21	a	18.2 ± 7.4	a	9.1 ± 1.3	a	13.6 ± 1.1	a	7.8 ± 0.6	a	4.45 ± 2.42	a	0.0256 ± 0.0035	a		
	B50	430 ± 40	a	6.8 ± 0.9	a	8.8 ± 0.7	a	11.9 ± 1.5	a	8.6 ± 0.4	a	2.12 ± 1.14	a	0.0262 ± 0.0009	a		
	B100	482 ± 54	a	7.4 ± 0.6	a	10.4 ± 0.8	a	12.3 ± 1.0	a	8.6 ± 1.3	a	4.09 ± 1.22	a	0.0360 ± 0.0029	a		
		n.s.		**n.s.**		**n.s.**		**n.s.**		**n.s.**		**n.s.**		**n.s.**		**-**	
72	B0	333 ± 21	a	0.78 ± 0.51	a	7.38 ± 0.60	a	37.1 ± 2.9	a	1.73 ± 0.18	a	4.40 ± 0.31	**ab**				
	B5	245 ± 36	a	2.57 ± 1.40	a	5.58 ± 1.22	a	26.6 ± 7.5	a	1.99 ± 0.37	a	3.32 ± 0.20	**b**				
	B10	327 ± 30	a	0.63 ± 0.38	a	7.03 ± 1.17	a	33.4 ± 6.5	a	2.68 ± 0.04	a	4.15 ± 0.35	**ab**	**N.D.**		**N.D.**	
	B20	276 ± 5	a	0.89 ± 0.60	a	7.36 ± 0.77	a	29.0 ± 2.9	a	1.92 ± 0.46	a	3.94 ± 0.19	**ab**				
	B50	323 ± 25	a	0.36 ± 0.31	a	8.30 ± 0.65	a	33.0 ± 7.0	a	2.47 ± 0.56	a	5.04 ± 0.39	**a**				
	B100	356 ± 47	a	1.16 ± 0.31	a	8.70 ± 1.24	a	39.8 ± 8.7	a	2.59 ± 0.42	a	4.61 ± 0.35	**ab**				
		n.s.		**n.s.**		**n.s.**		**n.s.**		**n.s.**		*		**-**		**-**	

Mean values ± one standard error are shown (n=3). “ANOVA” shows the results of one-way ANOVA, which was performed for detecting the significant differences among the treatments. Symbols († ,*,***) denote $p < 0.1, 0.05, 0.001$. “n.s.” denotes not significant ($p > 0.05$). Different letters indicate significant differences among the treatments determined via Tukey post hoc test.

(a)

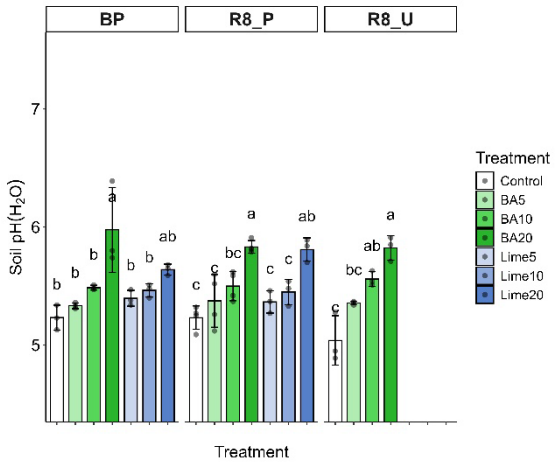
BP
R8_P
R8_U
Soil pH(H2O)
Treatment
Control
BA5
BA10
BA20
Lime5
Lime10
Lime20

(b)

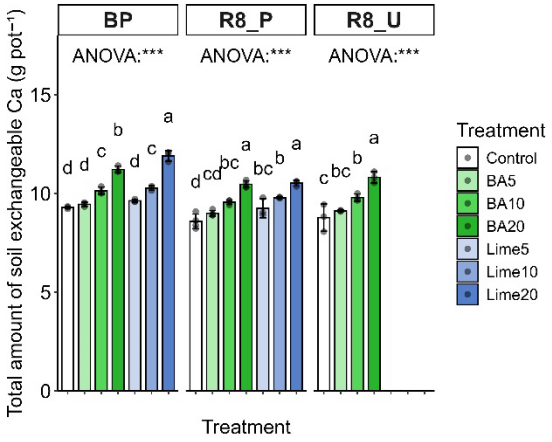
BP
R8_P
R8_U
ANOVA:***
Total amount of soil exchangeable Ca (g pot⁻¹)
Treatment
Control
BA5
BA10
BA20
Lime5
Lime10
Lime20

(c)

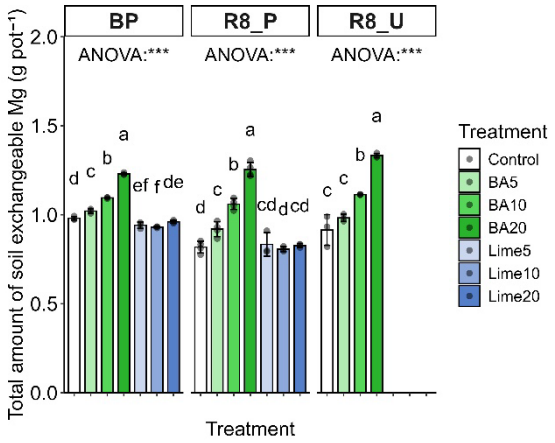
BP
R8_P
R8_U
ANOVA:***
Total amount of soil exchangeable Mg (g pot⁻¹)
Treatment
Control
BA5
BA10
BA20
Lime5
Lime10
Lime20

(d)

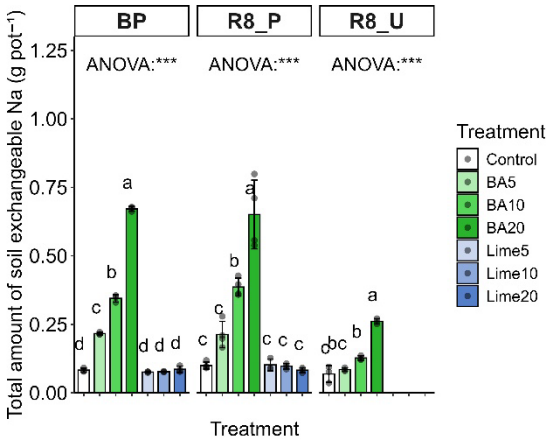
BP
R8_P
R8_U
ANOVA:***
Total amount of soil exchangeable Na (g pot⁻¹)
Treatment
Control
BA5
BA10
BA20
Lime5
Lime10
Lime20

(e)

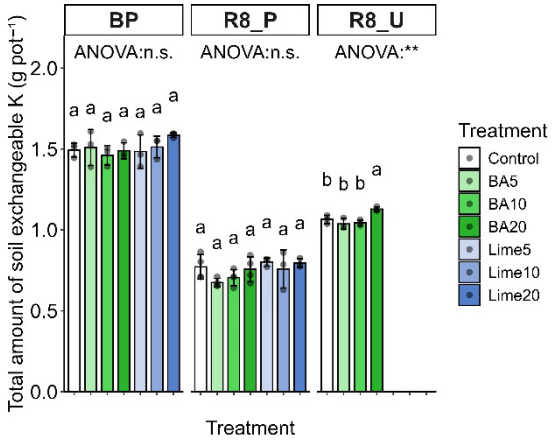
BP
R8_P
R8_U
ANOVA:n.s.
ANOVA:n.s.
ANOVA:**
Total amount of soil exchangeable K (g pot⁻¹)
Treatment
Control
BA5
BA10
BA20
Lime5
Lime10
Lime20

Figure 3-1. Soil chemical properties before planting and after harvest. (a) pH(H_2O) in water, total amount of exchangeable (b) Ca, (c) Mg, (d) Na, (e) K in a pot. Bars represents mean-value ± one standard error. “BP”, “R8_P”, and “R8_U” indicate-values of soil collected before planting, at R8 from planted plot, and at R8 from unplanted plot, respectively. Significant difference among the treatments within each sampling timing was determined using One-way ANOVA and its results are shown in upper part of bar plots. Asterisks(**, ***) indicate *p*-values < 0.01, 0.001, respectively. “n.s.” indicates *p*-values > 0.05. Different letters indicate significant differences among the treatments determined via Tukey post hoc test.

Table 3-1. Stem length and dry weight in each part of soybean at harvest.

Treatment	Stem length (cm)	Dry weight (g plant^{-1})						
		leaf	stem	pod	grain	shoot	root	total
Control	42.2 ± 1.5 a	7.2 ± 0.7 a	7.63 ± 0.41 a	6.9 ± 0.4 c	4.91 ± 1.43 a	26.6 ± 1.0 b	2.96 ± 0.19 a	29.6 ± 1.1 b
BA5	43.4 ± 2.5 a	8.5 ± 0.4 a	8.69 ± 0.56 a	9.0 ± 0.8 abc	5.33 ± 0.39 a	31.6 ± 1.2 ab	3.66 ± 0.10 a	35.3 ± 1.3 ab
BA10	47.7 ± 2.5 a	10.4 ± 1.3 a	9.59 ± 0.54 a	10.9 ± 0.4 ab	4.25 ± 0.40 a	35.1 ± 1.9 a	3.86 ± 0.20 a	39.0 ± 2.1 a
BA20	45.7 ± 2.4 a	9.5 ± 0.6 a	8.87 ± 0.65 a	11.2 ± 0.4 a	5.50 ± 1.15 a	35.1 ± 1.3 a	3.79 ± 0.22 a	38.9 ± 1.5 a
Lime5	42.7 ± 2.3 a	6.5 ± 0.7 a	7.24 ± 0.86 a	6.7 ± 0.7 c	3.88 ± 0.58 a	24.3 ± 2.7 b	2.86 ± 0.47 a	27.1 ± 3.1 b
Lime10	43.2 ± 1.4 a	8.2 ± 1.3 a	8.26 ± 0.60 a	9.6 ± 0.2 abc	4.86 ± 0.77 a	31.0 ± 2.5 ab	3.33 ± 0.18 a	34.3 ± 2.6 ab
Lime20	42.5 ± 2.3 a	6.8 ± 0.3 a	7.43 ± 0.17 a	8.0 ± 1.2 bc	5.23 ± 0.43 a	27.4 ± 1.1 ab	2.93 ± 0.12 a	30.4 ± 1.2 ab
ANOVA	**n.s.**	*	**n.s.**	***	**n.s.**	**	*	**

Mean-values ± one standard error are shown. Shoot dry weight is a sum of leaf, stem, pod, and grain dry weight. Total dry weight is a sum of shoot and root dry weight.One-way ANOVA was performed to detect significant differences among the treatments. Asterisks (*, **, ***) indicate *p*-values < 0.05, 0.01, 0.001, respectively. “n.s.” indicates *p*-values > 0.05. Different letters indicate significant differences among the treatments determined via Tukey post hoc test.

Table 3-2. Element concentration in soybean shoot.

Treatment	Element concentration in shoot (mg g^{-1} plant)																					
	N		P		K		Ca		Mg		S		Fe		Mn		Na	
Control	30.2 ± 2.3	a	4.85 ± 0.11	ab	16.8 ± 0.8	a	12.6 ± 0.7	ab	4.38 ± 0.17	a	3.72 ± 0.65	a	0.186 ± 0.022	a	0.197 ± 0.011	a	0.0745 ± 0.0020	a
BA5	29.8 ± 1.6	a	4.22 ± 0.17	bcd	16.6 ± 0.7	a	12.5 ± 0.4	ab	4.69 ± 0.11	a	3.06 ± 0.23	a	0.179 ± 0.024	a	0.146 ± 0.009	bc	0.0861 ± 0.0030	a
BA10	30.7 ± 1.6	a	4.03 ± 0.12	cd	16.3 ± 0.5	a	11.3 ± 0.3	b	4.17 ± 0.09	a	2.66 ± 0.13	a	0.199 ± 0.027	a	0.104 ± 0.005	d	0.0743 ± 0.0044	a
BA20	34.0 ± 0.8	a	3.92 ± 0.11	d	16.2 ± 0.5	a	12.0 ± 0.2	b	4.17 ± 0.13	a	2.58 ± 0.13	a	0.168 ± 0.013	a	0.062 ± 0.004	e	0.0767 ± 0.0043	a
Lime5	31.4 ± 1.4	a	5.05 ± 0.23	a	18.0 ± 0.4	a	14.5 ± 0.7	a	4.62 ± 0.20	a	3.74 ± 0.65	a	0.218 ± 0.012	a	0.159 ± 0.010	b	0.0761 ± 0.0099	a
Lime10	31.0 ± 2.3	a	4.19 ± 0.10	bcd	16.2 ± 0.2	a	13.1 ± 0.3	ab	4.39 ± 0.04	a	2.72 ± 0.06	a	0.219 ± 0.034	a	0.117 ± 0.006	cd	0.0723 ± 0.0025	a
Lime20	33.1 ± 0.6	a	4.61 ± 0.15	abc	17.3 ± 1.4	a	14.4 ± 0.6	a	4.26 ± 0.09	a	3.49 ± 0.77	a	0.171 ± 0.014	a	0.087 ± 0.002	de	0.0747 ± 0.0057	a
ANOVA	**n.s.**		***		**n.s.**		**		**n.s.**		**n.s.**		**n.s.**		***		**n.s.**	

Treatment	Element concentration in shoot (µg g^{-1} plant)													
	Zn		Cu		Mo		Ni		Sr		Cd		Cr	
Control	85.4 ± 4.6	a	12.5 ± 0.9	a	0.72 ± 0.08	b	2.34 ± 0.15	a	46.4 ± 2.4	a	0.539 ± 0.036	ab	2.97 ± 0.79	a
BA5	75.8 ± 2.6	ab	11.9 ± 0.5	a	0.88 ± 0.13	ab	2.02 ± 0.05	ab	46.0 ± 1.5	a	0.564 ± 0.026	ab	1.54 ± 0.36	a
BA10	66.4 ± 2.6	bc	12.6 ± 0.9	a	0.90 ± 0.07	ab	1.43 ± 0.11	bc	41.1 ± 0.5	a	0.421 ± 0.049	ab	2.22 ± 0.30	a
BA20	59.7 ± 2.4	c	11.8 ± 0.4	a	1.18 ± 0.03	a	1.35 ± 0.08	c	42.0 ± 0.7	a	0.361 ± 0.026	b	1.93 ± 0.41	a
Lime5	91.9 ± 4.3	a	12.4 ± 0.7	a	0.88 ± 0.17	ab	1.75 ± 0.25	abc	48.2 ± 2.6	a	0.606 ± 0.105	a	2.25 ± 0.48	a
Lime10	76.6 ± 2.7	ab	11.3 ± 0.5	a	0.85 ± 0.13	ab	1.75 ± 0.29	abc	42.6 ± 1.2	a	0.440 ± 0.023	ab	2.25 ± 0.75	a
Lime20	75.4 ± 5.0	abc	13.0 ± 1.2	a	1.32 ± 0.07	a	1.13 ± 0.11	c	45.3 ± 1.6	a	0.473 ± 0.038	ab	2.37 ± 0.42	a
ANOVA	***		**n.s.**		**		***		**n.s.**		*		**n.s.**	

Mean-values ± one standard error are shown. One-way ANOVA was performed to detect significant differences among the treatments. Asterisks (*, **, ***) indicate *p*-values < 0.05, 0.01, 0.001, respectively. “n.s.” indicates *p*-values > 0.05. Different letters indicate significant differences among the treatments determined via Tukey post hoc test.

Table 3-3. Element concentration in soybean root.

Treatment	Element concentration in root (mg g^{-1} plant)																					
	N		P		K		Ca		Mg		S		Fe		Mn		Na	
Control	17.5 ± 0.7	a	4.84 ± 0.28	a	11.2 ± 0.4	a	5.51 ± 0.22	a	2.25 ± 0.26	a	2.90 ± 0.37	a	1.60 ± 0.18	ab	0.0815 ± 0.0065	a	0.74 ± 0.13	c
BA5	17.0 ± 1.3	a	3.73 ± 0.27	ab	9.9 ± 0.6	ab	5.73 ± 0.15	a	2.20 ± 0.07	a	2.82 ± 0.14	a	1.81 ± 0.06	ab	0.0735 ± 0.0034	ab	1.15 ± 0.11	bc
BA10	19.7 ± 1.0	a	3.55 ± 0.16	b	8.8 ± 0.3	ab	5.37 ± 0.16	a	2.45 ± 0.07	a	2.86 ± 0.19	a	1.77 ± 0.09	ab	0.0601 ± 0.0020	ab	1.49 ± 0.22	b
BA20	19.8 ± 1.6	a	3.37 ± 0.30	b	7.7 ± 0.6	b	5.72 ± 0.16	a	2.62 ± 0.25	a	2.81 ± 0.09	a	1.98 ± 0.17	a	0.0561 ± 0.0043	b	2.21 ± 0.16	a
Lime5	20.1 ± 0.1	a	4.43 ± 0.28	ab	11.5 ± 0.9	a	5.51 ± 0.12	a	2.47 ± 0.41	a	3.17 ± 0.25	a	1.18 ± 0.25	b	0.0609 ± 0.0090	ab	0.71 ± 0.05	c
Lime10	19.6 ± 1.5	a	3.74 ± 0.32	ab	9.9 ± 1.1	ab	6.12 ± 0.19	a	2.71 ± 0.10	a	2.98 ± 0.15	a	1.86 ± 0.22	ab	0.0749 ± 0.0091	ab	0.49 ± 0.05	c
Lime20	17.6 ± 0.6	a	4.30 ± 0.20	ab	10.7 ± 1.4	ab	6.18 ± 0.14	a	2.56 ± 0.10	a	3.03 ± 0.51	a	1.62 ± 0.15	ab	0.0625 ± 0.0026	ab	0.67 ± 0.06	c
ANOVA	**n.s.**		**		*		*		**n.s.**		**n.s.**		**n.s.**		*		***	

Treatment	Element concentration in root (µg g^{-1} plant)													
	Zn		Cu		Mo	Ni		Sr		Cd		Cr	
Control	34.4 ± 1.8	a	24.2 ± 1.9	ab	N.D.	4.51 ± 1.02	a	31.8 ± 1.0	a	0.730 ± 0.036	a	12.8 ± 2.2	a
BA5	27.3 ± 0.7	abc	17.6 ± 1.7	ab	N.D.	3.77 ± 0.17	a	32.9 ± 0.7	a	0.834 ± 0.086	a	11.5 ± 2.1	a
BA10	22.0 ± 1.1	c	17.0 ± 2.2	b	N.D.	5.13 ± 0.98	a	30.7 ± 0.7	a	0.674 ± 0.052	a	15.3 ± 3.0	a
BA20	20.6 ± 1.2	c	15.8 ± 0.6	b	N.D.	2.78 ± 0.28	a	32.1 ± 1.0	a	0.716 ± 0.038	a	11.3 ± 0.7	a
Lime5	32.5 ± 4.5	ab	26.6 ± 4.3	a	N.D.	2.96 ± 0.24	a	30.5 ± 1.1	a	0.849 ± 0.070	a	7.5 ± 0.9	a
Lime10	28.6 ± 0.8	abc	15.5 ± 0.8	b	N.D.	5.08 ± 1.71	a	32.5 ± 1.3	a	0.845 ± 0.074	a	13.4 ± 3.5	a
Lime20	25.6 ± 1.0	bc	15.8 ± 1.1	b	N.D.	2.94 ± 0.50	a	31.5 ± 0.8	a	0.944 ± 0.024	a	10.3 ± 0.9	a
ANOVA	***		**		-	**n.s.**		**n.s.**		**n.s.**		**n.s.**	

Mean-values ± one standard error are shown. One-way ANOVA was performed to detect significant differences among the treatments. Asterisks (*, **, ***) indicate *p*-values < 0.05, 0.01, 0.001, respectively. “n.s.” indicates *p*-values > 0.05. Different letters indicate significant differences among the treatments determined via Tukey post hoc test. “N.D.” indicates not detected.

Table 3-4. Total element uptake in soybean.

Treatment	Total elemental uptake in soybean (mg plant^{-1})											
	Ca			Mg			Na			K		
Control	350	± 8	b	123	± 2	b	4.1	± 0.3	c	480	± 17	a
BA5	414	± 13	ab	156	± 6	a	7.0	± 0.5	b	563	± 35	a
BA10	418	± 30	ab	156	± 8	a	8.2	± 0.4	b	607	± 38	a
BA20	441	± 15	a	157	± 8	a	11.0	± 0.7	a	597	± 33	a
ANOVA	*			**			***			n.s.		

Mean-values ± one standard error are shown. One-way ANOVA was performed to detect significant differences among the treatments. Asterisks (*, **, ***) indicate *p*-values < 0.05, 0.01, 0.001, respectively. “n.s.” indicates *p*-values > 0.05. Different letters indicate significant differences among the treatments determined via Tukey post hoc test.

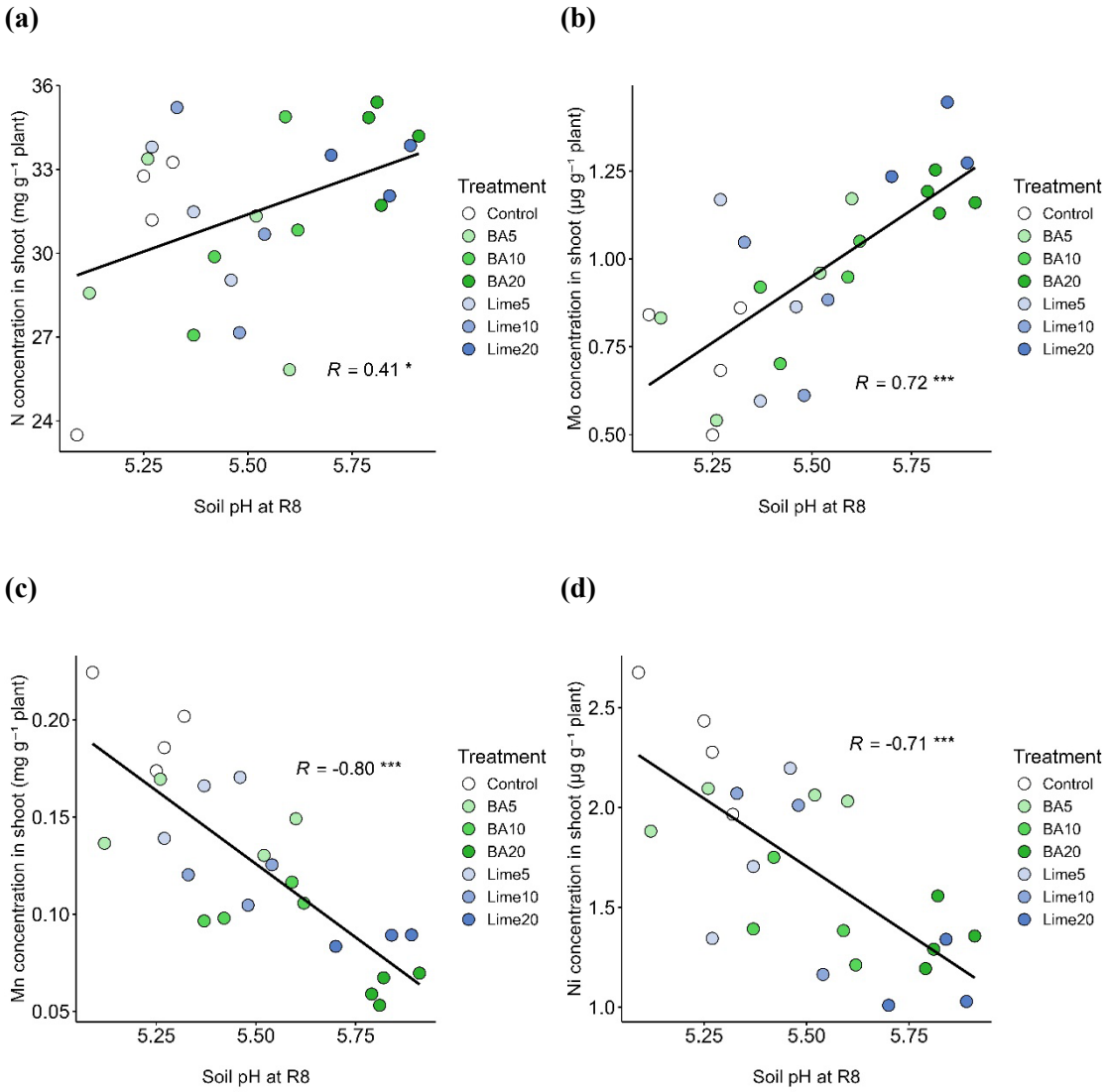

Figure 3-2. Relationships between soil pH at R8 and the concentrations of **(a)** N, **(b)** Mo, **(c)** Mn, and **(d)** Ni. Points represent values of each sample. Linear regression analysis was performed. *R* denotes the Pearson correlation coefficient. Asterisks (*,***) denote *p*-value < 0.05, 0.001, respectively.

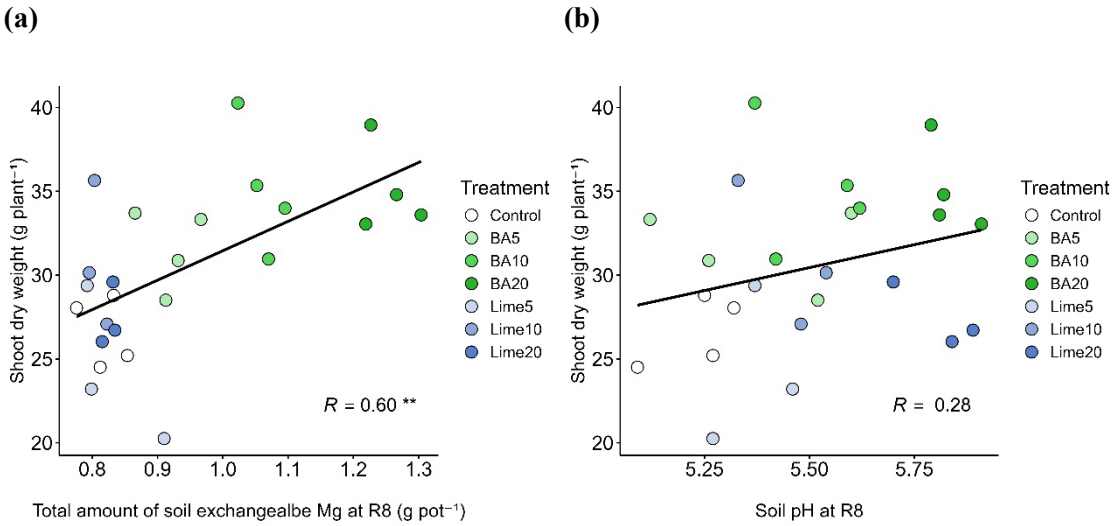

Figure 3-3. Relationships **(a)** between total amount of soil exchangeable Mg at R8 and shoot dry weight, and **(b)** between soil pH at R8 and shoot dry weight. Points represent values of each sample. Linear regression analysis was performed. *R* denotes the Pearson correlation coefficient. Asterisks (**) denote *p*-value < 0.01.

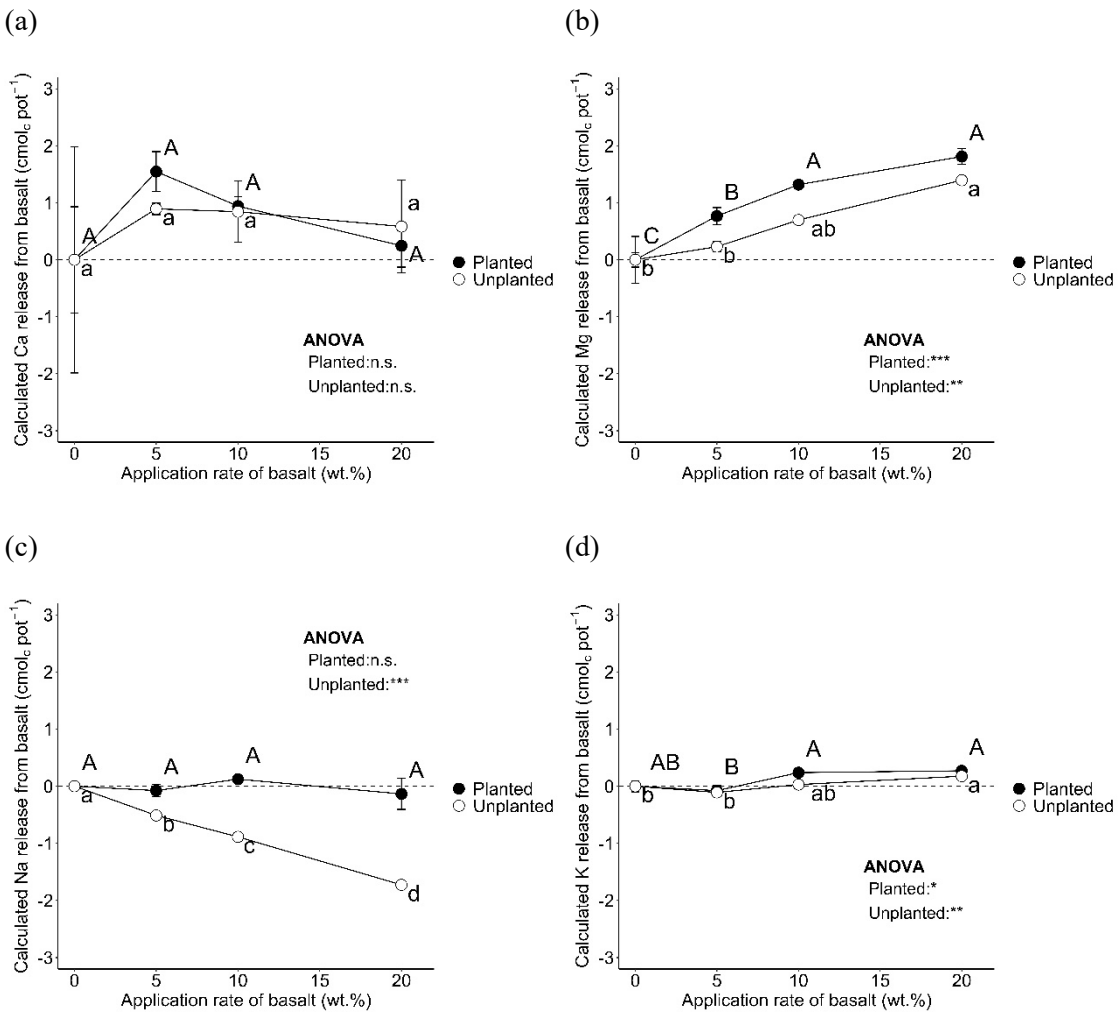

Figure 3-4. Calculated release of (a) Ca, (b) Mg, (c) Na and (d) K from basalt in planted and unplanted treatment. Points represent mean value of each application rate ± one standard error. One-way ANOVA was performed to detect significant differences among application rate of basalt in planted and unplanted plot each. Asterisks (*,**, ***) indicate *p*-values < 0.05, 0.01, 0.001, respectively. "n.s." indicates *p*-values > 0.05. Different uppercase letters and lowercase letters indicate significant differences among the treatments in planted and unplanted plot , respectively, determined via Tukey post hoc test.

Supplemental figure 3-1. Photographs of the soybean at R6 taken on August 29, 2023 with basalt and lime application treatments.

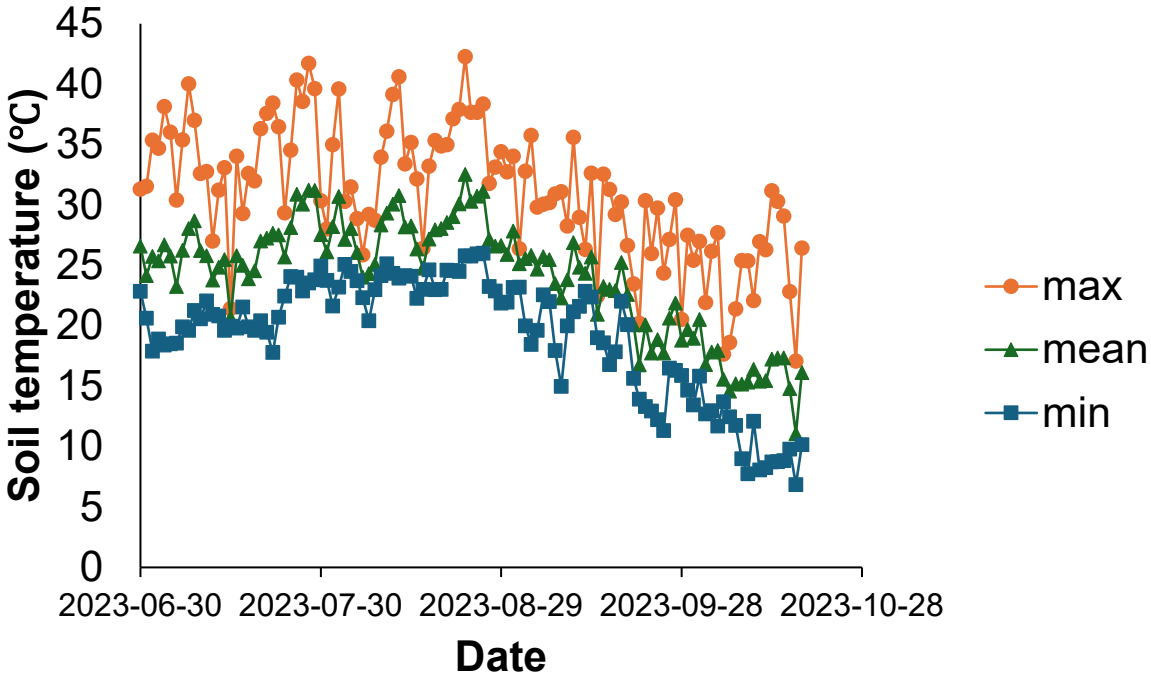

Supplemental figure 3-2. Daily soil temperature. Orange line shows maximum soil temperature, green line shows mean soil temperature, and blue line shows minimum soil temperature on a day.

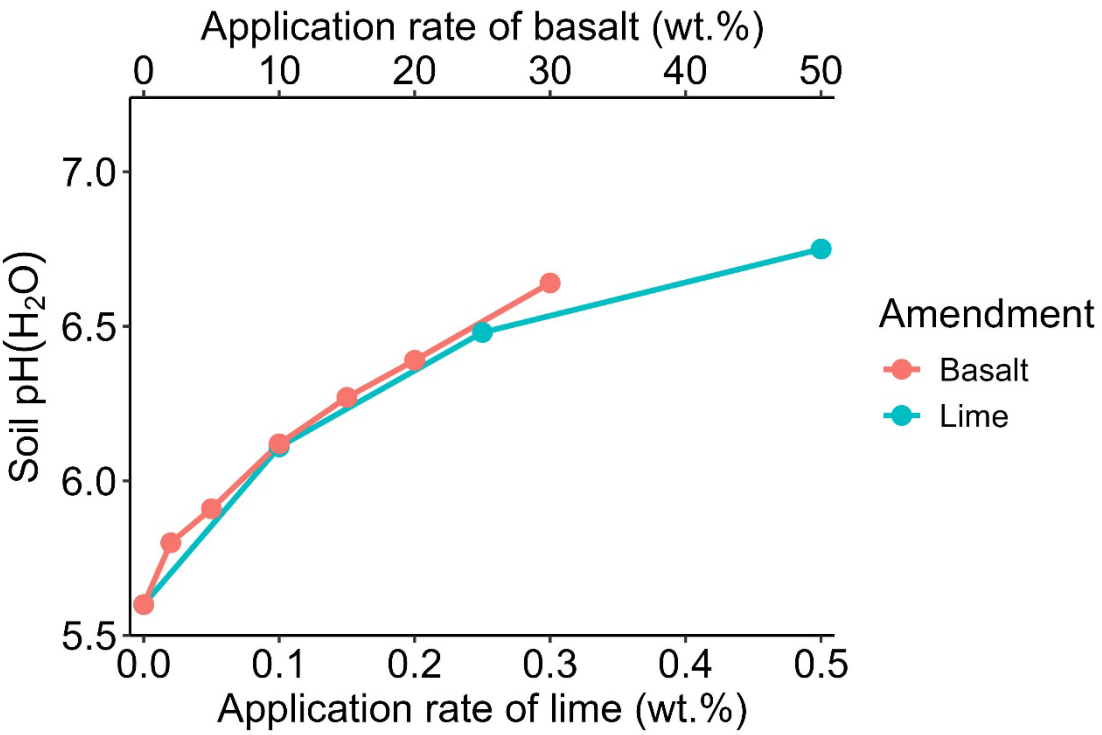

Supplemental figure 3-3. Neutralization curve by lime and basalt. Blue line shows the lime neutralization curve, and pink line shows basalt neutralization curve. The lower horizontal axis shows the application rate of lime, and upper horizontal axis shows the application rate of basalt.

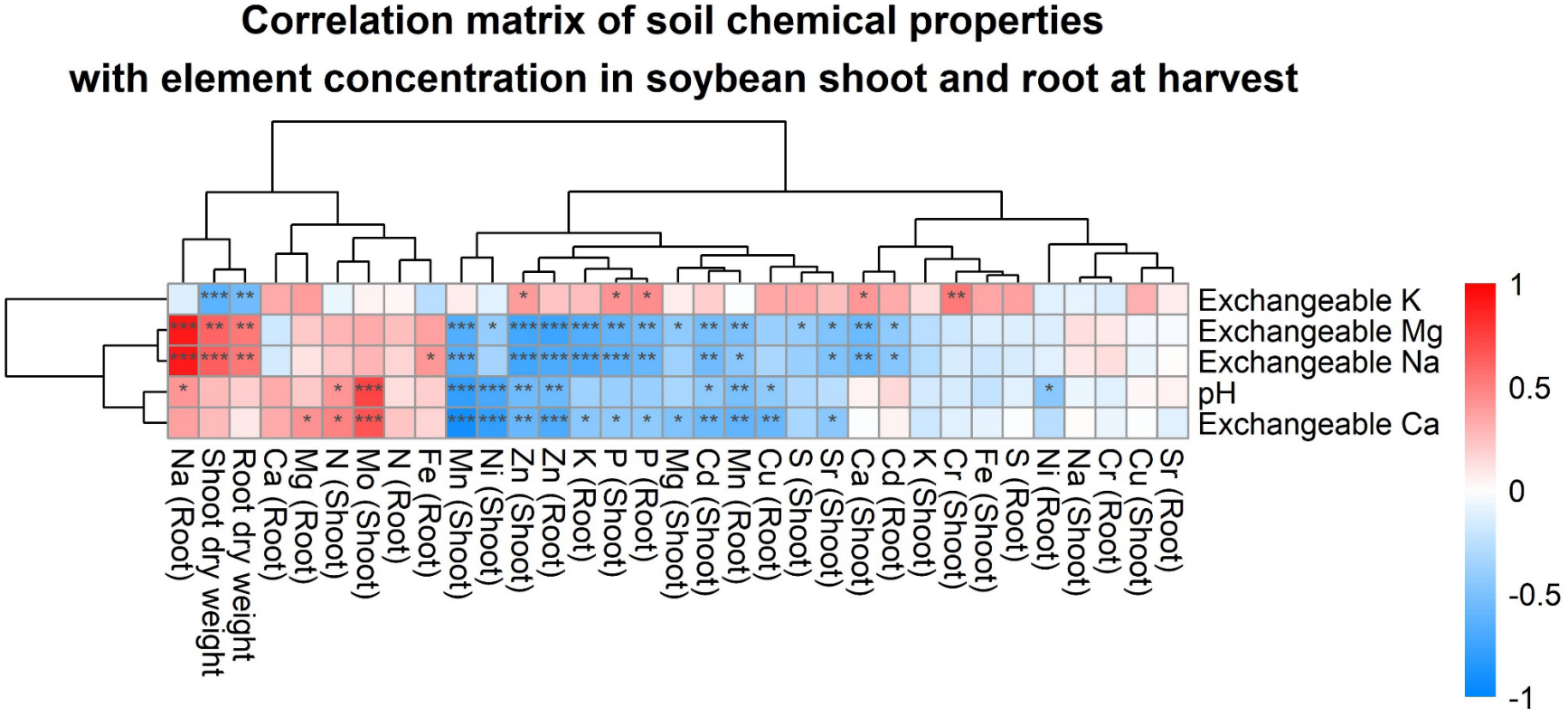

Supplemental figure 3-4. Correlation heatmap matrix of soil chemical properties at harvest with dry weight and elemental uptake in soybean at harvest across all treatments including Control, basalt and lime treatments. The heatmap was constructed using R with complete clustering method. Color expresses Pearson correlation coefficient based on the color scale bar. Asterisk (*, **, ***) denotes *p*-value < 0.05, 0.01, 0.001.

(a)

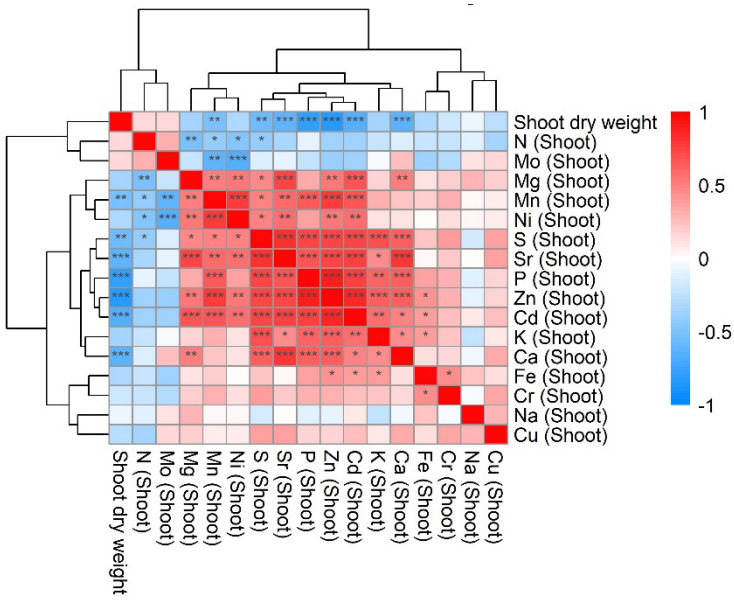

(b)

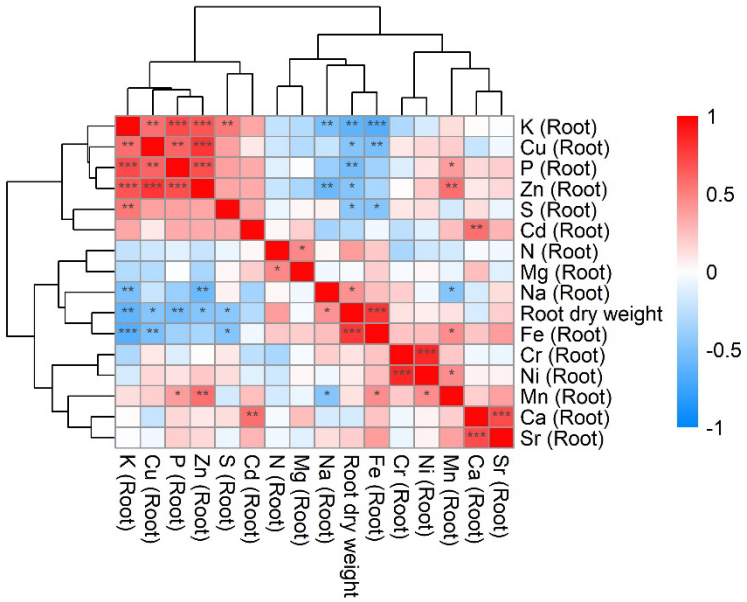

Supplemental figure 3-5. Correlation heatmap matrix of element concentration in soybean shoot**(a)** and root**(b)** at harvest. The heatmap was constructed using R with complete clustering method. Color expresses Pearson correlation coefficient based on the color scale bar. Asterisk (*, **, ***) denotes *p*-value < 0.05, 0.01, 0.001, respectively.

Supplemental table 3-1. Soil exchangeable cation concentrations before planting and after harvest.

Time	Treatment	Exchangeable cation concentration in soil (mg kg^{-1} soil)				Total cation ($cmol_c$ kg^{-1} soil)
		Ca	Mg	K	Na	
Before Planting (BP)	Control	3098 ± 13 cd	327 ± 2 bc	498 ± 8 ab	28 ± 1 d	19.7 ± 0.1 cd
	BA5	3002 ± 21 d	324 ± 2 bc	479 ± 20 ab	69 ± 1 c	19.3 ± 0.1 d
	BA10	3073 ± 33 cd	332 ± 1 b	443 ± 11 bc	104 ± 2 b	19.8 ± 0.2 cd
	BA20	3115 ± 28 cd	341 ± 1 a	414 ± 8 c	186 ± 1 a	20.3 ± 0.1 c
	Lime5	3211 ± 14 c	314 ± 3 de	495 ± 20 ab	25 ± 0 d	20.1 ± 0.0 c
	Lime10	3427 ± 22 b	310 ± 1 e	504 ± 13 ab	26 ± 0 d	21.2 ± 0.1 b
	Lime20	3969 ± 52 a	320 ± 2 cd	528 ± 3 a	29 ± 2 d	24.0 ± 0.3 a
	ANOVA	***	***	***	***	***
After Harvest (Planted) (AH_P)	Control	2863 ± 63 d	273 ± 6 b	257 ± 13 abc	33 ± 2 c	17.4 ± 0.3 d
	BA5	2858 ± 23 d	292 ± 7 b	214 ± 4 bc	68 ± 8 c	17.6 ± 0.2 cd
	BA10	2896 ± 17 cd	321 ± 5 a	214 ± 8 bc	117 ± 5 b	18.2 ± 0.1 bcd
	BA20	2910 ± 24 cd	348 ± 5 a	210 ± 11 c	181 ± 17 a	18.8 ± 0.3 bc
	Lime5	3086 ± 93 bc	278 ± 13 b	267 ± 5 a	34 ± 4 c	18.6 ± 0.6 bcd
	Lime10	3258 ± 5 b	269 ± 3 b	252 ± 23 abc	32 ± 2 c	19.3 ± 0.1 ab
	Lime20	3509 ± 27 a	276 ± 2 b	265 ± 5 ab	27 ± 2 c	20.6 ± 0.2 a
	ANOVA	***	***	**	***	***
After Harvest (Unplanted) (AH_U)	Control	2926 ± 132 a	305 ± 17 b	355 ± 5 a	23 ± 6 c	18.2 ± 0.8 a
	BA5	2896 ± 6 a	312 ± 4 b	329 ± 6 b	27 ± 1 bc	18.1 ± 0.0 a
	BA10	2968 ± 33 a	337 ± 0 ab	316 ± 3 b	38 ± 1 b	18.6 ± 0.2 a
	BA20	3006 ± 44 a	370 ± 2 a	313 ± 2 b	72 ± 2 a	19.2 ± 0.2 a
	ANOVA	n.s.	**	***	***	n.s.

Mean-values ± one standard error are shown. One-way ANOVA was performed to detect significant differences among the treatments within each sampling timing. Asterisks (**, ***) indicate *p*-values < 0.01, 0.001, respectively. “n.s.” indicates *p*-values > 0.05. Different letters indicate significant differences among the treatments determined via Tukey post hoc test. Total cation was calculated by following equation

$$\text{Total cation in soil} = \{(Ca\times2)/40.08 + (Mg\times2)/24.31 + K/39.10 + Na/22.99\}/10$$

, where Ca, Mg, K and Na are the concentration of exchangeable cation of each element in soil (mg kg^{-1} soil), and the unit of total cation in soil is $cmol_c$ kg^{-1} soil.

Table 4-1. Soil chemical properties during cultivation.

Treatment (T)	Planting (P)	pH (H_2O)			
		BP	R2	R6	R8
Control	Planted	5.55 ± 0.22 b	5.54 ± 0.05 b	5.55 ± 0.03 b	5.63 ± 0.04 c
	Unplanted		5.68 ± 0.11 ab	5.63 ± 0.07 b	5.75 ± 0.09 bc
BA5	Planted	5.97 ± 0.15 ab			5.89 ± 0.04 abc
	Unplanted				5.97 ± 0.15 abc
BA10	Planted	6.17 ± 0.08 ab	5.85 ± 0.06 ab	5.78 ± 0.08 ab	6.07 ± 0.08 ab
	Unplanted		5.96 ± 0.11 a	6.00 ± 0.07 a	6.10 ± 0.05 ab
BA20	Planted	6.44 ± 0.21 a			6.18 ± 0.08 a
	Unplanted				6.10 ± 0.10 ab
Lime	Planted	5.74 ± 0.15 ab	5.72 ± 0.09 ab	5.71 ± 0.06 ab	5.88 ± 0.08 abc
	Unplanted		5.82 ± 0.07 ab	5.73 ± 0.08 ab	5.92 ± 0.08 abc
ANOVA	(T)	**	**	***	***
	(P)	-	†	*	n.s.
	(T) x (P)	-	n.s.	n.s.	n.s.

Treatment (T)	Planting (P)	Exchangeable Ca (mg kg^{-1} soil)			
		BP	R2	R6	R8
Control	Planted	3056 ± 137 a	3204 ± 112 a	3126 ± 48 a	2989 ± 154 a
	Unplanted		3116 ± 169 a	3355 ± 169 a	3416 ± 146 a
BA5	Planted	3302 ± 181 a			3168 ± 59 a
	Unplanted				3166 ± 219 a
BA10	Planted	3144 ± 245 a	3295 ± 148 a	3053 ± 86 a	3148 ± 173 a
	Unplanted		3259 ± 155 a	3314 ± 141 a	3413 ± 187 a
BA20	Planted	3142 ± 113 a			3116 ± 165 a
	Unplanted				3233 ± 130 a
Lime	Planted	3547 ± 152 a	3481 ± 106 a	3484 ± 98 a	3598 ± 223 a
	Unplanted		3510 ± 180 a	3412 ± 144 a	3258 ± 117 a
ANOVA	(T)	n.s.	**	**	n.s.
	(P)	-	n.s.	*	n.s.
	(T) x (P)	-	n.s.	†	n.s.

Treatment (T)	Planting (P)	Exchangeable Mg (mg kg^{-1} soil)			
		BP	R2	R6	R8
Control	Planted	329 ± 12 a	317 ± 7 c	323 ± 6 b	320 ± 15 b
	Unplanted		317 ± 10 c	326 ± 1 b	349 ± 4 ab
BA5	Planted	377 ± 9 a			364 ± 7 ab
	Unplanted				369 ± 5 ab
BA10	Planted	375 ± 11 a	355 ± 8 ab	364 ± 1 a	367 ± 13 ab
	Unplanted		377 ± 10 a	369 ± 8 a	391 ± 11 ab
BA20	Planted	368 ± 23 a			389 ± 19 ab
	Unplanted				398 ± 25 a
Lime	Planted	358 ± 3 a	315 ± 1 c	324 ± 2 b	342 ± 9 ab
	Unplanted		335 ± 6 bc	329 ± 5 b	331 ± 17 ab
ANOVA	(T)	n.s.	***	***	***
	(P)	-	*	n.s.	n.s.
	(T) x (P)	-	n.s.	n.s.	n.s.

Table 4-1. continued.

Treatment (T)	Planting (P)	Exchangeable Na (mg kg^{-1} soil)							
		BP		R2		R6		R8	
Control	Planted	15.3 ± 2.2	b	42.7 ± 2.4	b	24.3 ± 1.4	b	10.2 ± 0.2	f
	Unplanted			32.4 ± 1.7	b	30.6 ± 1.7	b	11.4 ± 0.9	ef
BA5	Planted	46.5 ± 5.7	b					35.5 ± 2.2	d
	Unplanted							29.1 ± 1.2	de
BA10	Planted	72.4 ± 8.0	ab	83.7 ± 8.9	a	68.8 ± 11.2	a	59.9 ± 6.5	c
	Unplanted			78.7 ± 6.4	a	72.0 ± 4.3	a	70.5 ± 4.9	c
BA20	Planted	158.7 ± 45.0	a					104.6 ± 1.6	b
	Unplanted							130.5 ± 7.1	a
Lime	Planted	5.2 ± 2.1	b	34.3 ± 2.1	b	31.4 ± 2.9	b	9.7 ± 0.9	f
	Unplanted			33.5 ± 2.4	b	24.6 ± 2.4	b	8.4 ± 0.6	f
ANOVA	(T)	**		***		***		***	
	(P)	-		n.s.		n.s.		*	
	(T) x (P)	-		n.s.		n.s.		**	

Treatment (T)	Planting (P)	Exchangeable K (mg kg^{-1} soil)							
		BP		R2		R6		R8	
Control	Planted	170 ± 12	ab	209 ± 4	a	184 ± 2	ab	83 ± 24	a
	Unplanted			224 ± 7	a	242 ± 18	a	174 ± 19	a
BA5	Planted	196 ± 20	a					130 ± 14	a
	Unplanted							165 ± 14	a
BA10	Planted	150 ± 5	ab	234 ± 11	a	192 ± 17	ab	108 ± 13	a
	Unplanted			239 ± 14	a	214 ± 6	ab	147 ± 19	a
BA20	Planted	124 ± 20	b					94 ± 23	a
	Unplanted							88 ± 26	a
Lime	Planted	146 ± 1	ab	211 ± 27	a	163 ± 16	b	86 ± 16	a
	Unplanted			231 ± 7	a	205 ± 11	ab	163 ± 21	a
ANOVA	(T)	*		n.s.		n.s.		†	
	(P)	-		n.s.		**		***	
	(T) x (P)	-		n.s.		n.s.		†	

Mean-values ± one standard error are shown (n=3). “BP” indicates “before planting”, and R2, R6, and R8 indicate flowering stage, seed development stage, and full maturity stage, respectively. Samplings at R2 and R6 were conducted only in Control, BA10, and Lime treatments. Split-plot ANOVA was performed to detect significant differences among the “Treatments(T)”, “Planting(P)”, and their interaction “(T) x (P)” within each sampling timing. Symbols (†,*,**, ***) indicate *p*-values < 0.1, 0.05, 0.01, 0.001, respectively. “n.s.” indicates *p*-values > 0.1. Different letters indicate significant differences among the treatments determined via Tukey post hoc test.

Table 4-2. Stem length, shoot dry weight, and root dry weight of soybean at different growth stages.

Treatment	R2			R6			R8		
	Stem length (cm)	Shoot DW (g plant^{-1})	Root DW (g plant^{-1})	Stem length (cm)	Shoot DW (g plant^{-1})	Root DW (g plant^{-1})	Stem length (cm)	Shoot DW (g plant^{-1})	Root DW (g plant^{-1})
Control	50.4 ± 1.7 a	8.70 ± 0.21 a	1.65 ± 0.12 a	51.6 ± 2.2 a	23.9 ± 1.8 a	2.08 ± 0.04 a	53.4 ± 0.7 a	24.6 ± 0.8 a	1.80 ± 0.08 a
BA5							49.3 ± 0.8 bc	23.6 ± 1.4 a	1.70 ± 0.07 a
BA10	44.8 ± 3.5 a	6.63 ± 0.45 a	1.36 ± 0.13 a	48.7 ± 3.2 a	25.4 ± 0.2 a	2.06 ± 0.09 a	49.2 ± 0.7 bc	25.2 ± 1.0 a	1.69 ± 0.11 a
BA20							46.8 ± 0.8 c	24.6 ± 0.7 a	1.61 ± 0.06 a
Lime	50.0 ± 0.5 a	8.11 ± 0.72 a	1.60 ± 0.13 a	50.9 ± 1.1 a	22.3 ± 1.6 a	1.95 ± 0.14 a	51.2 ± 0.6 ab	24.0 ± 1.3 a	1.61 ± 0.04 a
ANOVA	**n.s.**	**n.s.**	**n.s.**	**n.s.**	**n.s.**	**n.s.**	***	**n.s.**	**n.s.**

Mean-values ± one standard error are shown. The sample size was three except for shoot length at R8, which was sixty. R2, R6, and R8 indicate flowering stage, seed development stage, and full maturity stage, respectively. Samplings at R2 and R6 were conducted only in Control, BA10, and Lime treatments. Split-plot ANOVA was performed to detect significant differences among the treatments. Asterisks (***) indicate p-values < 0.001. "n.s." indicates p-values > 0.1. Different letters indicate significant differences among the treatments determined via Tukey post hoc test. Dry weight of each part (i.e. leaf, stem, pod, grain) is shown in supplemental table 4-1.

Table 4-3. Yield-related indices of soybean.

Treatment	Yield-related indices			
	Yield (kg $10a^{-1}$)	100 grain weight (g)	pod number ($plant^{-1}$)	grain number (pod^{-1})
Control	316 ± 18 a	34.5 ± 0.5 a	22.8 ± 0.7 a	1.83 ± 0.02 a
BA5	308 ± 24 a	32.6 ± 1.3 a	24.0 ± 0.7 a	1.77 ± 0.04 a
BA10	339 ± 13 a	33.3 ± 0.6 a	25.3 ± 0.8 a	1.82 ± 0.05 a
BA20	331 ± 8 a	33.8 ± 1.6 a	25.1 ± 0.8 a	1.76 ± 0.03 a
Lime	313 ± 22 a	34.2 ± 1.4 a	23.1 ± 0.7 a	1.78 ± 0.08 a
ANOVA	n.s.	n.s.	†	n.s.

Mean-values ± one standard error are shown. The sample size was three except for pod number, which was sixty. Split-plot ANOVA was performed to detect significant differences among the treatments. Symbol (†) indicates *p*-values < 0.1. "n.s." indicates *p*-values > 0.1. Different letters indicate significant differences among the treatments determined via Tukey post hoc test.

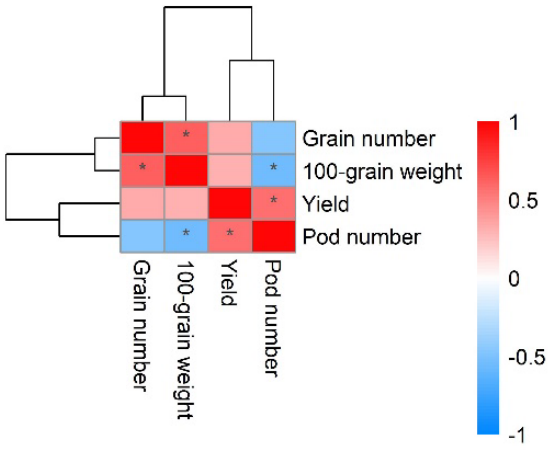

Figure 4-1. Correlation heatmap matrix of yield-related indices. The heatmap was constructed using R with complete clustering method. Color expresses Pearson correlation coefficient based on the color scale bar. Asterisk (*) denotes *p*-value < 0.05.

Table 4-4. Element concentrations of soybean in shoot at R2.

Treatment	Shoot element concentration at R2 (mg g^{-1} shoot)							
	N	P	K	Ca	Mg	S	Fe	Mn
Control	28.6 ± 0.6 a	2.83 ± 0.12 a	24.9 ± 0.9 a	11.6 ± 0.5 a	4.12 ± 0.09 a	4.36 ± 0.12 a	0.134 ± 0.006 a	0.0670 ± 0.0040 a
BA10	30.3 ± 0.3 a	2.80 ± 0.07 a	26.4 ± 1.0 a	11.2 ± 0.3 a	3.96 ± 0.06 a	4.53 ± 0.06 a	0.178 ± 0.009 a	0.0442 ± 0.0021 b
Lime	29.4 ± 0.5 a	2.61 ± 0.13 a	24.0 ± 1.1 a	11.7 ± 0.4 a	3.91 ± 0.05 a	4.32 ± 0.14 a	0.143 ± 0.017 a	0.0492 ± 0.0017 b
ANOVA	**	**n.s.**	**n.s.**	**n.s.**	**n.s.**	**n.s.**	**n.s.**	**

Treatment	Shoot element concentration at R2 (μg g^{-1} shoot)							
	Zn	Cu	Mo	Ni	Sr	Na	Cd	Cr
Control	52.1 ± 2.4 a	20.0 ± 2.9 a	N.D.	0.952 ± 0.246 a	40.8 ± 1.5 a	28.3 ± 3.3 a	0.134 ± 0.018 a	1.85 ± 0.25 a
BA10	45.0 ± 2.7 a	19.8 ± 2.8 a	0.257 ± 0.101	0.644 ± 0.034 a	40.4 ± 1.0 a	36.2 ± 2.7 a	0.062 ± 0.030 a	1.88 ± 0.30 a
Lime	43.0 ± 3.7 a	14.9 ± 1.1 a	0.278 ± 0.116	0.643 ± 0.044 a	38.9 ± 1.0 a	31.1 ± 4.6 a	0.119 ± 0.005 a	1.24 ± 0.09 a
ANOVA	**	**n.s.**	**-**	**n.s.**	**n.s.**	**n.s.**	†	†

Mean-values ± one standard error are shown (n=3). Sampling at R2 (flowering stage) was conducted only in Control, BA10, and Lime treatments. Split-plot ANOVA was performed to detect significant differences among the treatments. Symbols (†,**) indicate *p*-values < 0.1, 0.01. "n.s." indicates *p*-values > 0.1. "N.D." indicates not detected. Different letters indicate significant differences among the treatments determined via Tukey post hoc test.

Table 4-5. Element concentrations of soybean in shoot at R6.

Treatment	Shoot element concentration at R6 (mg g^{-1} shoot)															
	N		P		K		Ca		Mg		S		Fe		Mn	
Control	32.1 ± 1.5	a	3.12 ± 0.11	a	18.1 ± 0.1	a	8.81 ± 0.51	a	3.29 ± 0.15	a	3.97 ± 0.08	a	0.0852 ± 0.0076	a	0.0471 ± 0.0021	a
BA10	34.0 ± 0.8	a	3.14 ± 0.16	a	18.4 ± 0.3	a	8.90 ± 0.13	a	3.20 ± 0.03	a	4.00 ± 0.08	a	0.0841 ± 0.0024	a	0.0359 ± 0.0015	b
Lime	33.7 ± 1.2	a	3.22 ± 0.12	a	17.7 ± 0.6	a	9.55 ± 0.58	a	3.37 ± 0.21	a	3.96 ± 0.04	a	0.0799 ± 0.0072	a	0.0394 ± 0.0006	b
ANOVA	**n.s.**		**n.s.**		**n.s.**		**n.s.**		**n.s.**		**n.s.**		**n.s.**		**	

Treatment	Shoot element concentration at R6 (µg g^{-1} shoot)															
	Zn		Cu		Mo		Ni		Sr		Na		Cd		Cr	
Control	38.5 ± 2.8	a	15.8 ± 4.7	a	0.052 ± 0.013	a	0.905 ± 0.111	a	33.6 ± 1.7	a	29.3 ± 0.6	a	0.0574 ± 0.0223	a	2.37 ± 0.67	a
BA10	39.2 ± 3.9	a	22.1 ± 8.4	a	0.124 ± 0.018	a	0.625 ± 0.028	a	33.9 ± 1.0	a	30.0 ± 1.1	a	0.0830 ± 0.0093	a	2.03 ± 0.31	a
Lime	33.4 ± 2.4	a	10.2 ± 1.1	a	0.180 ± 0.066	a	0.632 ± 0.044	a	33.7 ± 2.3	a	31.7 ± 2.7	a	0.0529 ± 0.0132	a	1.79 ± 0.29	a
ANOVA	**n.s.**		**n.s.**		**n.s.**		*		**n.s.**		**n.s.**		**n.s.**		**n.s.**	

Mean-values ± one standard error are shown (n=3). Sampling at R6 (seed development stage) was conducted only in Control, BA10, and Lime treatments. Split-plot ANOVA was performed to detect significant differences among the treatments. Symbols (*,**) indicate *p*-values < 0.05, 0.01. "n.s." indicates *p*-values > 0.1. Different letters indicate significant differences among the treatments determined via Tukey post hoc test.

Table 4-6. Element concentrations in grain at R8.

Treatment	Grain element concentration at R8 (mg g^{-1} grain)							
	N	P	K	Ca	Mg	S	Fe	Mn
Control	60.1 ± 1.3 a	6.39 ± 0.23 a	23.6 ± 0.4 a	2.56 ± 0.07 a	2.81 ± 0.12 a	3.42 ± 0.07 a	0.0971 ± 0.0052 a	0.0252 ± 0.0008 a
BA5	62.1 ± 1.6 a	6.54 ± 0.25 a	22.7 ± 0.5 a	2.41 ± 0.15 a	2.75 ± 0.02 a	3.50 ± 0.11 a	0.0891 ± 0.0030 a	0.0223 ± 0.0005 a
BA10	61.1 ± 0.5 a	6.51 ± 0.04 a	23.5 ± 0.6 a	2.43 ± 0.09 a	2.79 ± 0.07 a	3.56 ± 0.23 a	0.0954 ± 0.0052 a	0.0231 ± 0.0013 a
BA20	61.6 ± 0.8 a	6.58 ± 0.26 a	23.4 ± 0.6 a	2.39 ± 0.11 a	2.74 ± 0.04 a	3.56 ± 0.03 a	0.0956 ± 0.0061 a	0.0215 ± 0.0006 a
Lime	61.3 ± 0.1 a	6.62 ± 0.23 a	23.4 ± 0.8 a	2.32 ± 0.04 a	2.73 ± 0.07 a	3.56 ± 0.10 a	0.0960 ± 0.0049 a	0.0219 ± 0.0008 a
ANOVA	**n.s.**	**n.s.**	**n.s.**	**n.s.**	**n.s.**	**n.s.**	**n.s.**	†

Treatment	Grain element concentration at R8 (µg g^{-1} grain)							
	Zn	Cu	Mo	Ni	Sr	Na	Cd	Cr
Control	55.7 ± 4.4 a	15.3 ± 1.6 a	0.401 ± 0.036 b	3.24 ± 0.12 a	3.89 ± 0.30 a	80.6 ± 26.1 a	0.0704 ± 0.0058 a	2.33 ± 0.28 a
BA5	52.9 ± 4.0 a	14.1 ± 1.1 a	0.483 ± 0.102 ab	2.53 ± 0.08 b	3.78 ± 0.03 a	72.3 ± 14.9 a	0.0693 ± 0.0178 a	1.87 ± 0.05 a
BA10	48.1 ± 2.5 a	15.7 ± 0.6 a	0.575 ± 0.060 ab	2.51 ± 0.11 b	4.08 ± 0.17 a	94.1 ± 8.5 a	0.0648 ± 0.0027 a	2.01 ± 0.03 a
BA20	48.1 ± 1.5 a	16.0 ± 1.7 a	0.935 ± 0.098 a	2.19 ± 0.02 b	3.69 ± 0.26 a	55.6 ± 11.4 a	0.0597 ± 0.0089 a	1.88 ± 0.04 a
Lime	52.6 ± 3.0 a	14.5 ± 0.8 a	0.579 ± 0.201 ab	2.37 ± 0.10 b	3.33 ± 0.17 a	72.9 ± 5.6 a	0.0506 ± 0.0045 a	2.01 ± 0.26 a
ANOVA	**n.s.**	**n.s.**	*	***	**n.s.**	**n.s.**	**n.s.**	**n.s.**

Mean-values ± one standard error are shown (n=3). Split-plot ANOVA was performed to detect significant differences among the treatments. Symbols (†, *, ***) indicates *p*-values < 0.1, 0.05, 0.001, respectively. “n.s.” indicates *p*-values > 0.1. Different letters indicate significant differences among the treatments determined via Tukey post hoc test.

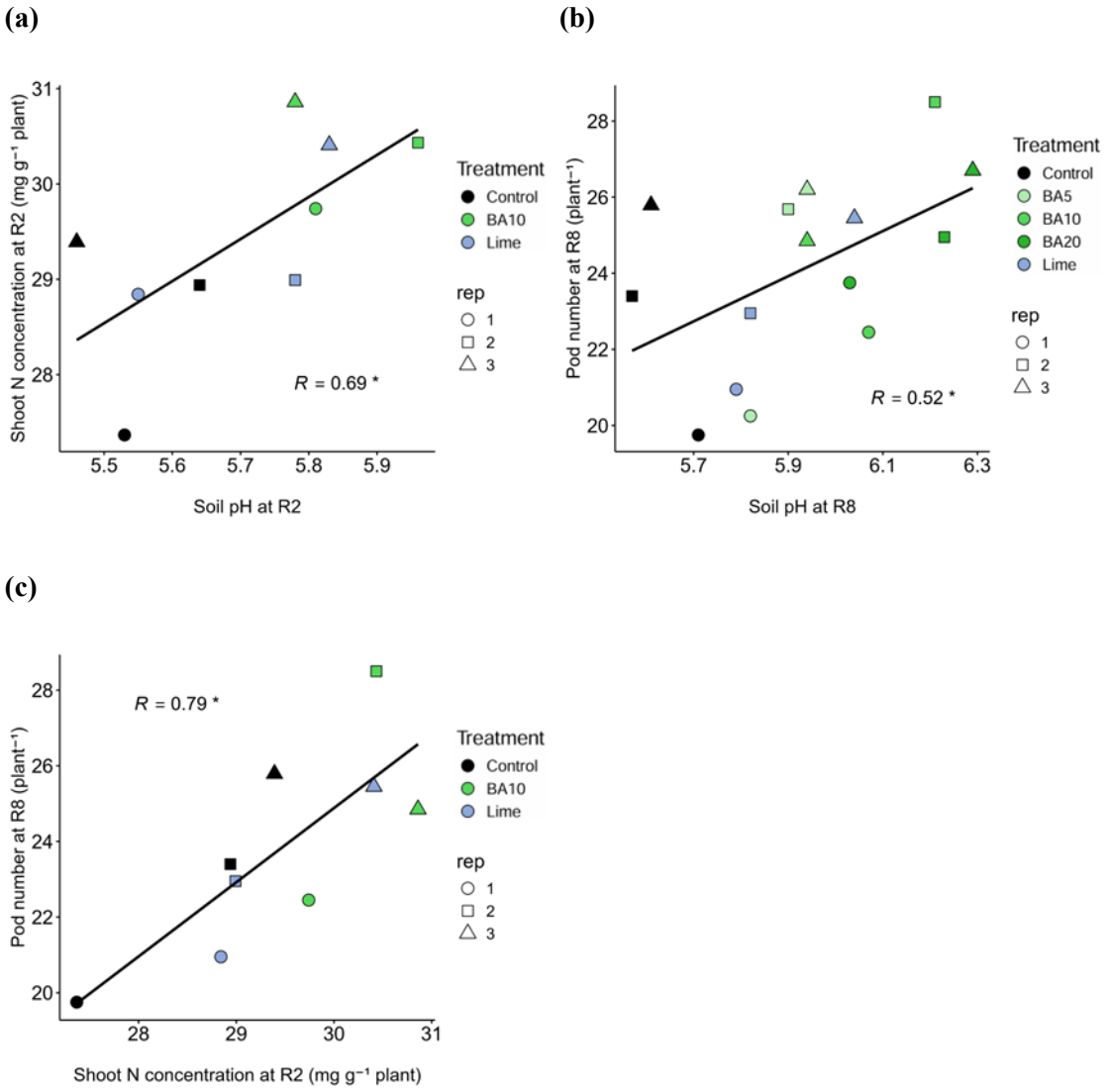

Figure 4-2. Relationships among soil pH, shoot N concentration at R2 and pod number at R8. **(a)**Correlation between soil pH at R2 and shoot N concentration at R2, **(b)**between soil pH at R8 and pod number at R8, **(c)**between shoot N concentration at R2 and pod number at R8**.** R2 and R8 indicate flowering stage and full maturity stage, respectively. Sampling at R2 was conducted only in Control, BA10, and Lime treatments. "rep" indicates plot replication. Linear regression analysis was performed. *R* denotes the Pearson correlation coefficient. Asterisks (*) denotes *p*-value < 0.05.

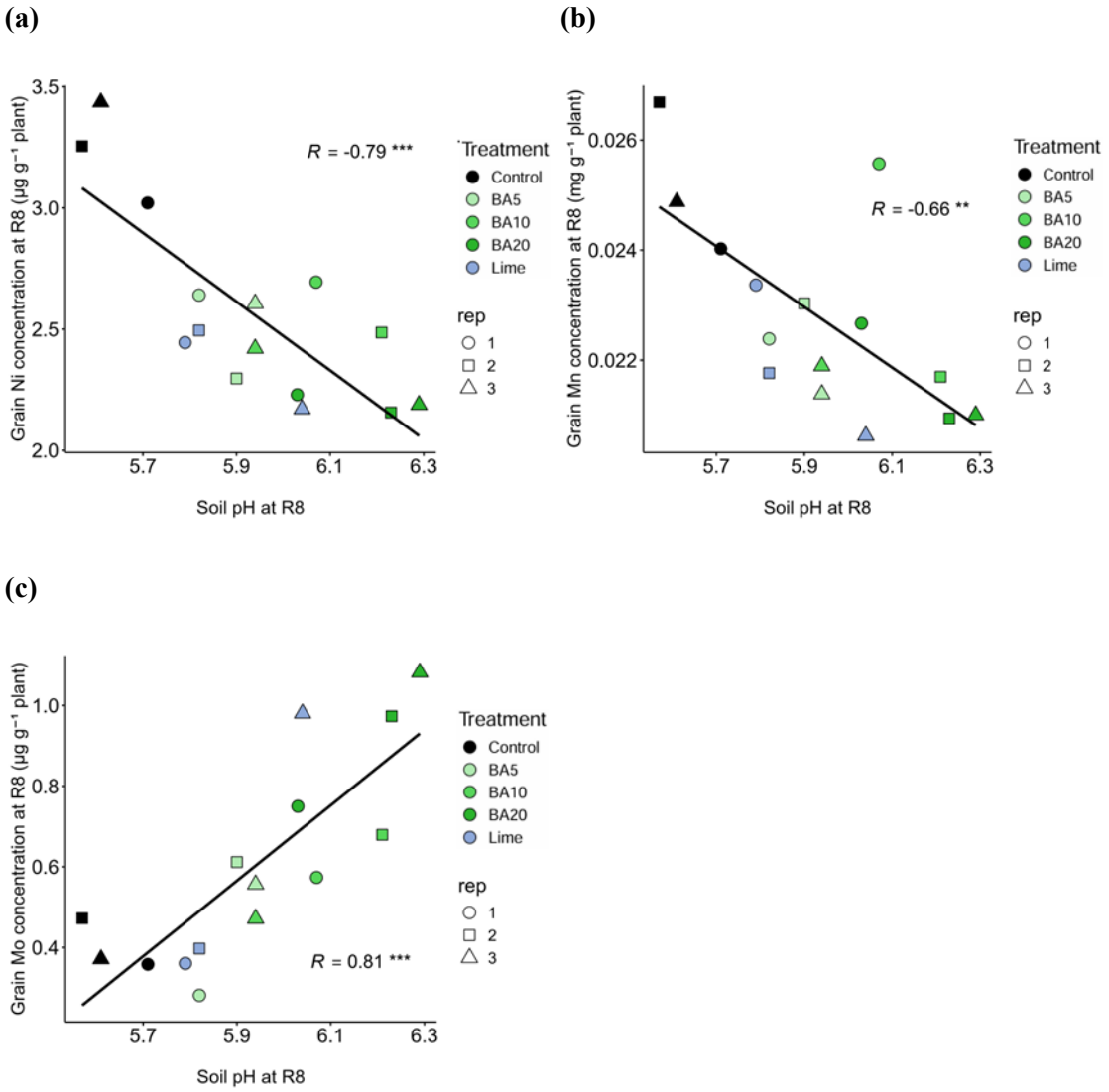

Figure 4-3. Relationships between soil pH and element concentrations of **(a)** Ni, **(b)** Mn, and **(c)** Mo in grain. "rep" indicates plot replication. Linear regression analysis was performed. *R* denotes the Pearson correlation coefficient. Asterisks (**,***) denote *p*-value < 0.01, 0.001, respectively.

Table 4-7. Changes in easily weatherable silicate mineral contents in soil during cultivation.

Treatment (T)	Planting (P)	Ca-plagioclase (g kg^{-1} soil)			Pyroxene (g kg^{-1} soil)		
		BP	R8	ΔCa-plagioclase	BP	R8	ΔPyroxene
Control	Planted	144 ± 5 b	137 ± 21 b	-7.4 ± 18.8 a	12.9 ± 1.4 a	11.4 ± 0.8 c	-1.49 ± 0.68 a
	Unplanted		146 ± 8 b	2.5 ± 12.6 a		10.1 ± 0.5 c	-2.83 ± 1.14 a
BA10	Planted	200 ± 9 ab	217 ± 10 a	17.1 ± 15.0 a	21.1 ± 4.4 a	17.7 ± 2.9 bc	-3.37 ± 1.67 a
	Unplanted		206 ± 6 a	5.5 ± 14.0 a		23.6 ± 3.4 ab	2.52 ± 7.62 a
BA20	Planted	259 ± 30 a	241 ± 3 a	-17.9 ± 31.2 a	28.1 ± 5.6 a	21.7 ± 0.7 ab	-6.46 ± 4.92 a
	Unplanted		230 ± 9 a	-28.6 ± 21.6 a		30.7 ± 0.6 a	2.61 ± 6.18 a
ANOVA	(T)	*	***	n.s.	n.s.	***	n.s.
	(P)	-	n.s.	n.s.	-	*	n.s.
	(T) x (P)	-	n.s.	n.s.	-	†	n.s.

Mean-values ± one standard error are shown (n=3). “BP” indicates “before planting”, and R8 indicates full maturity stage. “ΔCa-plagioclase” and “ΔPyroxene” were calculated as follows:

ΔCa-plagioclase = (Ca-plagioclase content at R8) – (Ca-plagioclase content at BP)

(ΔPyroxene = (Pyroxene content at R8) – (Pyroxene content at BP))

Soil mineral composition was measured only in Control, BA10, BA20. Split-plot ANOVA was performed to detect significant differences among the treatments. Symbols (†,*,***) indicate *p*-values < 0.1, 0.05, 0.001. “n.s.” indicates *p*-values > 0.1. Different letters indicate significant differences among the treatments determined via Tukey post hoc test.

(a)

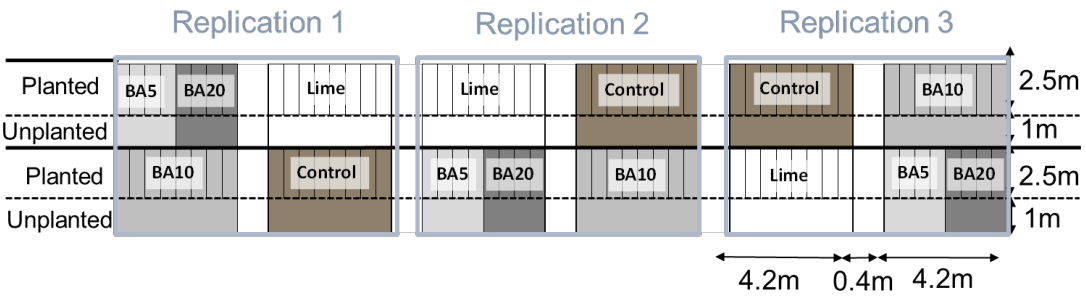

(b) **(c)**

Supplemental figure 4-1. The experimental field design. **(a)** schematic diagram of the field design. Control plots (white squares) had no basalt. BA5, BA10, BA20 (pale blue, blue, and deep blue squares) had 5, 10, 20 wt.% of basalt, respectively, in the 0-15 cm of surface layer. Lime plots (gray squares) had 0.01 wt.% of lime, which corresponds to the soil pH in BA10 plots. Each type of plot was prepared in triplicate. Each plot consists of planted and unplanted area. **(b)** Aerial photograph after the basalt application and **(c)** after the tillage on May 19, 2023.

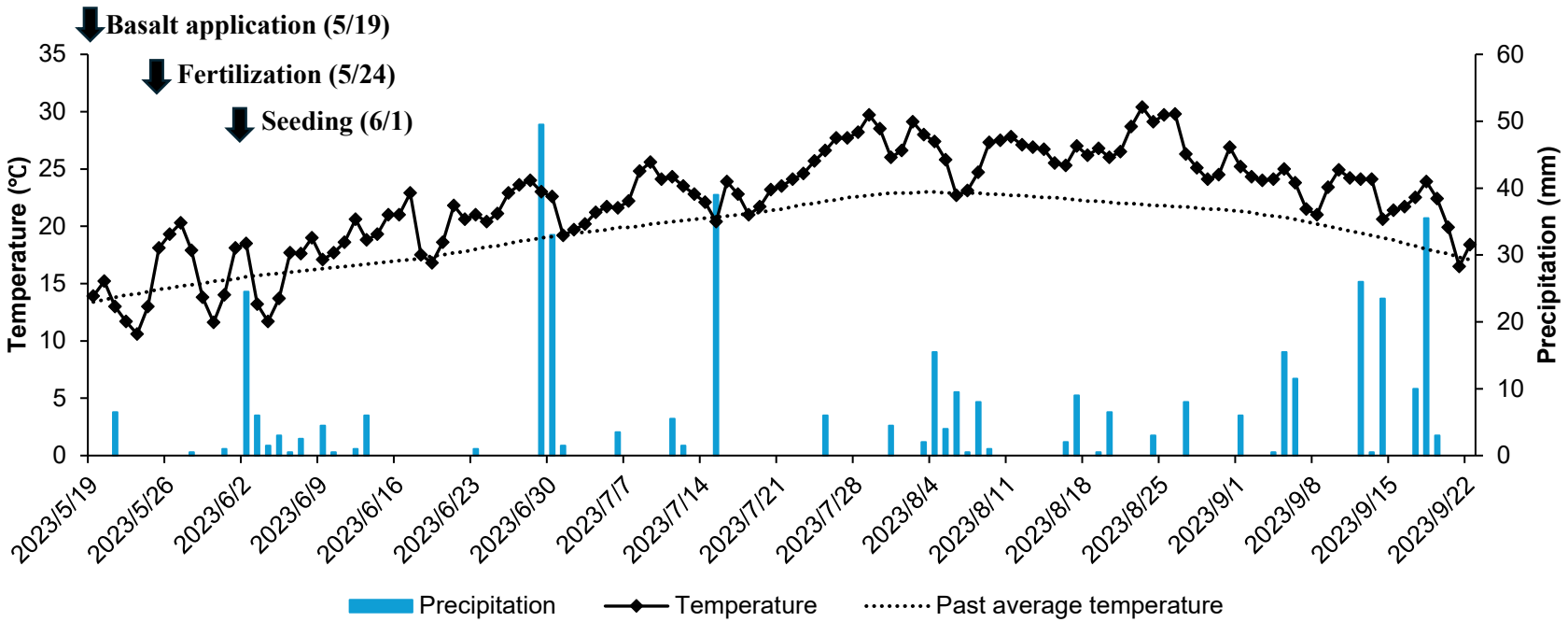

Supplemental figure 4-2. Climate conditions during the experiment. Points with solid line represent daily mean temperature during the experiment. Dotted line represents average daily mean temperature for the last 30 years. Bars represent the total daily precipitation.

(a)

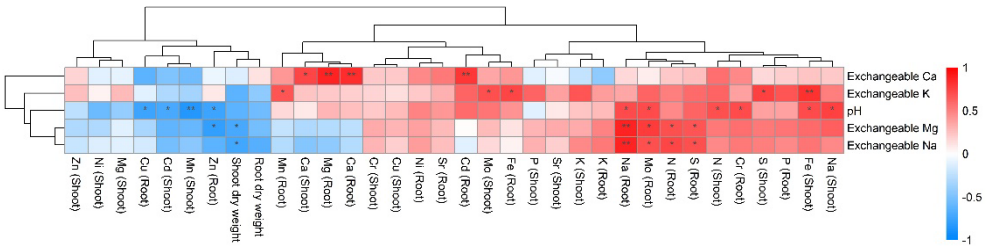

(b)

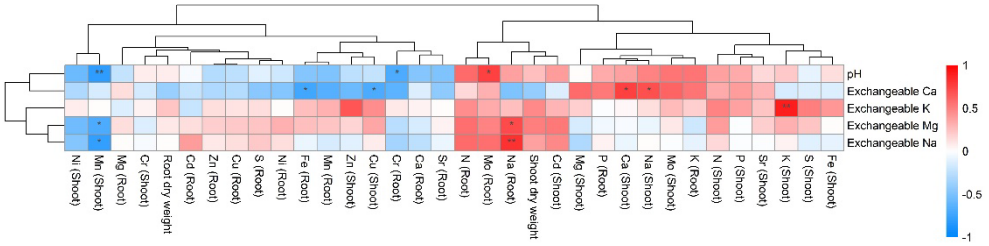

(c)

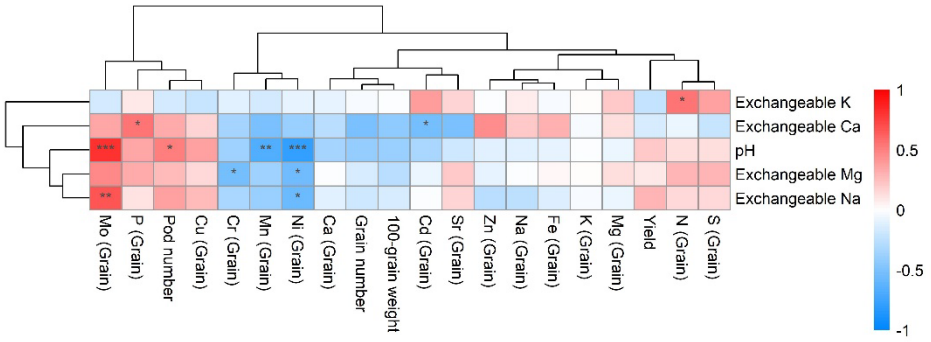

Supplemental figure 4-3. Correlation heatmap matrix of soil chemical properties with dry weight and element concentration in both shoot and root at R2**(a)** and R6**(b)**, and yield-related indices and element concentrations in grain at R8**(c)**. R2, R6, and R8 indicate flowering stage, seed development stage, and full maturity stage, respectively. Samplings at R2 and R6 were conducted only in Control, BA10, and Lime treatments. The heatmaps were constructed using R with complete clustering method. Color expresses Pearson correlation coefficient based on the color scale bar. Asterisks (*,**,***) denote *p*-value < 0.05, 0.01, 0.001, respectively.

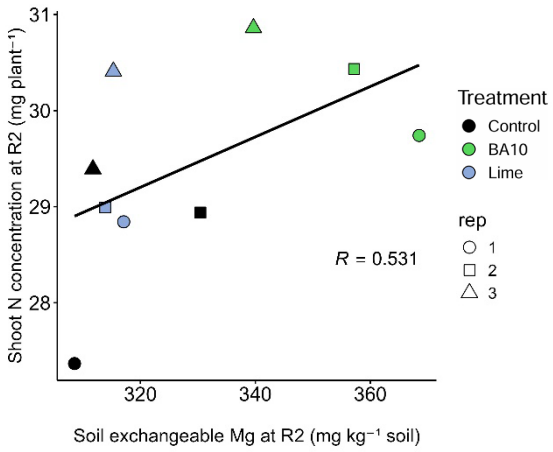

Supplemental figure 4-4. Correlation between soil exchangeable Mg at R2 and shoot N concentration at R2. Linear regression analysis was performed. *R* denotes the Pearson correlation coefficient. Significant correlation was not observed.

Supplemental table 4-1. Dry weight in each part at different growth stages.

Growth stage	Treatment	Dry weight in each part (g plant^{-1})						
		leaf	stem	pod	grain	shoot	root	total
R2	Control	4.72 ± 0.10 a	3.98 ± 0.14 a	-	-	8.70 ± 0.21 a	1.65 ± 0.12 a	10.3 ± 0.3 a
	BA10	3.74 ± 0.30 a	2.89 ± 0.43 b	-	-	6.63 ± 0.45 a	1.36 ± 0.13 a	8.0 ± 0.5 a
	Lime	4.48 ± 0.34 a	3.63 ± 0.39 ab	-	-	8.11 ± 0.72 a	1.60 ± 0.13 a	9.7 ± 0.8 a
	ANOVA	n.s.	n.s.			n.s.	n.s.	n.s.
R6	Control	6.52 ± 0.40 a	7.99 ± 0.64 a	4.58 ± 0.45 a	4.78 ± 0.31 a	23.9 ± 1.8 a	2.08 ± 0.04 a	25.9 ± 1.8 a
	BA10	6.68 ± 0.05 a	8.15 ± 0.11 a	5.15 ± 0.17 a	5.45 ± 0.13 a	25.4 ± 0.2 a	2.06 ± 0.09 a	27.5 ± 0.2 a
	Lime	6.29 ± 0.42 a	7.63 ± 0.41 a	4.32 ± 0.26 a	4.04 ± 0.71 a	22.3 ± 1.6 a	1.95 ± 0.14 a	24.2 ± 1.7 a
	ANOVA	n.s.	n.s.	n.s.	n.s.	n.s.	n.s.	n.s.
R8	Control	-	5.90 ± 0.19 a	4.42 ± 0.17 a	14.2 ± 0.8 a	24.6 ± 0.8 a	1.80 ± 0.08 a	26.4 ± 0.7 a
	BA5	-	5.31 ± 0.02 a	4.48 ± 0.36 a	13.9 ± 1.1 a	23.6 ± 1.4 a	1.70 ± 0.07 a	25.3 ± 1.4 a
	BA10	-	5.31 ± 0.25 a	4.65 ± 0.23 a	15.2 ± 0.6 a	25.2 ± 1.0 a	1.69 ± 0.11 a	26.9 ± 1.1 a
	BA20	-	5.04 ± 0.37 a	4.69 ± 0.07 a	14.9 ± 0.4 a	24.6 ± 0.7 a	1.61 ± 0.06 a	26.2 ± 0.8 a
	Lime	-	5.40 ± 0.23 a	4.51 ± 0.24 a	14.1 ± 1.0 a	24.0 ± 1.3 a	1.61 ± 0.04 a	25.6 ± 1.3 a
	ANOVA		n.s.	n.s.	n.s.	n.s.	n.s.	n.s.

Mean-values ± one standard error are shown (n=3). R2, R6, and R8 indicate flowering stage, seed development stage, and full maturity stage, respectively. Samplings at R2 and R6 were conducted only in Control, BA10, and Lime treatments. Shoot dry weight is a sum of leaf, stem, pod, and grain dry weight. Total dry weight is a sum of shoot and root dry weight. Split-plot ANOVA was performed to detect significant differences among the treatments. Asterisks (**) indicate p-values < 0.01. “n.s.” indicates p-values > 0.1. Different letters indicate significant differences among the treatments determined via Tukey post hoc test.

Supplemental table 4-2. Element concentrations of soybean in root at R2**.**

Treatment	Root element concentration at R2 (mg g^{-1} root)															
	N		P		K		Ca		Mg		S		Fe		Mn	
Control	15.8 ± 1.1	a	1.89 ± 0.09	a	12.9 ± 0.2	a	3.73 ± 0.18	a	1.83 ± 0.06	a	2.67 ± 0.11	a	0.442 ± 0.037	a	0.0266 ± 0.0007	a
BA10	18.0 ± 0.5	a	2.00 ± 0.05	a	13.4 ± 0.7	a	3.75 ± 0.32	a	1.88 ± 0.12	a	3.11 ± 0.04	a	0.829 ± 0.287	a	0.0292 ± 0.0075	a
Lime	15.7 ± 0.7	a	1.90 ± 0.11	a	12.9 ± 0.3	a	3.86 ± 0.18	a	2.10 ± 0.08	a	2.89 ± 0.10	a	0.703 ± 0.185	a	0.0313 ± 0.0053	a
ANOVA	**n.s.**		**n.s.**		**n.s.**		**n.s.**		**n.s.**		†		**n.s.**		**n.s.**	

Treatment	Root element concentration at R2 (µg g^{-1} root)															
	Zn		Cu		Mo		Ni		Sr		Na		Cd		Cr	
Control	24.3 ± 2.0	a	17.5 ± 1.8	a	0.94 ± 0.10	b	2.24 ± 0.22	a	24.5 ± 0.9	a	140 ± 25	b	0.190 ± 0.015	a	3.59 ± 0.37	a
BA10	19.3 ± 1.0	a	14.2 ± 0.6	a	1.87 ± 0.20	a	2.93 ± 0.94	a	25.6 ± 1.0	a	336 ± 28	a	0.247 ± 0.037	a	7.04 ± 1.77	a
Lime	22.4 ± 1.3	a	15.4 ± 3.1	a	1.27 ± 0.12	ab	1.91 ± 0.32	a	24.2 ± 0.6	a	161 ± 8	b	0.264 ± 0.054	a	4.21 ± 0.73	a
ANOVA	*		**n.s.**		*		**n.s.**		*		**		**n.s.**		**n.s.**	

Mean-values ± one standard error are shown (n=3). R2 indicates flowering stage. Samplings at R2 was conducted only in Control, BA10, and Lime treatments. Split-plot ANOVA was performed to detect significant differences among the treatments. Symbols (†,*,**) indicate *p*-values < 0.1, 0.05, 0.01. “n.s.” indicates *p*-values > 0.1. Different letters indicate significant differences among the treatments determined via Tukey post hoc test.

Supplemental table 4-3. Element concentrations of soybean in root at R6.

Treatment	Root element concentration at R6 (mg g^{-1} root)															
	N		P		K		Ca		Mg		S		Fe		Mn	
Control	7.01 ± 0.44	a	1.05 ± 0.11	a	8.26 ± 0.26	a	2.44 ± 0.07	a	1.44 ± 0.18	a	1.69 ± 0.21	a	0.761 ± 0.037	a	0.0245 ± 0.0016	a
BA10	9.59 ± 1.78	a	1.16 ± 0.21	a	8.19 ± 0.32	a	2.25 ± 0.03	a	1.59 ± 0.13	a	1.80 ± 0.06	a	0.823 ± 0.312	a	0.0254 ± 0.0101	a
Lime	7.93 ± 0.61	a	1.38 ± 0.08	a	8.69 ± 0.69	a	2.22 ± 0.08	a	1.66 ± 0.26	a	1.64 ± 0.11	a	0.487 ± 0.059	a	0.0168 ± 0.0016	a
ANOVA	**n.s.**		**n.s.**		**n.s.**		*		**n.s.**		**n.s.**		**n.s.**		**n.s.**	

Treatment	Root element concentration at R6 (µg g^{-1} root)															
	Zn		Cu		Mo		Ni		Sr		Na		Cd		Cr	
Control	117 ± 49	a	174 ± 79	a	0.369 ± 0.145	a	3.26 ± 0.97	a	17.4 ± 0.4	a	150 ± 12	ab	0.160 ± 0.045	a	43.3 ± 8.0	a
BA10	134 ± 20	a	207 ± 29	a	0.919 ± 0.398	a	2.83 ± 0.81	a	16.4 ± 0.2	a	223 ± 48	a	0.163 ± 0.034	a	26.5 ± 6.2	a
Lime	105 ± 15	a	161 ± 25	a	0.713 ± 0.123	a	1.43 ± 0.20	a	15.5 ± 0.6	a	81 ± 13	b	0.124 ± 0.024	a	18.5 ± 1.9	a
ANOVA	**n.s.**		**n.s.**		**n.s.**		**n.s.**		†		†		**n.s.**		†	

Mean-values ± one standard error are shown (n=3). R6 indicates seed development stage. Samplings at R6 was conducted only in Control, BA10, and Lime treatments. Split-plot ANOVA was performed to detect significant differences among the treatments. Symbols (†,*) indicate *p*-values < 0.1, 0.05. "n.s." indicates *p*-values > 0.1. Different letters indicate significant differences among the treatments determined via Tukey post hoc test.

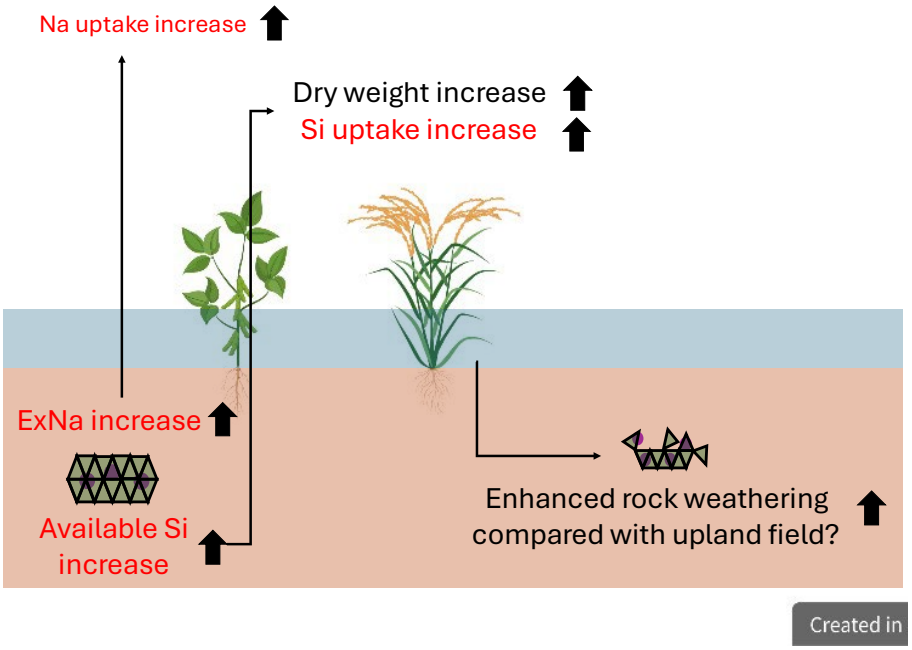

Figure 5-1. Graphical abstract of the paddy rice study.

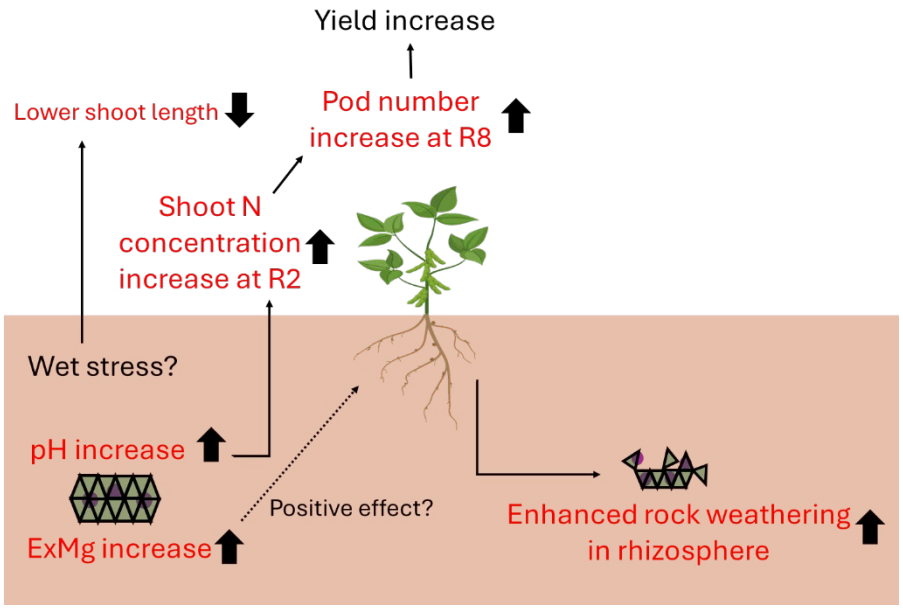

Figure 5-2. Graphical abstract of the soybean studies.

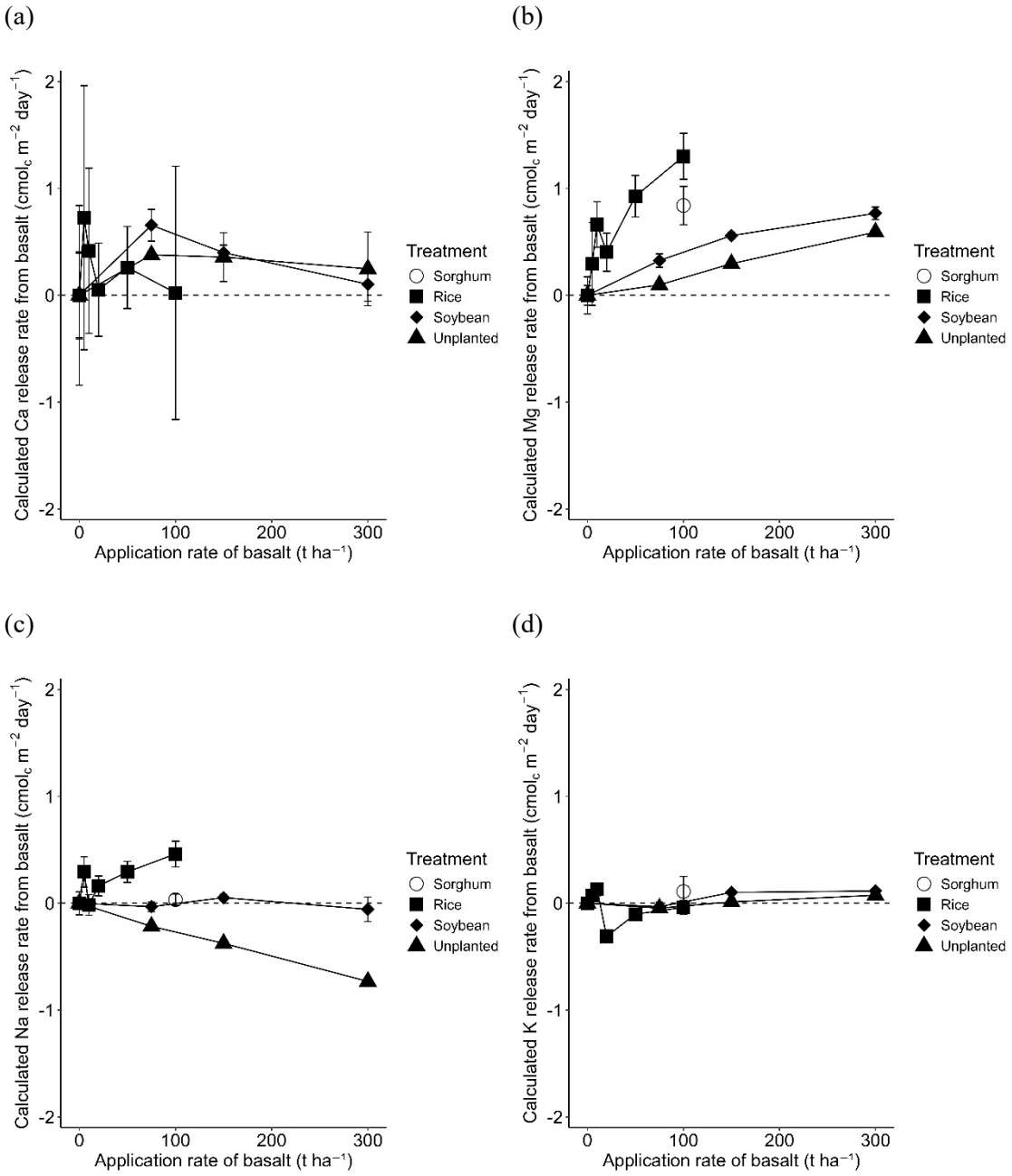

Figure 5-3. Comparisons of the calculated elemental release rate from basalt among different crops at different application rates. Points represent mean value ± one standard. The data of "Sorghum" was cited from Kelland et al. (2020). The data of "Rice" was obtained from Chapter 2, and "Soybean" and "Unplanted" were obtained from Chapter 3. The calculated Ca release rate in Sorghum was removed because of its high mean value ± one standard error (3.6 ± 2.8 $cmol_c$ m^{-2} day^{-1}).

The release rates of Ca, Mg, Na, and K in paddy rice pot experiment (Chapter 2) and soybean

pot experiment (Chapter 3) were calculated as follows:

Calculated release rate of M = calculated release of M from the basalt / land surface area / duration (eq. 5-1)

where calculated release of M from the basalt is a cation release from the basalt which was calculated based on (eq. 3-2) ($cmol_c\ pot^{-1}$), land surface area is an inner diameter of a pot (m^{-2}), and duration is the days from the application of the basalt to the sampling (day). Units of calculated release rate is represented in $cmol_c\ m^{-2}\ day^{-1}$. The units of the data of rice from Chapter 2 were firstly converted from $mmol\ pot^{-1}$ to $cmol_c\ pot^{-1}$ before the calculation.

References

1. AHMED, M., HASANUZZAMAN, M., RAZA, M. A., MALIK, A. & AHMAD, S. 2020. Plant nutrients for crop growth, development and stress tolerance. *Sustainable agriculture in the era of climate change***,** 43-92.
2. AKTER, M. & AKAGI, T. 2005. Effect of Fine Root Contact on Plant-Induced Weathering of Basalt. *Soil Science and Plant Nutrition,* 51**,** 861-871.
3. AKTER, M. & AKAGI, T. 2010. Dependence of plant-induced weathering of basalt and andesite on nutrient conditions. *GEOCHEMICAL JOURNAL,* 44**,** 137-150.
4. AMANN, T., HARTMANN, J., STRUYF, E., DE OLIVEIRA GARCIA, W., FISCHER, E. K., JANSSENS, I., MEIRE, P. & SCHOELYNCK, J. 2020. Enhanced Weathering and related element fluxes – a cropland mesocosm approach. Biogeosciences, 17, 103-119.
5. ANDA, M., SHAMSHUDDIN, J. & FAUZIAH, C. 2015. Improving chemical properties of a highly weathered soil using finely ground basalt rocks. Catena, 124, 147-161.
6. ANDREWS, M. G. & TAYLOR, L. L. 2019. Combating Climate Change Through Enhanced Weathering of Agricultural Soils. Elements, 15, 253-258.
7. BANERJEE, P. & NATH, R. 2022. Prospects of molybdenum fertilization in grain legumes-A review. *JOURNAL OF PLANT NUTRITION,* 45**,** 1425-1440.
8. BEERLING, D. J., EPIHOV, D. Z., KANTOLA, I. B., MASTERS, M. D., REERSHEMIUS, T., PLANAVSKY, N. J., REINHARD, C. T., JORDAN, J. S., THORNE, S. J., WEBER, J., VAL MARTIN, M., FRECKLETON, R. P., HARTLEY, S. E., JAMES, R. H., PEARCE, C. R., DELUCIA, E. H. & BANWART, S. A. 2024. Enhanced weathering in the US Corn Belt delivers carbon removal with agronomic benefits. *Proceedings of the National Academy of Sciences,* 121.
9. BEERLING, D. J., KANTZAS, E. P., LOMAS, M. R., WADE, P., EUFRASIO, R. M., RENFORTH, P., SARKAR, B., ANDREWS, M. G., JAMES, R. H., PEARCE, C. R., MERCURE, J.-F., POLLITT, H., HOLDEN, P. B., EDWARDS, N. R., KHANNA, M., KOH, L., QUEGAN, S., PIDGEON, N. F., JANSSENS, I. A., HANSEN, J. & BANWART, S. A. 2020. Potential for large-scale CO2 removal via enhanced rock weathering with croplands. *Nature,* 583**,** 242-248.
10. BEERLING, D. J., LEAKE, J. R., LONG, S. P., SCHOLES, J. D., TON, J., NELSON, P. N., BIRD, M., KANTZAS, E., TAYLOR, L. L., SARKAR, B., KELLAND, M., DELUCIA, E., KANTOLA, I., MÜLLER, C., RAU, G. & HANSEN, J. 2018. Farming with crops and rocks to address global climate, food and soil security. *Nature Plants,* 4**,** 138-147.

11. BERNARD, R. 1972. 2 GENES AFFECTING STEM TERMINATION IN SOYBEANS. *CROP SCIENCE,* 12**,** 235-+.
12. BURGHELEA, C., ZAHARESCU, D. G., DONTSOVA, K., MAIER, R., HUXMAN, T. & CHOROVER, J. 2015. Mineral nutrient mobilization by plants from rock: influence of rock type and arbuscular mycorrhiza. *Biogeochemistry,* 124**,** 187-203.
13. BUSS, W., HASEMER, H., FERGUSON, S. & BOREVITZ, J. 2024. Stabilisation of soil organic matter with rock dust partially counteracted by plants. *GLOBAL CHANGE BIOLOGY.*
14. BUTLER, B. & HILLIER, S. 2020. powdR: full pattern summation of X-ray powder diffraction data. R package version, 1.
15. BUTLER, B. M. & HILLIER, S. 2021. powdR: An R package for quantitative mineralogy using full pattern summation of X-ray powder diffraction data. Computers & Geosciences, 147.
16. CHINNUSAMY, V., JAGENDORF, A. & ZHU, J. K. 2005. Understanding and Improving Salt Tolerance in Plants. *Crop Science,* 45**,** 437-448.
17. CIPOLLA, G., CALABRESE, S., NOTO, L. & PORPORATO, A. 2021a. The role of hydrology on enhanced weathering for carbon sequestration I. Modeling rock-dissolution reactions coupled to plant, soil moisture, and carbon dynamics. *ADVANCES IN WATER RESOURCES,* 154.
18. CIPOLLA, G., CALABRESE, S., NOTO, L. & PORPORATO, A. 2021b. The role of hydrology on enhanced weathering for carbon sequestration II. From hydroclimatic scenarios to carbon-sequestration efficiencies. *ADVANCES IN WATER RESOURCES,* 154.
19. COCA, L., GONZÁLEZ, M., UNDAY, Z., HERNÁNDEZ, J., JÁUREGUI, M. & CANCIO, Y. 2023. Effects of Sodium Salinity on Rice (*Oryza sativa* L.) Cultivation: A Review. *SUSTAINABILITY.*
20. COLOMBO, C., PALUMBO, G., HE, J.-Z., PINTON, R. & CESCO, S. 2014. Review on iron availability in soil: interaction of Fe minerals, plants, and microbes. *Journal of Soils and Sediments,* 14**,** 538-548.
21. CONRAD, R. 2007. Microbial ecology of methanogens and methanotrophs. *ADVANCES IN AGRONOMY, VOL 96.*
22. DE MEDEIROS, D. S., SANCHOTENE, D. M., RAMOS, C. G., OLIVEIRA, L. F. S., SAMPAIO, C. H. & KAUTZMANN, R. M. 2021. Soybean crops cultivated with dacite rock by-product: A proof of a cleaner technology to soil remineralization. Journal of Environmental Chemical Engineering, 9, 106742.
23. DUPLA, X., MÖLLER, B., BAVEYE, P. & GRAND, S. 2023a. Potential accumulation of toxic trace elements in soils during enhanced rock weathering. *EUROPEAN JOURNAL OF*

SOIL SCIENCE, 74.

24. DUPLA, X., MÖLLER, B., BAVEYE, P. C. & GRAND, S. 2023b. Potential accumulation of toxic trace elements in soils during enhanced rock weathering. *European Journal of Soil Science,* 74.
25. EDENHOFER, O. 2015. *Climate change 2014: mitigation of climate change*, Cambridge University Press.
26. EL-NAGGAR, A., AHMED, N., MOSA, A., NIAZI, N. K., YOUSAF, B., SHARMA, A., SARKAR, B., CAI, Y. J. & CHANG, S. X. 2021. Nickel in soil and water: Sources, biogeochemistry, and remediation using biochar. *Journal of Hazardous Materials,* 419.
27. EPIHOV, D. Z., BANWART, S. A., MCGRATH, S. P., MARTIN, D. P., STEELEY, I. L., COBBOLD, V., KANTOLA, I. B., MASTERS, M. D., DELUCIA, E. H. & BEERLING, D. J. 2024. Iron Chelation in Soil: Scalable Biotechnology for Accelerating Carbon Dioxide Removal by Enhanced Rock Weathering. *Environmental Science & Technology,* 58**,** 11970-11987.
28. EPIHOV, D. Z., BATTERMAN, S. A., HEDIN, L. O., LEAKE, J. R., SMITH, L. M. & BEERLING, D. J. 2017. N_2-fixing tropical legume evolution: a contributor to enhanced weathering through the Cenozoic? *Proceedings of the Royal Society B: Biological Sciences,* 284**,** 20170370.
29. EPIHOV, D. Z., SALTONSTALL, K., BATTERMAN, S. A., HEDIN, L. O., HALL, J. S., VAN BREUGEL, M., LEAKE, J. R. & BEERLING, D. J. 2021. Legume–microbiome interactions unlock mineral nutrients in regrowing tropical forests. *Proceedings of the National Academy of Sciences,* 118**,** e2022241118.
30. FAWE, A., ABOU-ZAID, M., MENZIES, J. G. & BÉLANGER, R. R. 1998. Silicon-mediated accumulation of flavonoid phytoalexins in cucumber. *Phytopathology,* 88**,** 396-401.
31. GILLMAN, G. P., BURKETT, D. C. & COVENTRY, R. J. 2001. A laboratory study of application of basalt dust to highly weathered soils: effect on soil cation chemistry. *Soil Research,* 39**,** 799.
32. GOLDICH, S. 1938. A study in rock-weathering. *JOURNAL OF GEOLOGY,* 46**,** 17-58.
33. GUO, F., SUN, H., YANG, J., ZHANG, L., MU, Y., WANG, Y. & WU, F. 2023a. Improving food security and farmland carbon sequestration in China through enhanced rock weathering: Field evidence and potential assessment in different humid regions. *SCIENCE OF THE TOTAL ENVIRONMENT,* 903.
34. GUO, F., WANG, Y., ZHU, H., ZHANG, C., SUN, H., FANG, Z., YANG, J., ZHANG, L., MU, Y., MAN, Y. & WU, F. 2023b. Crop productivity and soil inorganic carbon change mediated by enhanced rock weathering in farmland: A comparative field analysis of multi-

agroclimatic regions in central China. *AGRICULTURAL SYSTEMS,* 210.

35. HAQUE, F., SANTOS, R. M. & CHIANG, Y. W. 2020. Optimizing Inorganic Carbon Sequestration and Crop Yield With Wollastonite Soil Amendment in a Microplot Study. *Frontiers in Plant Science,* 11.
36. HAQUE, F., SANTOS, R. M., DUTTA, A., THIMMANAGARI, M. & CHIANG, Y. W. 2019. Co-Benefits of Wollastonite Weathering in Agriculture: CO_2 Sequestration and Promoted Plant Growth. *ACS Omega,* 4**,** 1425-1433.
37. HARTMANN, A., SCHMID, M., TUINEN, D. V. & BERG, G. 2009. Plant-driven selection of microbes. *Plant and Soil,* 321**,** 235-257.
38. HARTMANN, J., WEST, A. J., RENFORTH, P., KÖHLER, P., DE LA ROCHA, C. L., WOLF-GLADROW, D. A., DÜRR, H. H. & SCHEFFRAN, J. 2013. Enhanced chemical weathering as a geoengineering strategy to reduce atmospheric carbon dioxide, supply nutrients, and mitigate ocean acidification. *Reviews of Geophysics,* 51**,** 113-149.
39. HASEMER, H., BOREVITZ, J. & BUSS, W. 2024. Measuring enhanced weathering: inorganic carbon-based approaches may be required to complement cation-based approaches. *FRONTIERS IN CLIMATE,* 6.
40. HAYNES, R. 1983. SOIL ACIDIFICATION INDUCED BY LEGUMINOUS CROPS. *GRASS AND FORAGE SCIENCE,* 38**,** 1-11.
41. HE, Z., YANG, X. & STOFFELLA, P. 2005. Trace elements in agroecosystems and impacts on the environment. *JOURNAL OF TRACE ELEMENTS IN MEDICINE AND BIOLOGY,* 19**,** 125-140.
42. HERMANSKÁ, M., VOIGT, M., MARIENI, C., DECLERCQ, J. & OELKERS, E. 2023. A comprehensive and consistent mineral dissolution rate database: Part II: Secondary silicate minerals. *CHEMICAL GEOLOGY,* 636.
43. HINSINGER, P., BARROS, O. N. F., BENEDETTI, M. F., NOACK, Y. & CALLOT, G. 2001. Plant-induced weathering of a basaltic rock: Experimental evidence. *Geochimica Et Cosmochimica Acta,* 65**,** 137-152.
44. HINSINGER, P., GOBRAN, G. R., GREGORY, P. J. & WENZEL, W. W. 2005. Rhizosphere geometry and heterogeneity arising from root-mediated physical and chemical processes. *New Phytologist,* 168**,** 293-303.
45. Hokkaido Research Organization. 2020. Hokkaido Fertilizer Recommendations 2020. 1-226. Hokkaido Government Department of Agriculture.
46. ISHIKAWA, S., MAKINO, T., ITO, M., HARADA, K., NAKADA, H., NISHIDA, I., NISHIMURA, M., TOKUNAGA, T., SHIRAO, K., YOSHIZAWA, C., MATSUYAMA, M., ABE, T. & ARAO, T. 2016. Low-cadmium rice (*Oryza sativa* L.) cultivar can simultaneously reduce arsenic and cadmium concentrations in rice grains. *Soil Science and*

Plant Nutrition, 62**,** 327-339.

47. IUSS Working Group WRB. 2022. World reference base for soil resources. International soil classification system for naming soil sand creating legends for soil maps (4th ed.). International Union of Soil Sciences (IUSS). https://wrb.isric.org/
48. Intergovernmental Panel on Climate Change (IPCC). 2023. AR6 Synthesis Report Climate change 2023. https://www.ipcc.ch/report/ar6/syr/
49. KAISER, B., GRIDLEY, K., BRADY, J., PHILLIPS, T. & TYERMAN, S. 2005. The role of molybdenum in agricultural plant production. *ANNALS OF BOTANY,* 96**,** 745-754.
50. KAMEWADA, K. 1997a. Exchangeable cations and anions. *In:* ENVIRONMENT, E. C. F. A. M. F. S. (ed.) *Dojo-Kankyo-Bunseki-Ho (analytical Methods for Soil Environment).* Tokyo: Hakuyusya.
51. KAMEWADA, K. 1997b. pH (glass electrode method). *In:* ENVIRONMENT, E. C. F. A. M. F. S. (ed.) *Dojo-Kankyo-Bunseki-Ho (analytical Methods for Soil Environment).* Tokyo: Hakuyusya.
52. KANTOLA, I. B., BLANC-BETES, E., MASTERS, M. D., CHANG, E., MARKLEIN, A., MOORE, C. E., VON HADEN, A., BERNACCHI, C. J., WOLF, A., EPIHOV, D. Z., BEERLING, D. J. & DELUCIA, E. H. 2023. Improved net carbon budgets in the US Midwest through direct measured impacts of enhanced weathering. *Global Change Biology,* 29**,** 7012-7028.
53. KANTOLA, I. B., MASTERS, M. D., BEERLING, D. J., LONG, S. P. & DELUCIA, E. H. 2017. Potential of global croplands and bioenergy crops for climate change mitigation through deployment for enhanced weathering. *Biology Letters,* 13**,** 20160714.
54. KASTING, J. 2019. The Goldilocks Planet? How Silicate Weathering Maintains Earth "Just Right". *ELEMENTS,* 15**,** 235-240.
55. KELLAND, M. E., WADE, P. W., LEWIS, A. L., TAYLOR, L. L., SARKAR, B., ANDREWS, M. G., LOMAS, M. R., COTTON, T. E. A., KEMP, S. J., JAMES, R. H., PEARCE, C. R., HARTLEY, S. E., HODSON, M. E., LEAKE, J. R., BANWART, S. A. & BEERLING, D. J. 2020. Increased yield and CO_2 sequestration potential with the C_4 cereal *Sorghum bicolor* cultivated in basaltic rock dust-amended agricultural soil. *Global Change Biology,* 26**,** 3658-3676.
56. KOHRI, K., SAITOH, K., KURODA, T. & KUMANO, S. 1998. Significance of Flower Differentiation and Development in the Process of Determining Soybean Yield. Effects of shading treatment on the number of floral buds and pod sets. *Japanese Journal of Crop Science,* 67**,** 79-84.
57. KUMAR, A., JIGYASU, D. K., SUBRAHMANYAM, G., MONDAL, R., SHABNAM, A. A., CABRAL-PINTO, M. M. S., MALYAN, S. K., CHATURVEDI, A. K., GUPTA, D. K.,

FAGODIYA, R. K., KHAN, S. A. & BHATIA, A. 2021. Nickel in terrestrial biota: Comprehensive review on contamination, toxicity, tolerance and its remediation approaches. *Chemosphere,* 275.

58. KUMP, L., BRANTLEY, S. & ARTHUR, M. 2000. Chemical, weathering, atmospheric CO_2, and climate. *ANNUAL REVIEW OF EARTH AND PLANETARY SCIENCES,* 28**,** 611-667.
59. KUROKAWA, K., AZUMA, K., NAKAO, A., SUZUKI, A., WAKABAYASHI, S., FUJIMURA, S., SHINANO, T. & YANAI, J. 2024. Examination of the reliability of X-ray powder diffraction analysis to determine mineral composition of soils. *Soil Science Society of America Journal,* 88**,** 1942-1958.
60. KUSA, K., MORIIZUMI, M., HOBARA, S., KANEKO, M., MATSUMOTO, S., KASUGA, J. & AE, N. 2021. Mineral weathering and silicon uptake by rice plants promote carbon storage in paddy fields. *Soil Science and Plant Nutrition,* 67**,** 162-170.
61. KUSA, K., MORIIZUMI, M., HOBARA, S., KANEKO, M., MATSUMOTO, S., KASUGA, J. & AE, N. 2021. Mineral weathering and silicon uptake by rice plants promote carbon storage in paddy fieldsma. Soil Science and Plant Nutrition, 67, 162-170.
62. LARKIN, C., ANDREWS, M., PEARCE, C., YEONG, K., BEERLING, D., BELLAMY, J., BENEDICK, S., FRECKLETON, R., GORING-HARFORD, H., SADEKAR, S. & JAMES, R. 2022. Quantification of CO_2 removal in a large-scale enhanced weathering field trial on an oil palm plantation in Sabah, Malaysia. *FRONTIERS IN CLIMATE,* 4.
63. LEWIS, A. L., SARKAR, B., WADE, P., KEMP, S. J., HODSON, M. E., TAYLOR, L. L., YEONG, K. L., DAVIES, K., NELSON, P. N., BIRD, M. I., KANTOLA, I. B., MASTERS, M. D., DELUCIA, E., LEAKE, J. R., BANWART, S. A. & BEERLING, D. J. 2021. Effects of mineralogy, chemistry and physical properties of basalts on carbon capture potential and plant-nutrient element release via enhanced weathering. *Applied Geochemistry,* 132.
64. LIN, M.-H., GRESSHOFF, P. M. & FERGUSON, B. J. 2012. Systemic Regulation of Soybean Nodulation by Acidic Growth Conditions. *Plant Physiology,* 160**,** 2028-2039.
65. LUCHESE, A., LEITE, I., GIARETTA, A., ALVES, M. & MISSIO, R. 2023. Use of quarry waste basalt rock powder as a soil remineralizer to grow soybean and maize. *HELIYON,* 9.
66. MA, J. F. & YAMAJI, N. 2008. Functions and transport of silicon in plants. *Cellular and Molecular Life Sciences,* 65**,** 3049-3057.
67. MA, J. F. 2004. Role of silicon in enhancing the resistance of plants to biotic and abiotic stresses. *Soil Science and Plant Nutrition,* 50**,** 11-18.
68. MINISTRY OF AGRICULTURE, FORESTRY AND FISHERIES. 2024. "Statistics of

Agricultural Land Area." https://www.e-stat.go.jp/stat-search/files/data?sinfid=000040217091&ext=xls. accessed 13, December , 2024.

69. MINX, J., LAMB, W., CALLAGHAN, M., FUSS, S., HILAIRE, J., CREUTZIG, F., AMANN, T., BERINGER, T., GARCIA, W., HARTMANN, J., KHANNA, T., LENZI, D., LUDERER, G., NEMET, G., ROGELJ, J., SMITH, P., VICENTE, J., WILCOX, J. & DOMINGUEZ, M. 2018. Negative emissions-Part 1: Research landscape and synthesis. *ENVIRONMENTAL RESEARCH LETTERS,* 13.
70. MORIIZUMI, M., AE, N., OZAWA, K., YOSHIDA, Y., HAMANO, R. & NUMADATE, K. 2021. Effects of weathering and silicic acid uptake by rice plants on weathered products -Quantitative changes in potassium, silica, and aluminum in granitic Fluvisol. *SOIL SCIENCE AND PLANT NUTRITION,* 67**,** 439-445.
71. MOULTON, K., WEST, A. & BERNER, R. 2000. Solute flux and mineral mass balance approaches to the quantification of plant effects on silicate weathering. *AMERICAN JOURNAL OF SCIENCE.*
72. Ministry of Agriculture, Forestry and Fisheries (MAFF), 2024. *Fertilizer Control Act and its standards*. [online] Available at: https://www.maff.go.jp/ [Accessed 3 Feb. 2025].
73. NAKAMURA, T., OSAKI, M. & WATANABE, T. 2024. Zero-valent iron reduces cadmium and arsenic accumulation in spinach (Spinacia oleracea L.). *JOURNAL OF PLANT NUTRITION.*
74. NASER, H. M., NAGATA, O., SULTANA, S. & HATANO, R. 2020. Carbon Sequestration and Contribution of CO2, CH_4 and N_2O Fluxes to Global Warming Potential from Paddy-Fallow Fields on Mineral Soil Beneath Peat in Central Hokkaido, Japan. Agriculture-Basel, 10.
75. OBAMA, R., KUMAGAI, K., MARUYAMA, H., SHINANO, T. & WATANABE, T. 2024. Effect of different light conditions on the growth response of sugar beet to NaCl. *Soil Science and Plant Nutrition***,** 1-9.
76. OBARA, H., T. OHKURA, Y. TAKATA, K. KOHYAMA, Y. MAEJIMA, AND T. HAMAZAKI. 2011. “Comprehensive Soil Classification System of Japan First Approximation.” Bulletin of National Institute for Agro-Environmental Sciences 29:1–73 doi:http://doi.org/10.24514/00002990.
77. PALANDRI, J. L. & KHARAKA, Y. K. 2004. A compilation of rate parameters of water-mineral interaction kinetics for application to geochemical modeling. US Geological Survey.
78. PENG, W., QI, W., NIE, M., XIAO, Y., LIAO, H. & CHEN, Z. 2020. Magnesium supports

nitrogen uptake through regulating *NRT2.1/2.2* in soybean. *PLANT AND SOIL,* 457**,** 97-111.

79. PENG, W., ZHANG, L., ZHOU, Z., FU, C., CHEN, Z. & LIAO, H. 2018. Magnesium promotes root nodulation through facilitation of carbohydrate allocation in soybean. *PHYSIOLOGIA PLANTARUM,* 163**,** 372-385.
80. RENFORTH, P. & HENDERSON, G. 2017. Assessing ocean alkalinity for carbon sequestration. *Reviews of Geophysics,* 55**,** 636-674.
81. RIBEIRO, I., GAZOLLA VOLPIANO, C., VARGAS, L., GRANADA, C., LISBOA, B. & PASSAGLIA, L. 2020. Use of Mineral Weathering Bacteria to Enhance Nutrient Availability in Crops: A Review. *Frontiers in Plant Science,* 11.
82. SAHRAWAT, K. 2005. Fertility and organic matter in submerged rice soils. *CURRENT SCIENCE.*
83. SAITOH, K., ISOBE, S. & KURODA, T. 1998. Significance of Flower Differentiation and Development in the Process of Determining Soybean Yield. Relation between the Number of Pods and Flowers. *Japanese Journal of Crop Science,* 67**,** 70-78.
84. SHIGEZUMI, M., KITTA, Y., KUBO, S. & MIZUOCHI, T. 2002. The evaluation of the available silica in paddy soil by the phosphate buffer extraction method. *Japanese Journal of Soil Science and Plant Nutrition,* 73**,** 383-390.
85. SKOV, K., WARDMAN, J., HEALEY, M., MCBRIDE, A., BIEROWIEC, T., COOPER, J., EDEH, I., GEORGE, D., KELLAND, M. E., MANN, J., MANNING, D., MURPHY, M. J., PAPE, R., TEH, Y. A., TURNER, W., WADE, P. & LIU, X. 2024. Initial agronomic benefits of enhanced weathering using basalt: A study of spring oat in a temperate climate. *PLOS ONE,* 19**,** e0295031.
86. SWOBODA, P., DÖRING, T. & HAMER, M. 2022. Remineralizing soils? The agricultural usage of silicate rock powders: A review. *Science of the Total Environment,* 807.
87. TAKAMOTO, A., TAKAHASHI, T. & TOGAMI, K. 2021. Effect of changes in the soil calcium-to-magnesium ratio by calcium application on soybeans, *Glycine max* (L.) Merr., growth. *Soil Science and Plant Nutrition,* 67**,** 139-149.
88. TAYLOR, L., QUIRK, J., THORLEY, R., KHARECHA, P., HANSEN, J., RIDGWELL, A., LOMAS, M., BANWART, S. & BEERLING, D. 2016. Enhanced weathering strategies for stabilizing climate and averting ocean acidification. *NATURE CLIMATE CHANGE,* 6**,** 402-+.
89. TEN BERGE, H. F. M., VAN DER MEER, H. G., STEENHUIZEN, J. W., GOEDHART, P. W., KNOPS, P. & VERHAGEN, J. 2012. Olivine Weathering in Soil, and Its Effects on Growth and Nutrient Uptake in Ryegrass (Lolium perenne L.): A Pot Experiment. PLoS ONE, 7, e42098.

90. THILAKARATHNA, M. & RAIZADA, M. 2017. A meta-analysis of the effectiveness of diverse rhizobia inoculants on soybean traits under field conditions. *SOIL BIOLOGY & BIOCHEMISTRY,* 105**,** 177-196.
91. TRIPATHI, P., NA, C. I. & KIM, Y. 2021. Effect of silicon fertilizer treatment on nodule formation and yield in soybean (*Glycine max* L.). *European Journal of Agronomy,* 122.
92. TSUBOUCHI, H. & SAITO, M. 2010. Soil Properties of the Soybean Fields in [paddy rice – barley – soybean – paddy rice] Rotation System, and its Amelioration with Lime or Micronutrients Fertilizer. *Bulletin of the Fukui Agricultural Experiment Station,* 47: 9–14.
93. VAN DER BAUWHEDE, R., MUYS, B., VANCAMPENHOUT, K. & SMOLDERS, E. 2024. Accelerated weathering of silicate rock dusts predicts the slow-release liming in soils depending on rock mineralogy, soil acidity, and test methodology. *GEODERMA,* 441.
94. VAN VUUREN, D. P., STEHFEST, E., DEN ELZEN, M. G. J., KRAM, T., VAN VLIET, J., DEETMAN, S., ISAAC, M., KLEIN GOLDEWIJK, K., HOF, A., MENDOZA BELTRAN, A., OOSTENRIJK, R. & VAN RUIJVEN, B. 2011. RCP2.6: exploring the possibility to keep global mean temperature increase below 2°C. *Climatic Change,* 109**,** 95-116.
95. VERBRUGGEN, E., STRUYF, E. & VICCA, S. 2021. Can arbuscular mycorrhizal fungi speed up carbon sequestration by enhanced weathering? *PLANTS, PEOPLE, PLANET,* 3**,** 445-453.
96. VIENNE, A., POBLADOR, S., PORTILLO-ESTRADA, M., HARTMANN, J., IJIEHON, S., WADE, P. & VICCA, S. 2022. Enhanced Weathering Using Basalt Rock Powder: Carbon Sequestration, Co-benefits and Risks in a Mesocosm Study With Solanum tuberosum. *Frontiers in Climate,* 4.
97. WANG, F. N., ZHU, F. F., LIU, D. Z., QU, Y. Y., LIU, D., XIE, J., WANG, A., KANG, R. H., QUAN, Z., LI, Y. H., CHEN, X., LI, G. C., HOBBIE, E. A. & FANG, Y. T. 2024. Wollastonite powder application increases rice yield and CO_2 sequestration in a paddy field in Northeast China. *Plant and Soil*.
98. WHITE, A. & BRANTLEY, S. 2003. The effect of time on the weathering of silicate minerals: why do weathering rates differ in the laboratory and field? *CHEMICAL GEOLOGY,* 202**,** 479-506.
99. YANAI, J., TANIGUCHI, H. & NAKAO, A. 2016. Evaluation of available silicon content and its determining factors of agricultural soils in Japan. Soil Science and Plant Nutrition, 62, 511-518.
100. YANG, Y., G. KOSAKA, H. UCHIBAYASHI, Y. ZHU, K. KUROMOCHI, T. SHINANO, T. WATANABE, H. MARUYAMA, S. HAMAMOTO, A. NAKAO, Y & TOMA. 2024. “Enhanced CO2 Removal and Improved Carbon Budget by Enhanced Rock Weathering:

A Field Experiment in Hokkaido, Japan." *Nutrient Cycling in Agroecosystem*. (under review).

101. ZENG, L. & SHANNON, M. C. 2000. Salinity Effects on Seedling Growth and Yield Components of Rice. *Crop Science,* 40**,** 996-1003.
102. ZULFIQAR, U., HAIDER, F. U., AHMAD, M., HUSSAIN, S., MAQSOOD, M. F., ISHFAQ, M., SHAHZAD, B., WAQAS, M. M., ALI, B., TAYYAB, M. N., AHMAD, S. A., KHAN, I. & ELDIN, S. M. 2023. Chromium toxicity, speciation, and remediation strategies in soil-plant interface: A critical review. *Frontiers in Plant Science,* 13.

Acknowledgements

The work presented in this thesis was mostly carried out at Laboratory of Plant Nutrition in Graduate School of Agriculture, Hokkaido University (Hokkaido University; Sapporo, Japan).

First of all, I would like to express my great appreciation to my supervisor, Professor Takuro Shinano, for giving me the opportunity to investigate the effect of basalt powder application on soil chemical properties and crop growth and element uptake. I also appreciate all the support, knowledge, observation, and comment that he gave to me. I am indebted to him for introducing me to many experienced scientists.

I would like to thank Dr. Toshihiro Watanabe, associate professor of our laboratory. He was so kind as to provide me with many insights through comments on experiments and paper.

I am very grateful to Dr. Hayato Maruyama, assistant professor of our laboratory, for sharing his own time and technical knowledge for sampling and experiments in my research. His willing cooperation and warm teaching have always been a great encouragement for me to complete this work.

I am thankful to Professor Yo Toma (Laboratory of Soil Science in Hokkaido University; Sapporo, Japan) for giving me opportunity to analyze soil total carbon and nitrogen as well as other measurement items related with carbon.

I am also thankful to Professor Shoichiro Hamamoto (Laboratory of Soil Conservation in Hokkaido University; Sapporo, Japan) for sharing many insights about element and water transport in soil.

Once again, I would like to thank Professor Shinano, Dr. Watanabe, Dr. Maruyama, Professor Toma, and Professor Hamamoto for their helpful comments to improve the thesis as the official referees of the dissertation.

I must not forget to express my thankfulness to Dr. Atsushi Nakao (Laboratory of Soil Science in Kyoto Prefecture University; Kyoto, Japan) for giving me great opportunities to learn mineralogy and analyze soil with XRD analysis.

Great thanks to all members of ERW project teams: especially Professor Takao Nakagaki, Professor Tsutomu Sato, Professor Junta Yanai, Professor Taku Nishimura, Dr. Rota Wagai, Dr.

Kazutoshi Kinjo, Dr. Saiko Yada, Dr. Ryosuke Kikuchi, Dr. Shinya Iwasaki, Dr. Jumpei Fukumasu, and Ms. Minori Umahashi for spending time with me in conferences and samplings.

My special thanks go to all our laboratory members and graduates, and my friends for supporting each other during tough times.

At last, but not the least, I would like to express my sincere gratitude to my family for all support, joy and comfort you have given me during all years I was engaged in the research work.

Hiroshi Uchibayashi

March 2025, Hokkaido, Japan